Spatiotemporal cat: a chaotic field theory

P Cvitanović and H Liang

Center for Nonlinear Science, School of Physics, Georgia Institute of Technology, Atlanta, GA 30332-0430, USA

E-mail: predrag.cvitanovic@physics.gatech.edu

November 30, 2020

Abstract.

While the global dynamics of an extended, spatiotemporally turbulent system can be extraordinarily complex, the local dynamics, observed through small spatiotemporal windows, can be thought of as a visitation sequence through a finite repertoire of finite patterns. To compute spatiotemporal expectation values of observables from the defining equations of such systems, one needs to know how often a given pattern occurs. Here we address this fundamental question by constructing a spatiotemporal cat, a classical d-dimensional chaotic lattice field theory. Treating the temporal and spatial directions on equal footing, we abandon initial state evolution, local in time, and enumerate instead global solutions compatible with system's defining equations. In such field theory any spatiotemporal state is labeled by a unique d-dimensional lattice block of symbols from a finite alphabet, a state of the system over a finite spatiotemporal region is specified uniquely and with exponential precision by a finite blocks of such symbols, and the likelihood of such state occurring is given by the Hill determinant of its spatiotemporal orbit Jacobian matrix.

PACS numbers: 02.20.-a, 05.45.-a, 05.45.Jn, 47.27.ed

Submitted to: *Nonlinearity*

A temporally chaotic system is exponentially unstable with time: double the time, and exponentially more orbits are required to cover its strange attractor to the same accuracy. For large spatial extents, the complexity of the spatial shapes also needs to be taken into account; double the spatial extent, and exponentially as many distinct spatiotemporal patterns will be required to describe the repertoire of system's shapes to the same accuracy. The systems whose temporal and spatial correlations decay sufficiently fast, and whose "physical" dimension [36, 48] grows with system size, are said to be "spatiotemporally chaotic."

Our goal here is to make this "spatiotemporal chaos" tangible and precise, by offering the reader what we believe is its simplest explicit example, the *spatiotemporal cat* [52, 55] (a screened Poisson or Yukawa equation)

$$(\Box - d(s-2))\,\Phi = -\mathsf{M}\,,$$

a classical field theory on a d-dimensional hyper-cubic lattice, with an "anti-harmonic" rotor ϕ_z at each site z coupled to its nearest neighbors. In contrast to a field governed by its close relative, Helmholtz equation, with oscillatory solutions, spatiotemporal cat solutions are hyperbolic and 'turbulent', in the same sense that in contrast to stable oscillations of a harmonic oscillator, Bernoulli coin flip solutions are unstable and chaotic.

Spatiotemporally homogenous turbulent flows offer one physical motivation for considering such models: a very rough approximation to such flows is discretizing them into spatiotemporal cells, with each cell turbulent, and cells coupled to their nearest neighbors. Spatiotemporal cat is arguably the simplest such model, no closer to physical turbulence than the Lorenz model [76] is to weather, but still capturing the essential qualitative features of spatiotemporal chaos.

The main thrust of this paper is, however, more radical: we've been doing 'turbulence' all wrong, and we know that since Poincaré's times. In "explaining" chaos we talk the talk as though we have never moved beyond Newton; here is an initial state of a system, local in time, and here are the differential equations that evolve it forward in time. But when we -all of us- do the work, we do something altogether different, closer to Lagrange, and to the 20th century 'spacetime' physics. This paper realigns the theory to what we actually *do* when solving "chaos" equations, using not much more than linear algebra. In this formulation, there is no time, and there is no "Lyapunov" horizon; every solution Φ is a global solution of a spatiotemporal fixed point condition $F[\Phi] = 0$, and there is no exponential blowup of anything.

As we shall here have to traverse territory unfamiliar to many, we follow Mephistopheles pedagogical dictum "You have to say it three times" [49], and sing our song thrice.

The first time, for a reader too busy [25] to read the book [30], we disguise a brief course on chaos theory as something everyone understands, a Bernoulli coin toss, section 1. In section 1.2 we introduce the 'temporal Bernoulli', a lattice reformulation of the Bernoulli map. The deep insight here is the realization that the *Hill determinant*, i.e., the volume (16) of the *orbit Jacobian matrix* (figure 2, 3 and 4) counts all global solutions of given defining equations.

The second time, as a 'temporal cat', a 1-dimensional lattice of rotors that all dynamicists understand, section 2. In section 2.1 we review the traditional cat map in its Hamiltonian formulation (but relegate to Appendix C the explicit Adler-Weiss generating partition of the cat map phase space). In section 2.2 we introduce the 'temporal cat', a lattice reformulation of the cat map. The periodic orbits theory of cat maps can be developed in either formulation: both the forward-in-time Hamiltonian cat map, Appendix C.2, and the Lagrangian temporal cat lead to the same topological zeta function (68) count of *prime* periodic orbits, with the two formulations related by Hill's formula (67).

The third time, herding cats all over spacetime, as a field theory similar to ones studied by statistical mechanicians and field theorists, section 3. In section 3.1 we

review the traditional coupled map lattice model discretizations of dissipative PDEs, as well as many-body Hamiltonian models, section 3.2. In section 3.3 we generalize the temporal cat model to the d-dimensional *spatiotemporal* cat, and in section 3.5 show that the system admits a d-dimensional symbolic code with a finite alphabet. We then turn to study of admissible finite spatiotemporal symbol blocks. The key to solution counting problem is the enumeration of *prime* periodic orbits, with the notion of 'prime' now subtler than what it was for 1-dimensional lattices, different for the integer lattice coordinate system, section 3.6, from periodic orbits, i.e., the fields over these coordinates, section 3.7. Section 3.8 illustrates our periodic orbit spatiotemporal cat solutions by several explicit examples. In section 3.10 we use the spatiotemporal cat symbolic dynamics to show that spatiotemporal periodic orbits that share finite spatiotemporal symbol blocks shadow each other to exponential precision (the symbolic dynamics definitions used throughout the paper are collected in Appendix F).

Section 4 tabulates our prime periodic orbits counts. Hill's formula for the 2-dimensional lattice spatiotemporal cat is derived in section 5.3. We evaluate and cross-check Hill determinants by two methods, either the 'fundamental fact' evaluation, section Appendix A.4.3, or by the discrete Fourier transform diagonalization, Appendix A.

The results are summarized and some open questions discussed in the section 6.

1. A fair coin toss

The very simplest example of a deterministic law of evolution that gives rise to 'chaos' is the *Bernoulli* map, figure 1 (a), which models a coin toss. Starting with a random initial state, the map generates, deterministically, a sequence of tails and heads with the 50-50% probability.

We introduce the model in its conventional, time-evolution dynamical formulation, than reformulate it as a lattice 'field theory', solved by enumeration of all admissible *lattice states*, field configurations that satisfy a global fixed point condition, and use this simple setting to motivate (1) the *fundamental fact*: for a given lattice period, the *Hill determinant* of stabilities of global solutions counts their number, and (2) the topological zeta function counts their symmetry orbits, with a *prime* lattice state per each orbit.

1.1. Bernoulli map

The base-2 *Bernoulli* shift map,

$$x_{t+1} = \begin{cases} f_0(x_t) = 2x_t\,, & x_t \in \mathcal{M}_0 = [0, 1/2) \\ f_1(x_t) = 2x_t \pmod 1\,, & x_t \in \mathcal{M}_1 = [1/2, 1) \end{cases}\,, \tag{1}$$

is shown in figure 1 (a). If the linear part of such map has an integer-valued slope, or 'stretching' parameter $s \geq 2$,

$$x_{t+1} \;=\; s x_t \tag{2}$$

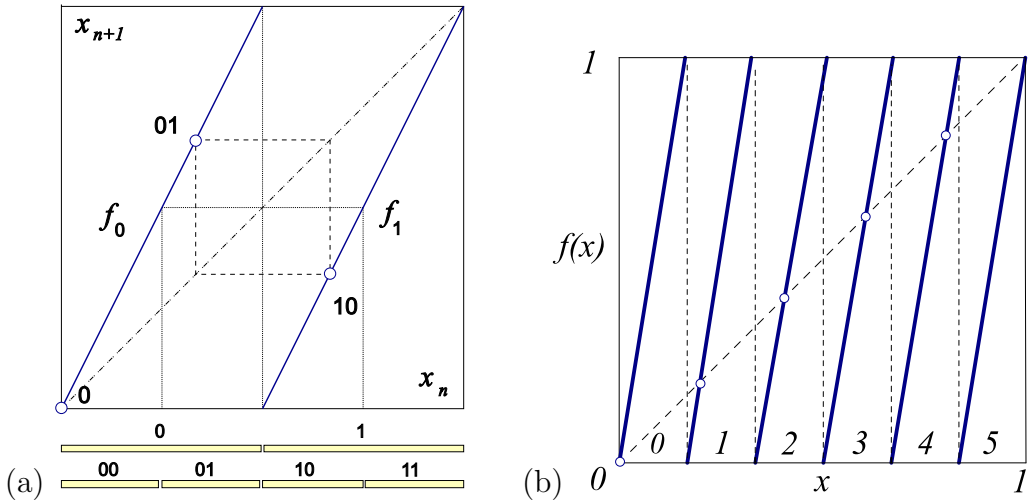

Figure 1. (a) The 'coin toss' map (1), together with the $\overline{0}$ fixed point, and the $\overline{01}$ 2-cycle. Preimages of the critical point $x_c = 1/2$ partition the unit interval into $\{\mathcal{M}_0, \mathcal{M}_1\}$, $\{\mathcal{M}_{00}, \mathcal{M}_{01}, \mathcal{M}_{10}, \mathcal{M}_{11}\}$, ..., subintervals. (b) The base-s Bernoulli map, here with the 'dice throw' stretching parameter $s = 6$, partitions the unit interval into 6 subintervals $\{\mathcal{M}_m\}$, labeled by the 6-letter alphabet (5). As the map is a circle map, $x_5 = 1 = 0 = x_0 \pmod 1$.

that maps state x_t into a state in the 'extended state space', outside the unit interval, the (mod 1) operation results in the base-s Bernoulli circle map,

$$\phi_{t+1} = s\phi_t \pmod 1 , \tag{3}$$

sketched as a dice throw in figure 1 (b). The (mod 1) operation subtracts $m_{t+1} = \lfloor s\phi_t \rfloor$, the integer part of $s\phi_t$, or the circle map *winding number*, to keep ϕ_{t+1} in the unit interval $[0, 1)$, and partitions the unit interval into s subintervals $\{\mathcal{M}_m\}$,

$$\phi_{t+1} = s\phi_t - m_{t+1} , \qquad \phi_t \in \mathcal{M}_{m_t} , \tag{4}$$

where m_t takes values in the s-letter alphabet

$$m \in \mathcal{A} = \{0, 1, 2, \cdots, s-1\} . \tag{5}$$

The Bernoulli map is a highly instructive example of a hyperbolic dynamical system. Its symbolic dynamics is simple: the base-s expansion of the initial point ϕ_0 is also its temporal itinerary, with symbols from alphabet (5) indicating that at time t the orbit visits the subinterval $\mathcal{M}_{m_t}$. The map is a 'shift': a multiplication by s acts on the base-s representation of $\phi_0 = .m_1 m_2 m_3 \cdots$ (for example, binary, if $s = 2$) by shifting its digits,

$$\phi_1 = f(\phi_0) = .m_2 m_3 \cdots . \tag{6}$$

Periodic points can be counted by observing that the preimages of critical points $\{\phi_{c1}, \phi_{c2}, \cdots \phi_{c,s-1}\} = \{1/s, 2/s, \cdots, (s-1)/s\}$ partition the unit interval into $\{\mathcal{M}_0, \mathcal{M}_1, \cdots, \mathcal{M}_{s-1}\}$, $\{\mathcal{M}_{m_1 m_2}\}$, ..., s^n subintervals, each containing *one* unstable period-n periodic point $\phi_{m_1 m_2 \cdots m_n}$, with stability multiplier s^n, see figure 1. The Bernoulli map is a full shift, in the sense that every itinerary is admissible, with one

exception: on the circle, the rightmost fixed point is the same as the fixed point at the origin, $\phi_{s-1} = \phi_0 \pmod 1$, so these fixed points are identified and counted as one, see figure 1. The total number of periodic points of period n is thus

$$N_n = s^n - 1\,. \tag{7}$$

1.2. Temporal Bernuolli

To motivate our formulation of a spatiotemporal chaotic field theory to be developed below, we now recast the local initial value, time-evolution Bernoulli map problem as a *temporal lattice* fixed point condition, the problem of enumerating and determining all global solutions.

'Temporal' here refers to the state (field) ϕ_t, and the winding number (source) m_t taking their values on the lattice sites of a 1-dimensional *temporal* integer lattice $t \in \mathbb{Z}$. Over a finite lattice segment, these can be written compactly as a *lattice state* and the corresponding *symbol block*

$$\Phi^\top = (\phi_{t+1}, \cdots, \phi_{t+n})\,, \quad \mathsf{M}^\top = (m_{t+1}, \cdots, m_{t+n})\,, \tag{8}$$

where $(\cdots)^\top$ denotes a transpose. The Bernoulli equation (4), rewritten as a first-order difference equation

$$\phi_t - s\phi_{t-1} = -m_t\,, \qquad \phi_t \in [0, 1)\,, \tag{9}$$

takes the matrix form

$$\mathcal{J}\,\Phi = -\mathsf{M}\,, \qquad \mathcal{J} = 1 - s\sigma^{-1}\,, \tag{10}$$

where the $[n \times n]$ matrix

$$\sigma_{jk} = \delta_{j+1,k}\,, \qquad \sigma = \begin{pmatrix} 0 & 1 & & & \\ & 0 & 1 & & \\ & & & \ddots & \\ & & & 0 & 1 \\ 1 & & & & 0 \end{pmatrix}\,, \tag{11}$$

implements the shift operation (6), a cyclic permutation that translates forward in time the lattice state Φ by one site, $(\sigma\Phi)^\top = (\phi_2, \phi_3, \cdots, \phi_n, \phi_1)$. The time evolution law (4) must be of the same form for all times, so the shift operator σ has to be time-translation invariant, with $\sigma_{n+1,n} = \sigma_{1n} = 1$ matrix element enforcing the periodicity. After n shifts, a lattice state returns to the initial state,

$$\sigma^n = 1\,. \tag{12}$$

As the temporal Bernoulli condition (10) is a linear relation, a given block M, or 'code' in terms of alphabet (5), corresponds to a unique temporal lattice state Φ. That is why Percival and Vivaldi [90] refer to such symbol block M as a *linear code*.

1.3. Orbit Jacobian matrix

The temporal lattice reformulation gives us deep insights into how to enumerate and determine all global solutions of such systems. The temporal Bernoulli condition (10) can be viewed as a search for zeros of the function

$$F[\Phi] = \mathcal{J}\Phi + \mathsf{M} = 0\,, \tag{13}$$

with the entire periodic *lattice state* Φ_{M} treated as a single fixed *point* $(\phi_1, \phi_2, \cdots, \phi_n)$ in the n-dimensional state space unit hyper-cube $\Phi \in [0,1)^n$, where the $[n\times n]$ matrix $\mathcal{J}$ is given by (10).

The $F[\Phi] = 0$ fixed point condition (13) is central to the theory of global methods for finding periodic orbits. Instead of requiring forward-in-time numerical integrations, in multi-shooting searches for periodic orbits one discretizes a periodic orbit into n segments [21, 32, 36–38, 50, 68], and lists a point for each segment

$$\Phi^{\top} = (\phi_1, \phi_2, \cdots, \phi_n)\,. \tag{14}$$

Starting with an initial guess for Φ, the zero of function (13) is then found by Newton iteration, which requires an evaluation of the $[n\times n]$ *orbit Jacobian matrix*

$$\mathcal{J}_{ij} = \frac{\delta F[\Phi]_i}{\delta \phi_j}\,. \tag{15}$$

For the particularly simple, linear case at hand, the orbit Jacobian matrix (10) is the same for all lattice states of period n.

1.4. Fundamental fact

The orbit Jacobian matrix $\mathcal{J}$ stretches the state space unit hyper-cube $\Phi \in [0,1)^n$ into the n-dimensional *fundamental parallelepiped*, and maps each periodic point Φ_{M} into an integer lattice $\mathbb{Z}^n$ site, which is then translated by the winding numbers M into the origin, in order to satisfy the fixed point condition (13). Hence N_n, the total number of the solutions of the fixed point condition equals the number of integer lattice points within the fundamental parallelepiped, a number given by what Baake *et al* [9] call the 'fundamental fact',

$$N_n = |\mathrm{Det}\,\mathcal{J}|\,, \tag{16}$$

i.e., fact that the number of integer points in the fundamental parallelepiped is equal to its volume, or, what we refer to as the 'Hill determinant' below. In two dimensions this formula is known since 1899 as Pick's theorem, in higher dimensions it was given by Nielsen [16, 87] in 1920, and rederived several times since in different contexts, for example by Baake *et al* [9]. For the task at hand, Barvinok [10] lectures offer a clear and simple introduction to integer lattices, and a proof of (16).

The action of orbit Jacobian matrix $\mathcal{J}$ for the period-2 lattice states (periodic points) of the Bernoulli map of figure 1 (a), suffices to convey the idea. In this case, the

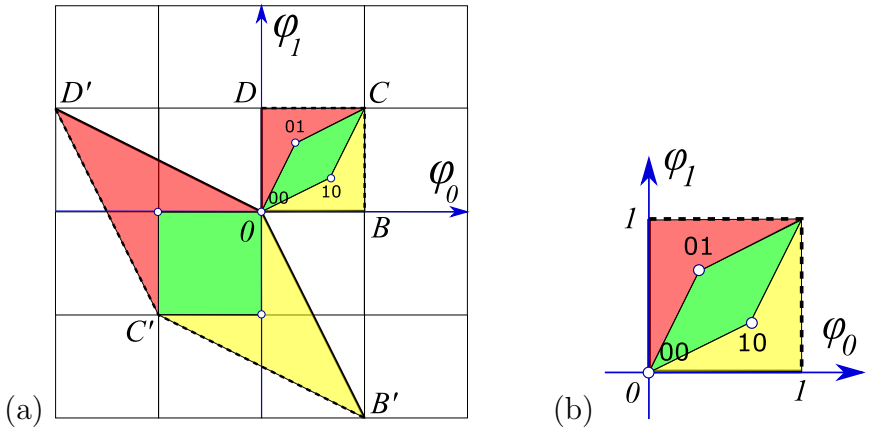

Figure 2. (a) The Bernoulli map (1) periodic points $\Phi_{\mathsf{M}} = (\phi_0, \phi_1)$ of period 2 are the $\overline{0} = (0, 0)$ fixed point, and the 2-cycle $\Phi_{01} = (1/3, 2/3)$, see figure 1 (a). They all lie within the unit square $[0BCD]$, which is mapped by the orbit Jacobian matrix $\mathcal{J}$ (17) into the fundamental parallelepiped $[0B'C'D']$. Periodic points Φ_{M} are mapped by $\mathcal{J}$ onto the integer lattice, $\mathcal{J}\Phi_{\mathsf{M}} \in \mathbb{Z}^n$, and are sent back into the origin by integer translations M, in order to satisfy the fixed point condition (13). Note that this fundamental parallelepiped is covered by 3 unit area quadrilaterals, hence $|\det \mathcal{J}| = 3$. (b) Conversely, in the flow conservation sum rule (27) sum over all lattice states M of period n, the inverse of the Hill determinant defines the 'neighborhood' of a lattices state as the corresponding fraction of the unit hypercube volume.

$[2\times 2]$ orbit Jacobian matrix (10), the unit square basis vectors, and their images are

$$\mathcal{J} = \begin{pmatrix} 1 & -2 \\ -2 & 1 \end{pmatrix}$$

$$\Phi^{(B)} = \begin{pmatrix} 1 \\ 0 \end{pmatrix} \ \to \ \Phi^{(B')} = \mathcal{J}\,\Phi^{(B)} = \begin{pmatrix} 1 \\ -2 \end{pmatrix}, \quad \cdots$$

i.e., the columns of the orbit Jacobian matrix are the edges of the fundamental parallelepiped,

$$\mathcal{J} = \left(\Phi^{(B')}\Phi^{(D')}\right), \tag{17}$$

see figure 2 (a), and $N_2 = |\det \mathcal{J}| = 3$, in agreement with the periodic orbit count (7).

In general, the unit vectors of the state space unit hyper-cube $\Phi \in [0, 1)^n$ point along the n axes; orbit Jacobian matrix $\mathcal{J}$ maps them into a fundamental parallelepiped basis vectors $\Phi^{(j)}$, each one given by a column of the $[n\times n]$ matrix

$$\mathcal{J} = \left(\Phi^{(1)}\Phi^{(2)}\cdots\Phi^{(n)}\right). \tag{18}$$

The Hill determinant is then

$$\det \mathcal{J} = \det\left(\Phi^{(1)}\Phi^{(2)}\cdots\Phi^{(n)}\right), \tag{19}$$

the volume of the fundamental parallelepiped whose edges are basis vectors $\Phi^{(j)}$. Note that the unit hypercubes and fundamental parallelepipeds are half-open, as indicated by dashed lines in figure 2 (a), so that their translates form a partition of the extended

state space (2). For further examples of fundamental parallelepipeds, see figure 3 and (117).

Note that in the temporal lattice reformulation, the Bernoulli system exhibits two unrelated lattices:

(i) In the latticization of a time continuum, one replaces *any* dynamical system's time-dependent field $\phi(t) \in \mathbb{R}$ at time $t \in \mathbb{R}$ by a discrete set of its values $\phi_t = \phi(t\Delta T)$ at time instants $t \in \mathbb{Z}$. Here the index t is a *coordinate* over which the field ϕ is defined.

(ii) Specific to the Bernoulli system is the fact that the *state* ϕ_t (3) is confined to the unit interval $[0, 1)$, imparting integer lattice structure onto the intermediate calculational steps in the extended state space (2) on which the orbit Jacobian matrix $\mathcal{J}$ (10) acts.

1.5. Counting temporal Bernoulli lattice states

To evaluate the Hill determinant (16), observe that from (10) it follows that

$$\det(-\mathcal{J}) = \det(s/\sigma)\det(1-\sigma/s)\,,$$

where $|\det(s/\sigma)| = s^n$. Expand $\ln\det(1-\sigma/s) = \operatorname{Tr}\ln(1-\sigma/s)$ as a series in $1/s$,

$$\operatorname{Tr}\ln\left(1-\frac{\sigma}{s}\right) = -\sum_{k=1}^{\infty}\frac{1}{k}\frac{\operatorname{Tr}(\sigma^k)}{s^k}\,. \tag{20}$$

It follows from $\sigma^n = \mathbb{1}$ that $\operatorname{Tr}\sigma^k = n\delta_{k,rn}$ is non-vanishing if k is a multiple of n, 0 otherwise:

$$\ln\det(1-\sigma/s) = -\sum_{r=1}^{\infty}\frac{1}{r}\frac{1}{s^{nr}} = \ln(1-s^{-n})\,.$$

So for the temporal Bernoulli the volume is

$$N_n = |\det\mathcal{J}(s)| = s^n - 1\,, \tag{21}$$

in agreement with the time-evolution count (7); all itineraries are allowed, except that the periodicity of $\sigma^n = \mathbb{1}$ accounts for $\overline{0}$ and $\overline{s-1}$ fixed points (see figure 1) being a single periodic point.

1.6. Stability of an orbit vs. its time-evolution stability

The orbit Jacobian matrix $\mathcal{J}_{ij}$ (15) is a high–dimensional linear stability matrix for a *zero* of function $F[\Phi_{\mathsf{M}}] = 0$, evaluated on the lattice state Φ_{M}. How is the stability so computed related to the conventional dynamical systems, forward-in-time stability? To motivate the answer, consider a temporal lattice with a set of d fields $\phi_t = \{\phi_{t,1}, \phi_{t,2}, \ldots, \phi_{t,d}\}$ on each lattice site t, and time evolution given by a d–dimensional map $\phi_{t+1} = f(\phi_t)$. The 1-time step $[d\times d]$ Jacobian matrix of this dynamical system is

$$J(\phi_t)_{ij} = \left.\frac{\partial f(\phi)_i}{\partial\phi_j}\right|_{\phi_i=\phi_{t,i}}\,. \tag{22}$$

Bernoulli systems stretch uniformly, so for the example at hand it suffices to consider the case of a Jacobian matrix not depending on the field value ϕ_t or time t, $J(\phi_t) = J$. For a n-periodic lattice state Φ_{M}, the orbit Jacobian matrix (15) is now a $[nd \times nd]$ matrix function of the $[d \times d]$ block matrix J,

$$\mathcal{J}(J) \;=\; \begin{pmatrix} \mathbf{1} & & & & -J \\ -J & \mathbf{1} & & & \\ & -J & \ddots & & \\ & & & \mathbf{1} & \\ & & & -J & \mathbf{1} \end{pmatrix} , \tag{23}$$

where $\mathbf{1}$ is a d–dimensional identity matrix.

The evaluation of the Hill determinant of this orbit Jacobian matrix proceeds as in the Bernoulli case, the only difference being that the Bernoulli Hill determinant is replaced by a function of a matrix, $\mathrm{Det}\,\mathcal{J}(s) \to \mathrm{Det}\,\mathcal{J}(J)$, resulting in (21) being replaced by $|\mathrm{Det}\,\mathcal{J}(J)| = |\det(1 - J_{\mathsf{M}})|$. (Were the 1-step Jacobian matrix J_t varying with time t, by chain rule the period-n Jacobian matrix would be of form $J_{\mathsf{M}} = \prod_{t=1}^{n} J_t$). The orbit Jacobian matrix evaluated on a lattice state Φ_{M}, and the dynamical, forward in time Jacobian matrix are related by *Hill's formula*

$$|\mathrm{Det}\,\mathcal{J}_{\mathsf{M}}| = |\det(1 - J_{\mathsf{M}})| \,, \tag{24}$$

of which (21) is the simplest example. We work that out in detail in section 5.3.

1.7. Periodic orbit theory

How come that a 'Det' in (16) counts lattice states?

For a general, nonlinear fixed point condition $F[\Phi] = 0$, expansion (20) in terms of traces is a cycle expansion [8, 24, 30], with support on *periodic orbits*. Ozorio de Almeida and Hannay [4] were the first to relate the number of periodic points to a Jacobian matrix generated volume; in 1984 they used such relation as an illustration of their 'principle of uniformity': "periodic points of an ergodic system, counted with their natural weighting, are uniformly dense in phase space." In periodic orbit theory [24, 28] this principle is stated as a flow conservation sum rule, a sum over all lattice states M of period n,

$$\sum_{|\mathsf{M}|=n} \frac{1}{|\det(1 - J_{\mathsf{M}})|} \;= 1 \,, \tag{25}$$

or, by Hill's formula (24),

$$\sum_{|\mathsf{M}|=n} \frac{1}{|\mathrm{Det}\,\mathcal{J}_{\mathsf{M}}|} \;= 1 \,. \tag{26}$$

For the Bernoulli system the 'natural weighting' takes a particularly simple form, as the Hill determinant of the orbit Jacobian matrix is the same for all periodic points of

period n, $\mathrm{Det}\,\mathcal{J}_{\mathsf{M}} = \mathrm{Det}\,\mathcal{J}$, whose number is thus given by (16). For example, the sum over the $n = 2$ lattice states is,

$$\frac{1}{|\mathrm{Det}\,\mathcal{J}_{00}|} + \frac{1}{|\mathrm{Det}\,\mathcal{J}_{01}|} + \frac{1}{|\mathrm{Det}\,\mathcal{J}_{10}|} = 1\,, \tag{27}$$

see figure 2 (b). Furthermore, for any piece-wise linear system all curvature corrections [27] for orbits of periods $k > n$ vanish, leading to explicit lattice state-counting formulas of kind reported in this paper.

1.8. Shadowing

As the temporal Bernoulli condition (10) is a linear relation, a given block M, or 'code' in terms of alphabet (5), corresponds to a unique temporal lattice state Φ given by the temporal lattice Green's function

$$\Phi_{\mathsf{M}} = \mathsf{g}\,\mathsf{M}\,, \qquad \mathsf{g} = \frac{\sigma/s}{1-\sigma/s}\,. \tag{28}$$

For an infinite lattice $t \in \mathbb{Z}$, this Green's function can be expanded as a series in Λ^{-k},

$$\mathsf{g} = \frac{\sigma/\Lambda}{1-\sigma/\Lambda} = \sum_{k=1}^{\infty} \frac{\sigma^k}{\Lambda^k}\,, \tag{29}$$

where $\Lambda = s$ is the 1-time step stability multiplier for the Bernoulli system. From (28) it follows that the influence of a source $m_{t'}$ back in the past, at site t', falls off exponentially with the temporal lattice distance $t - t'$,

$$\phi_t = \sum_{t'=-\infty}^{t-1} g_{tt'} m_{t'}\,, \quad g_{tt'} = \frac{1}{\Lambda^{t-t'}}\,, \quad t > t'\,, \quad 0 \text{ otherwise}\,. \tag{30}$$

That means that an ergodic lattice state segment of length n (or a periodic lattice state of a longer period) is shadowed by the periodic lattice state (8) with the same n-sites symbol block M,

$$\phi_t = \frac{1}{1-1/\Lambda^n}\left(\frac{m_1}{\Lambda} + \frac{m_2}{\Lambda^2} + \cdots + \frac{m_{n-1}}{\Lambda^{n-1}} + \frac{m_n}{\Lambda^n}\right), \tag{31}$$

with exponentially decreasing shadowing error of order $O(1/\Lambda^{n+1})$. The error is controlled by the (24) prefactor $1/|\mathrm{Det}\,\mathcal{J}| = 1/|\det(1 - J_{\mathsf{M}})|$, with the determinant arising from inverting the orbit Jacobian matrix $\mathcal{J}$ to obtain the Green's function (10).

This error estimate is deeper than what it might seem at the first glance. In fluid dynamics, pattern recognition, neuroscience and other high or ∞-dimensional settings distances between 'close solutions' (let's say pixel images of two faces in a face recognition code) are almost always measured using some arbitrary yardstick, let's say a Euclidean L_2 norm, even though the state space that has no Euclidean symmetry. Not so in the periodic orbit theory: here $1/|\mathrm{Det}\,\mathcal{J}|$ is the *intrinsic, coordinatization and norm independent* measure of the distance between similar spatiotemporal states.

1.9. Topological zeta function

Now that we have the numbers of lattice states N_n for any period n, we can combine them all into a single generating function by substituting N_n into the *topological* or *Artin-Mazur* zeta function [7, 27],

$$1/\zeta_{\rm top}(z) = \exp\left(-\sum_{n=1}^{\infty}\frac{z^n}{n}N_n\right)\,, \tag{32}$$

which, when expanded as a Taylor series in z, is built from *primitive* (or *prime*), i.e., non-repeating lattice states [24]. Conversely, given the topological zeta function, the number of periodic points of period n is given by the logarithmic derivative of the topological zeta function (see ChaosBook [27])

$$\sum_{n=1} N_n z^n \;=\; -\;\frac{1}{1/\zeta_{\rm top}}\,z\frac{d}{dz}(1/\zeta_{\rm top})\,. \tag{33}$$

For a Bernoulli system (21),

$$\begin{aligned} 1/\zeta_{\rm top}(z) \;&=\; \exp\left(-\sum_{n=1}^{\infty}\frac{z^n}{n}(s^n-1)\right) \;=\; \exp\left[\ln(1-sz)-\ln(1-z)\right] \\ &= \frac{1-sz}{1-z}\,. \end{aligned} \tag{34}$$

The numerator $(1-sz)$ says that a Bernoulli system is a full shift [27]: there are s fundamental lattice states, in this case fixed points $\{\phi_0,\phi_1,\cdots,\phi_{s-1}\}$, and every other lattice state is built from their concatenations and repeats. The denominator $(1-z)$ compensates for the single overcounted lattice state, the fixed point $\phi_{s-1}=\phi_0 \pmod 1$ of figure 1 and its repeats.

1.10. Counting temporal Bernoulli prime periodic orbits

Substituting the Bernoulli map topological zeta function (34) into (33) we obtain

$$\begin{aligned} \sum_{n=1} N_n z^n = {}& z+3z^2+7z^3+15z^4+31z^5+63z^6+127z^7 \\ &+255z^8+511z^9+1023z^{10}+2047z^{11}\cdots\,, \end{aligned} \tag{35}$$

in agreement with the lattice states count (21). The number of *prime* cycles of period n is given recursively by subtracting repeats of shorter prime cycles [27],

$$M_n \;=\; \frac{1}{n}\left(N_n-\sum_{d|n}^{d<n} dM_d\right)\,, \tag{36}$$

where d's are all divisors of n, hence

$$\begin{aligned} \sum_{n=1} M_n z^n = {}& z+z^2+2z^3+3z^4+6z^5+9z^6+18z^7 \\ &+30z^8+56z^9+99z^{10}+186z^{11}\cdots\,, \end{aligned} \tag{37}$$

in agreement with the usual numbers of binary symbolic dynamics prime cycles [27].

1.11. Bernoulli as a continuous time dynamical system

The discrete time derivative of a lattice state Φ evaluated at the lattice site t is given by the *difference operator* [44]

$$\dot{\Phi}_t = \left[\frac{\partial \Phi}{\partial t}\right]_t = \frac{\phi_t - \phi_{t-1}}{\Delta t} \tag{38}$$

The temporal Bernoulli condition (9) can be thus viewed as a time-discretized, first-order ODE dynamical system

$$\dot{\Phi} \;=\; v(\Phi)\,, \tag{39}$$

where the 'velocity' vector field v is given by

$$v(\Phi) \;=\; (s-1)\,\sigma^{-1}\,\Phi - \mathsf{M}\,,$$

with the time increment set to $\Delta t = 1$, and perturbations that decay (or grow) with rate $(s-1)$. By inspection of figure 1 (a), it is clear that for *shrinking*, $s < 1$ parameter values the orbit is stable forward in time, with a single linear branch, 1-letter alphabet $\mathcal{A} = \{0\}$, and the only periodic lattice states being the single fixed point $\phi_0 = 0$, and its repeats $\Phi = (0, 0, \cdots, 0)$. However, for *stretching*, $s > 1$ parameter values Bernoulli systems that we study here, every periodic lattice state Φ_{M} is unstable, and there is a periodic orbit solution for each symbol block M.

As far as the time-evolution stability is concerned, the $|\mathrm{Det}\,\mathcal{J}_{\mathsf{M}}| = |\det(1 - J_{\mathsf{M}})|$ formula (24) is correct for all first-order difference equations (systems whose evolution laws are first order in time), for any $[d \times d]$ one-time-step Jacobian matrix. For the Bernoulli system that is a $[1 \times 1]$ matrix $J = s$, with the periodic points count (21) trivially verified.

The orbit Jacobian matrix $\mathcal{J} = \partial/\partial t - (s-1)\,\sigma^{-1}$ is a differential operator whose determinant one usually computes by a Fourier transform diagonalization (see Appendix A). The Fourier discretization approach goes all the way back to Hill's 1886 paper [56]; in the limit of $n \to \infty$ multi-shooting steps (14), this is a remarkable formula, relating a field-theoretic, ∞-dimensional *functional* Hill determinant $\mathrm{Det}\,\mathcal{J}_{\mathsf{M}}$ to a determinant of the finite, $[d \times d]$ matrix J_{M}, and it took Poincaré [95] to prove that Hill's Fourier modes calculation is correct in the continuum limit. Historically, in periodic orbit theory calculations one always computes J_{M}. However, as we shall show here, and in more generality in section 5, it is the Hill determinant $\mathrm{Det}\,\mathcal{J}$ that is the computationally robust quantity that one should evaluate.

A fair coin toss, summarized. We refer to the *global* temporal lattice condition (10) as the '*temporal* Bernoulli', in order to distinguish it from the one-time step Bernoulli evolution *map* (3), in preparation for the study of *spatiotemporal* systems to be undertaken in section 3. In the lattice formulation, a *global* temporally periodic lattice state Φ_{M} is determined by the requirement that the *local* temporal lattice condition (9) is satisfied at every lattice site. For temporal Bernoulli there is no need for forward-in-time searches for the returning periodic points. Instead, one determines each global

temporally periodic lattice state Φ_{M} at one go, by solving the fixed point condition (13), and one determines the total number of lattice states by computing the Hill determinant (16) of the *orbit Jacobian matrix*. The most importantly for what follows, this calculation requires no recourse to any *explicit coordinatization of system's state space* (as, for example, the Adler-Weiss partition of figure C1 below), and *no explicit symbolic dynamics*. This is the 'periodic orbit theory'. And if you don't know, now you know.

The observation that a Bernoulli system can be viewed as a discretization of a first-order in time ODE, eq. (39), with solutions whose temporal global linear stability is described by the orbit Jacobian matrix $\mathcal{J}_{ij} = \delta F[\Phi]_i/\delta\phi_j$, has profound implications for dissipative spatiotemporal systems such as Navier-Stokes and Kuramoto-Sivashinsky [51]. However, the goal here is to formulate a classical spatiotemporally chaotic field theory, Hamiltonian and energy conserving, because (a) that is physics, and (b) cannot do quantum theory without it. We need a system as simple as the Bernoulli map, but mechanical. So, we move on from running in circles, to a mechanical rotor to kick.

2. A kicked rotor

The 1-degree of freedom maps that describe kicked rotors subject to discrete time sequences of angle-dependent impulses $P(q_t)$, $t \in \mathbb{Z}$,

$$q_{t+1} - q_t = p_{t+1} \qquad (\text{mod } 1), \tag{40}$$

$$p_{t+1} - p_t = P(q_t)\,, \tag{41}$$

with $2\pi q$ the angle of the rotor, p the momentum conjugate to the angular coordinate q, and the angular pulse $P(q) = P(q+1)$ periodic with period 1, play a key role in the theory of classical and quantum chaos in atomic physics, from the Taylor, Chirikov and Greene standard map [20, 74], to the cat maps discussed below. The equations are of the canonical Hamiltonian form: (40) is $\dot{q} = p/m$ in terms of discrete time derivative (38), i.e., the configuration trajectory starting at q_t reaches $q_{t+1} = q_t + p_{t+1}\Delta t/m$ in one time step Δt, and (41) is the time-discretized $\dot{p} = -\partial V(q)/\partial q$: at each kick the angular momentum p_t is accelerated to p_{t+1} by the force pulse $P(q_t)\Delta t$, with the time step set to $\Delta t = 1$, and the rotor mass m set to 1.

For an atomic physics kicked rotor, the values of the angle q differing by integers are identified, but the momentum p is unbounded. As for the Bernoulli map (2), one compactifies the momentum by adding (mod 1) to (41). This reduces the phase space to a square $[0,1) \times [0,1)$ of unit area, with the opposite edges identified.

2.1. Cat map

The simplest kicked rotor is subject to a force is proportional to displacement, that is, Hooke's law force $P(q) = Kq$ linear in the angular displacement q. The (mod 1) added

to (41) makes the map a discontinuous 'sawtooth,' unless K is an integer. In the integer K case, the map (40,41) is of form

$$\begin{pmatrix} q_{t+1} \\ p_{t+1} \end{pmatrix} = J \begin{pmatrix} q_t \\ p_t \end{pmatrix} \pmod 1 , \qquad J = \begin{pmatrix} a & c \\ d & b \end{pmatrix} , \tag{42}$$

where a, b, c, d are integers whose precise values do not matter, as long as $\det J = 1$, i.e., the map is area-preserving. The map is then a Continuous Automorphism of the Torus, or a *'cat map'*, a linear area-preserving map on the unit 2-torus phase space, with the field at the temporal lattice site t, $\phi_t = (q_t, p_t) \in (0, 1] \times (0, 1]$ interpreted as the angular position and its conjugate momentum at time instant t.

We consider the case of stability multipliers $(\Lambda\,,\ \Lambda^{-1})$ real, with a positive Lyapunov exponent $\lambda > 0$,

$$\Lambda = e^{\lambda} = (s + \sqrt{(s-2)(s+2)})/2 , \qquad s = \mathrm{tr}\, J = \Lambda + \Lambda^{-1} . \tag{43}$$

The eigenvalues are functions of the single stretching parameter s, and for $|s| > 2$ the cat map (42) is a fully chaotic Hamiltonian dynamical system. Cat maps with the same s are equivalent up to a similarity transformation, so it suffices to work out a single convenient realization, as we shall do here for the Percival-Vivaldi example (45).

Cat maps are beloved by ergodicists and statistical mechanicians because, even though the field (q_t, p_t) is 2-dimensional, for integer values of the stretching parameter s, a cat map has a finite alphabet linear code, just like the Bernoulli map, and its unit torus can be tiled by two rectangles (see figure C1 (a)), in analogy with the forward-in-time Bernoulli map subinterval partitioning of figure 1. From this it follows that all admissible symbol blocks can be generated as shifts of finite type, and all periodic points determined and counted.

As all that is well known, and a side issue for this paper, we relegate the details of the Hamiltonian cat map dynamics and periodic orbit counting to Appendix C. Here we focus on reformulating the cat dynamics as a temporal lattice (or discrete Lagrangian) problem, as we have done for the Bernoulli system in section 1.2.

2.2. Temporal cat

To motivate our formulation of a spatiotemporal chaotic field theory to be developed in section 3, we again recast the local initial value, time-evolution cat *map* (42) as a global *temporal lattice* condition that we shall refer to as the *temporal cat*.

The discrete time Hamilton's equations (40,41) induce forward-in-time evolution on a 2-torus (q_t, p_t) *phase space*. For the problem at hand, it pays to go from the Hamiltonian (configuration, momentum) phase space formulation to the discrete Lagrangian (ϕ_{t-1}, ϕ_t) formulation. If the momentum is replaced by the discrete time velocity,

$$(q_t, p_t) \to \left(\phi_t, \frac{\phi_t - \phi_{t-1}}{\Delta t} \right) , \tag{44}$$

and the time step set to $\Delta t = 1$, a cat map can be brought to the Percival-Vivaldi 'two-configuration representation' [90]

$$\begin{pmatrix} \phi_t \\ \phi_{t+1} \end{pmatrix} = J_{PV} \begin{pmatrix} \phi_{t-1} \\ \phi_t \end{pmatrix} - \begin{pmatrix} 0 \\ m_t \end{pmatrix} , \qquad J_{PV} = \begin{pmatrix} 0 & 1 \\ -1 & s \end{pmatrix} , \tag{45}$$

with matrix J_{PV} acting on the 2-dimensional space of successive configuration points $(\phi_{t-1}, \phi_t)^\top$. As was case for the Bernoulli map (9), the cat map (mod 1) condition (42) is enforced by integers $m_t \in \mathcal{A}$, where for a given integer stretching parameter s the alphabet $\mathcal{A}$ ranges over $|\mathcal{A}| = s+1$ possible values for m_t,

$$\mathcal{A} = \{\underline{1}, 0, \ldots s-1\} , \tag{46}$$

necessary to keep ϕ_t for all times t within the unit interval $[0, 1)$. We find it convenient to have symbol $\underline{m_t}$ denote m_t with the negative sign, i.e., '$\underline{1}$' stands for symbol '-1'. As for the Bernoulli system, m_t can be interpreted as 'winding numbers' [66], or, as they shepherd stray points back into the unit torus, as 'stabilising impulses' [90]. Here we shall refer to them as a 'code', or, in the field-theoretical parlance, as 'sources'.

Written out as a second-order difference equation, the Percival-Vivaldi map (45) takes a particularly elegant, *temporal cat* form

$$\phi_{t+1} - s\,\phi_t + \phi_{t-1} = -m_t , \tag{47}$$

or, in terms of a lattice state Φ, the corresponding symbol block M (8), and the $[n \times n]$ shift operator σ (11),

$$(\sigma - s1 + \sigma^{-1})\,\Phi = -\mathsf{M} , \tag{48}$$

very much like the temporal Bernoulli condition (10). 'Temporal' again refers to the global lattice state (field) Φ, and the winding numbers (sources) M taking their values on the lattice sites of a 1-dimensional *temporal* lattice $t \in \mathbb{Z}$.

For a finite lattice segment Φ, one needs to specify the boundary conditions (bc's). The companion article [52] tackles the Dirichlet bc's, a difficult, time-translation symmetry breaking, and from the periodic orbit theory perspective, a wholly unnecessary, self-inflicted pain. All that one needs to solve the temporal cat is the n-periodic, time-translation invariant bc's used here.

2.3. Orbit Jacobian matrix

Again, the temporal lattice reformulation gives us a different perspective into how to enumerate and determine global solutions of such systems. The temporal cat condition (48) can be viewed as a search for zeros (13) of the function

$$F[\Phi] = \mathcal{J}\Phi + \mathsf{M} = 0 , \tag{49}$$

with the entire periodic *lattice state* Φ_{M} treated as a single fixed *point* $(\phi_1, \phi_2, \cdots, \phi_n)$ in the n-dimensional phase space unit hyper-cube $\Phi \in [0, 1)^n$, where the $[n \times n]$ orbit Jacobian matrix $\mathcal{J}$ is now given by

$$\mathcal{J} = \sigma - s1 + \sigma^{-1} \tag{50}$$

a tri-diagonal Toeplitz matrix (constant along each diagonal, $\mathcal{J}_{k\ell} = j_{k-\ell}$) of circulant form,

$$\mathcal{J} = \begin{pmatrix} -s & 1 & 0 & 0 & \dots & 0 & 1 \\ 1 & -s & 1 & 0 & \dots & 0 & 0 \\ 0 & 1 & -s & 1 & \dots & 0 & 0 \\ \vdots & \vdots & \vdots & \vdots & \ddots & \vdots & \vdots \\ 0 & 0 & \dots & \dots & \dots & -s & 1 \\ 1 & 0 & \dots & \dots & \dots & 1 & -s \end{pmatrix} . \tag{51}$$

2.4. Integer lattices

As in section 1.4, the fundamental parallelepiped given the stretching of the n-dimensional phase space unit hyper-cube $\Phi \in [0,1)^n$ by the orbit Jacobian matrix counts periodic lattice states, with the admissible lattice states of period n constrained to field values within $0 \leq \phi_t < 1$. The fundamental parallelepiped contains images of all periodic lattice states Φ_{M}, which are then translated by integer winding numbers M into the origin, in order to satisfy the fixed point condition (49). The total number of periodic lattice states is again, as for the Bernoulli system (16), given by the 'fundamental fact'

$$N_n = |\mathrm{Det}\, \mathcal{J}| \,. \tag{52}$$

Period-1, or fixed point lattice states are easy to count: the orbit Jacobian matrix is a 1-dimensional matrix, so it follows from (47) that

$$N_1 = s - 2 \,, \tag{53}$$

The action of the temporal cat orbit Jacobian matrix is harder to visualize than the 2-dimensional fundamental parallelepiped of forward-in-time cat map of Appendix C.2: a period-2 solution temporal cat is a 2-torus, period-3 solution a 3-torus, etc.. Still, the fundamental parallelepiped for the period-2 and period-3 lattice states, figure 3, should suffice to convey the idea. The fundamental parallelepiped basis vectors (18) are the columns of $\mathcal{J}$. The [2×2] orbit Jacobian matrix (51) and its Hill determinant are

$$\mathcal{J} = \begin{pmatrix} -s & 2 \\ 2 & -s \end{pmatrix} , \qquad N_2 = \mathrm{Det}\, \mathcal{J} = (s-2)(s+2) \,, \tag{54}$$

(compare with the lattice states count (69)), with the resulting fundamental parallelepiped shown in figure 3 (a). The period-3 lattice states for $s = 3$ are contained in the half-open fundamental parallelepiped of figure 3 (b), defined by the columns of [3×3] orbit Jacobian matrix

$$\mathcal{J} = \begin{pmatrix} -s & 1 & 1 \\ 1 & -s & 1 \\ 1 & 1 & -s \end{pmatrix} , \qquad N_3 = |\mathrm{Det}\, \mathcal{J}| = (s-2)(s+1)^2 \,, \tag{55}$$

again in agreement with the periodic orbit count (69).

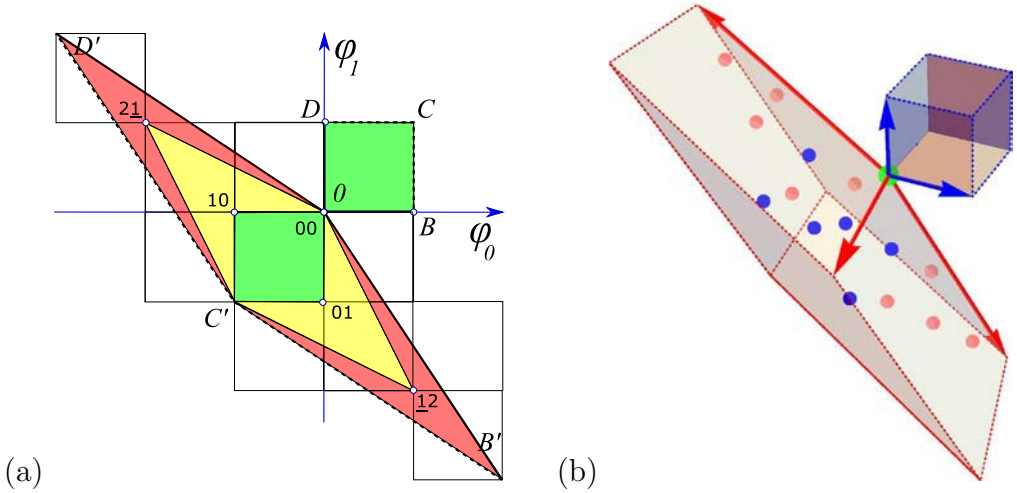

Figure 3. (a) For $s = 3$, the temporal cat (48) has 5 period-2 lattice states $\Phi_{\mathsf{M}} = (\phi_0, \phi_1)$: Φ_{00} fixed point and 2-cycles $\{\Phi_{01}, \Phi_{10}\}$, $\{\Phi_{\underline{1}2}, \Phi_{2\underline{1}}\}$. They lie within the unit square $[0BCD]$, and are mapped by the $[2\times 2]$ orbit Jacobian matrix $\mathcal{J}$ (54) into the fundamental parallelepiped $[0B'C'D']$, as in, for example, Bernoulli figure 2. The images of periodic points Φ_{M} land on the integer lattice, and are sent back into the origin by integer translations $\mathsf{M} = m_0 m_1$, in order to satisfy the fixed point condition $\mathcal{J}\Phi_{\mathsf{M}} + \mathsf{M} = 0$. (b) A 3-dimensional [blue basis vectors] unit-cube stretched by $\mathcal{J}$ (55) into the [red basis vectors] fundamental parallelepiped. For $s = 3$, the temporal cat (48) has 16 period-3 lattice states: a Φ_{000} fixed point at the vertex at the origin, [pink dots] 3 period-3 orbits on the faces of the fundamental parallelepiped, and [blue dots] 2 period-3 orbits in its interior. An n-dimensional phase space unit hyper-cube $\Phi \in [0,1)^n$ and the corresponding fundamental parallelepiped are half-open, as indicated by dashed lines, so the integer lattice points on the far corners, edges and faces do not belong to it.

The 16 period-3 lattice states $\Phi_{\mathsf{M}} = (\phi_0, \phi_1, \phi_3)$ are the Φ_{000} fixed point at the vertex at the origin, 3 period-3 orbits on the faces of the fundamental parallelepiped, and 2 period-3 orbits in its interior, all five of form $\{\Phi_{m_0 m_1 m_2}, \Phi_{m_1 m_2 m_0} \Phi_{m_2 m_0 m_1}\}$.

Note that in the temporal lattice reformulation, the temporal cat happens to involve two unrelated lattices:

(i) In the latticization of a time continuum, one replaces a time-dependent field $\phi(t)$ at time $t \in \mathbb{R}$ of *any* dynamical system by a discrete set of its values $\phi_t = \phi(t\Delta T)$, $t \in \mathbb{Z}$. Here the index 't' is a *coordinate* over which the field ϕ lives.

(ii) A peculiarity of the temporal cat is that the *field* ϕ_t (45) is confined to the unit interval $[0, 1)$, imparting a $\mathbb{Z}^1$ lattice structure onto the calculationally intermediate fundamental parallelepiped $\mathcal{J}$ basis vectors (18).

2.5. Counting temporal cat lattice states (unwritten)

We now count the number of periodic lattice states (67) in the temporal cat (or, 'discrete Lagrangian') formulation (for counting using the Hamiltonian formulation, see Appendix C.2).

[...] one can write the Hill determinant compactly as

$$N_n = |\det(\mathcal{J})| = 2\,T_n(s/2) - 2\,, \tag{56}$$

where $T_n(s/2)$ is the Chebyshev polynomial of the first kind.

2.6. Counting temporal cat lattice states (experimental)

The temporal cat equation (47) is a linear 2nd-order inhomogeneous difference equation (a 3-term recurrence relation) with constant coefficients that can be solved by standard methods [44] that parallel the theory of linear differential equations. Inserting a solution of form $\phi_t = \Lambda^t$ into the associated (m_t=0) homogenous 2nd-order difference equation

$$\phi_{t+1} - s\,\phi_t + \phi_{t-1} = 0 \tag{57}$$

yields the characteristic equation

$$\Lambda^2 - s\Lambda + 1 = 0\,, \tag{58}$$

which, for $|s| > 2$, has two real roots $\{\Lambda\,,\ \Lambda^{-1}\}$,

$$\Lambda = \frac{1}{2}(s + \sqrt{(s-2)(s+2)})\,, \tag{59}$$

and the so-called *complementary* solution of form

$$\phi_{c,t} = a_1\Lambda^t + a_{-1}\Lambda^{-t}\,. \tag{60}$$

A difference of any pair of solutions to the temporal cat inhomogenous equation (47) is a solution of the homogenous difference equation (57), so the general solution is a sum of the complementary solution (60) and a *particular* solution ϕ_p,

$$\phi_t = \phi_{c,t} + \phi_{p,t}\,. \tag{61}$$

Eq. (57) is time-reversal invariant, $\phi_t = \phi_{-t}$, so $a_1 = a_{-1} = a$. To determine the particular solution, assume that both the source $m_t = m$ and $\phi_{p,t} = \phi_p$ in (47) are site-independent,

$$\phi_p - s\,\phi_p + \phi_p = -m\,, \tag{62}$$

so $\phi_p = m/(s-2)$. Hence the solution is

$$\phi_t = \phi_{c,t} + \phi_{p,t} = a\left(\Lambda^t + \Lambda^{-t}\right) + m/(s-2)\,, \tag{63}$$

with a_i determined by fields at two lattice sites,

$$\phi_0 = 2a + m/(s-2)\,, \quad \phi_1 = a\left(\Lambda + \Lambda^{-1}\right) + m/(s-2)\,, \quad .$$

Temporal cat starts with $N_0 = 0$, and according to (53), $N_1 = s - 2$, so $a = 1$, $m = -2(s-2)$, and the number of temporal lattice states of period n is

$$N_n = \Lambda^n + \Lambda^{-n} - 2\,. \tag{64}$$

2.7. Shadowing

As the relation between the symbol blocks M and the corresponding lattice states Φ_{M} is linear, for M an admissible symbol block, the corresponding lattice state Φ_{M} is given by the Green's function

$$\Phi_{\mathsf{M}} = \mathsf{g}\,\mathsf{M}\,, \qquad \mathsf{g} = \frac{1}{-\sigma + s\mathbf{1} - \sigma^{-1}}\,, \tag{65}$$

as in the Bernoulli case (28).

As in section 1.8, the Green's function (65) decays exponentially with the distance from the origin, a fact that is essential in establishing the 'shadowing' between lattice states sharing a common sub-block M. For an infinite temporal lattice $t \in \mathbb{Z}$, the lattice field at site t is determined by the sources $m_{t'}$ at all sites t', by the Green's function $g_{tt'}$ for one-dimensional discretized heat equation [81, 90],

$$\phi_t = \sum_{t'=-\infty}^{\infty} g_{tt'} m_{t'}\,, \qquad g_{tt'} = \frac{1}{\Lambda - \Lambda^{-1}}\,\frac{1}{\Lambda^{|t-t'|}}\,, \tag{66}$$

with Λ is the expanding stability multiplier defined in (43).

Suppose there is a non-vanishing point source $m_0 \neq 0$ only at the present, $t' = 0$ temporal lattice site. Its contribution to $\phi_t \sim \Lambda^{-|t|}$ decays exponentially with the distance from the origin. More generally, as in the Bernoulli case (31), if two lattice states Φ, Φ' share a common sub-block M of length n, they shadow each other with accuracy of order of $O(1/\Lambda^n)$.

2.8. Topological zeta function

The number of lattice states of period n is given by the area of the fundamental parallelepiped (52) (Hill's formula)

$$N_n = |\mathrm{Det}\,\mathcal{J}| = |\det(J^n - \mathbf{1})| = \Lambda^n + \Lambda^{-n} - 2\,, \tag{67}$$

where the Λ is the stability multiplier (43) of the one-time-step evolution matrix J (42).

Substituting the numbers of lattice states N_n into the *topological zeta function* (32) we obtain

$$\begin{aligned} 1/\zeta_{\mathrm{top}}(z) &= \exp\left(-\sum_{n=1}^{\infty}\frac{z^n}{n}N_n\right) = \exp\left(-\sum_{n=1}^{\infty}\frac{z^n}{n}(\Lambda^n + \Lambda^{-n} - 2)\right) \\ &= \exp\left[\ln(1-z\Lambda) + \ln(1-z\Lambda^{-1}) - 2\ln(1-z)\right] \\ &= \frac{(1-z\Lambda)(1-z\Lambda^{-1})}{(1-z)^2} = \frac{1-sz+z^2}{(1-z)^2}\,, \end{aligned} \tag{68}$$

in agreement with Isola [59], as well as the Adler-Weiss generating partition topological zeta function (C.4). Topological zeta functions count *prime orbits*, i.e., time invariant *sets* of equivalent lattice states related by translations (cyclic permutations), and other symmetries [27].

Conversely, given the topological zeta function, the generating function for the number of temporal lattice states of period n is given by the logarithmic derivative of the topological zeta function (33),

$$\begin{aligned}\sum_{n=0}^{\infty} N_n z^n &= \frac{2-sz}{1-sz+z^2} - \frac{2}{1-z} \\ &= (s-2)\left[z + (s+2)z^2 + (s+1)^2 z^3 \right. \\ &\qquad \left. + (s+2)\, s^2 z^4 + (s^2+s-1)^2 z^5 + \cdots\right] , \end{aligned} \tag{69}$$

which is indeed the generating function for $T_n(s/2)$, the Chebyshev polynomial of the first kind of (56).

2.9. Temporal cat as a continuous time dynamical system

Recall how the Bernoulli first-order difference equation could be viewed as a time-discretization of the first-order linear ODE (39). The second-order difference equation (47) can be interpreted as the second order discrete time derivative d^2/dt^2, or the temporal lattice Laplacian,

$$\Box\, \phi_t \equiv \phi_{t+1} - 2\phi_t + \phi_{t-1} = (s-2)\phi_t - m_t\,, \tag{70}$$

with the time step set to $\Delta t = 1$. But that is nothing but Newton's Second Law: "acceleration equals force," so Percival and Vivaldi [90] refer to this formulation as 'Newtonian', while Allroth [3], Mackay, Meiss, Percival, Kook & Dullin [42, 67, 77, 78, 80], and Li and Tomsovic [72] refer to it as the 'Lagrangian' formulation.

In other words, for a cat map the force pulse $P(q) = (s-2)\, q$ in (41) is linear in the angular displacement q, so the temporal lattice equation takes form

$$(-\Box + (s-2)1)\, \Phi = \mathsf{M}\,. \tag{71}$$

For small stretching parameter values, $s < 2$, this equation describes a set of coupled penduli, with oscillatory solutions, known as the discrete Helmholtz equation or the tight-binding model, with Hamiltonian [43]

$$H = \sum_{\ell} |\ell\rangle \epsilon_0 \langle \ell| + \sum_{\ell m} |\ell\rangle V_{\ell m} \langle m|\,, \quad V_{\ell m} = \begin{cases} V & \text{if } \ell, m \text{ nearest neighbors} \\ 0 & \text{otherwise} \end{cases}$$

corresponding to the stretching factor $s = -\epsilon_0/V$ in eq. (71).

Here we study the strong stretching, $s > 2$ case, known as the discrete *screened Poisson equation* (hyperbolic, damped solutions) [39, 45, 99]. We refer to eq. (71) as the '*temporal cat*', both to distinguish it from the forward-in-time Hamiltonian cat *map* (42), and in the anticipation of the spatiotemporal cat of section 3.

Temporal cat, summarized. In the spatiotemporal formulation a *global* temporal lattice state

$$\Phi^{\top} = (\phi_t, \phi_{t+1}, \cdots, \phi_{t+k}) \tag{72}$$

is not determined by a forward-in-time 'cat map' evolution (42), but rather by the fixed point requirement (49) that the *local*, 3-term discrete temporal lattice condition (47) is satisfied at every lattice point. The Lagrangian formulation requires only temporal lattice states and their actions, replacing the phase space 'cat map' (42) by a 'temporal cat' lattice (71). The temporal cat has no generating partition analogue of the Adler-Weiss partition for a Hamiltonian cat map (see section Appendix C.1).

As we have shown here, no funky Hamiltonian phase space partitioning magic (such as figure C1) is needed to count the periodic lattice states of a temporal cat. Not only are no such partitions needed to solve the system, but the Lagrangian, temporal 1-dimensional lattice formulation is the bridge that takes us from the single cat map (42) to the higher–dimensional coupled infinity "multi-cat" spatiotemporal lattices (80).

And did you know that the cute Arnold cat is but the screened Poisson equation in disguise?

3. Spatiotemporal cat

The *temporal cat* of section 2 is a 1-dimensional example of the simplest spatiotemporally chaotic, or 'turbulent' field theory, the *spatiotemporal cat* to which we turn now. Spatiotemporal cat lives on a d-dimensional discretized spacetime, a spatiotemporal $\mathbb{Z}^d$ integer lattice, with a cat map (a 'rotor') on each site, coupled to its nearest neighbors. Another way of visualizing a spatiotemporal cat is as a lattice of locally hyperbolic 'anti' oscillators, as opposed to the classical free field theory, with an oscillator at each site ('Gaussian model' [46, 61]).

The temporal cat lives on a 1-dimensional temporal integer lattice $\mathbb{Z}$, with very simple 'tilings'. For every integer temporal period T, we first determine N_T, the number of all periodic *lattice state* Φ_{M} solutions on a tile of length T. However, if $T = mT_p$, the T-tile can be tiled by m repeats of a smaller T_p-tile, so some of T-periodic orbit solutions are repeats of the already determined shorter T_p *prime* solution Φ_p. Furthermore, due to the time invariance of the defining equations, there are T_p physically equivalent copies of a given solution in the time orbit of every Φ_p. So all we really have to do is to enumerate M_T *prime orbits* of the time-invariance equivalent periodic orbit solutions, whose generating function is the analytically elegant topological zeta function.

For the d-dimensional spatiotemporal cat the repertoire of periodic tilings is richer. In $d = 2$ and 3 the basic facts are well known both from crystallography, and from the number theory of integer lattices. In this paper we systematically construct and enumerate distinct $d = 2$ tilings, or Bravais lattices $[L \times T]_S$, of increasing spacetime periodicities, and determine $N_{[L\times T]_S}$, the number of *doubly periodic lattice state* solutions, by evaluating the associated Hill determinants. For $d = 2$ and higher-dimensional lattices counting the spatiotemporal 'prime' tilings requires some thought. We determine $M_{[L\times T]_S}$, the numbers of doubly-periodic prime orbits, invariant under spacetime translations. We, however, fail to find an analytic form for the associated doubly-periodic topological zeta function.

We start by a brief review of physical origin of coupled map lattices (CMLs) models. The impatient reader should proceed directly to the spatiotemporal cat, introduced in section 3.3, and solved in section 3.8.

3.1. Coupled map lattices

In order to solve a partial differential equation (PDE) on a computer, one represents it by a finite number of computational elements. The simplest discretization of a scalar spacetime field $\phi(\vec{q},\tau)$ is by specifying its values $\phi_{n_1 n_2 \cdots n_{d-1} t} = \phi(q_n, \tau_t)$ on lattice points $(\vec{n}, t) \in \mathbb{Z}^d$. Once spatial and temporal derivatives are replaced by their discretizations, the PDE is reduced to dynamics of a coupled map lattice, a spatially extended system with discrete time, discrete space, and a set of continuous fields on each site. For many PDEs, CML conceptual advantage is not only numerical, but also that the technical problems such as existence and uniqueness of the field theory are regularized away, and the essence of spatiotemporal chaos is revealed in a transparent form.

Often one starts out by coupling neighbors harmonically, and thinks of this starting, free field theory formulation as a spring mattress [108] to which weakly coupled nonlinear terms are then added. Similarly, the conventional CML models, mostly motivated by discretizations of dissipative PDEs, start out with chaotic on-site dynamics weakly coupled to neighboring sites, with a strong space-time asymmetry. An example are the diffusive coupled map lattices introduced by Kaneko [62, 63], with time evolution given by

$$\begin{aligned} \phi_{n,t+1} &= (1+\epsilon\,\Box) g(\phi_{nt}) \\ &= g(\phi_{nt}) + \epsilon[g(\phi_{n-1,t}) - 2g(\phi_{nt}) + g(\phi_{n+1,t})]\,, \end{aligned} \tag{73}$$

where the individual spatial site's dynamical system $g(x)$ is a 1-dimensional map, such as the logistic map, coupled to its nearest neighbors by $\Box$, the spatial version of the Laplacian (70) for the discretized second order *spatial* derivative d^2/dx^2 (we always set the lattice spacing constant equal to unity).

The form of time-step map $g(\phi_{nt})$ is the same for all times, i.e., the law of temporal evolution is invariant under the group of discrete *time translations*. Spatially homogenous lattice models also invariant under discrete *space translations* were studied by Bunimovich and Sinai [17] in the case when $g(\phi_{nt})$ is a one-dimensional expanding map.

The observation that for spatiotemporally chaotic systems space and time should be considered on the same footing goes back to the 'chronotopic' program of Politi and collaborators [47, 70, 71, 98] who, in their studies of propagation of spatiotemporal disturbances in extended systems, discovered that the spatial stability analysis can be combined with the temporal stability analysis, with orbit weights depending exponentially both on the space and the time variables, $t_p \propto e^{-LT\lambda_p}$. Politi and Torcini [96] study of periodic orbits of *spatiotemporal Hénon*, a (1+1)-spacetime lattice of Hénon maps with solutions periodic both in space and time is the closest to the present investigation. They explain why the dependence of the lattice field at time ϕ_{t+1} on the

two previous time steps prevents an interpretation of dynamics as the composition of a local chaotic evolution with a diffusion process (73). In the CML tradition, they study the weak coupling regime $\epsilon \approx 0$, but note that the $b = -1$ case could be an interesting example of a nonlinear Hamiltonian lattice field theory.

3.2. Hamiltonian coupled map lattices

For quantum mechanics and statistical mechanics applications, one needs the dynamics to be Hamiltonian, motivating models such as coupled standard map lattice [64] and ϕ^4 lattice [57]. Lattice recurrence relations [84] of the type studied below arise in the Frenkel-Kontorova lattice, Hamiltonian lattice models for ferromagnetism, many-body quantum chaos [53–55, 85, 102], and in discretizations of elliptic PDEs.

Pesin and Sinai [92] were the first to study such lattices, with chains of coupled Anosov maps. In order to establish rigorously the desired statistical properties of coupled map lattices, such as the continuity of their SRB measures, they, and most of the subsequent statistical mechanics literature, relied on the structural stability of Anosov automorphisms under small perturbations. For such lattices the neighboring sites have to be coupled sufficiently weakly (small ϵ in (73)) so that the site cat maps could be conjugated to a lattice of uncoupled Anosov automorphisms, with a finite Markov partition, the key ingredient required for the proofs.

This exploration, as well as the companion paper [52] for Dirichlet bc's, starts with the study of a coupled L-body Hamiltonian system undertaken by Gutkin and Osipov [55]. If the reader wants to quantize an L-body Hamiltonian system, Gutkin and Osipov article covers the formalism in depth, so we do not review the Hamiltonian formulation here.

3.3. Spatiotemporal cat

In their paper, Gutkin and Osipov also note that if the single 'body' dynamics is described by a cat map coupled to its nearest spatial neighbors, and if the spatial coupling strength is taken to be the same as temporal coupling strength, one obtains a spatiotemporally symmetric 5-term recurrence relation

$$\phi_{n,t+1} + \phi_{n,t-1} - 2s\,\phi_{nt} + \phi_{n+1,t} + \phi_{n-1,t} = -m_{nt}\,, \tag{74}$$

that adds one spatial lattice direction to the temporal cat 3-term recurrence relation (47). As these equations are symmetric under interchange of the 'space' and the 'time' directions, their temporal and spatial dynamics are strongly coupled, corresponding to $\epsilon \approx O(1)$ in (73), in contrast to the traditional spatially weakly coupled CML [17].

Now that we have mastered the *temporal cat* (47), a generalization to the *spatiotemporal cat* (74) is immediate. Consider a 1-dimensional spatial lattice, with field ϕ_{nt} (the angle of a kicked rotor (40) at instant t) at spatiotemporal site $z = (n, t) \in \mathbb{Z}^2$. If each site couples only to its nearest spatial neighbors $\phi_{n\pm1,t}$, and if we require (1) invariance under spatial translations, (2) invariance under spatial reflections, and (3)

invariance under the space-time exchange, we arrive at the 2-dimensional Euclidean lattice difference equations (74).

Gutkin and Osipov –for reasons that make sense in context of L-body quantum systems– call this recurrence relation a 'non-perturbed coupled cat map'. A well-established name [39, 45] for this system is the 'discrete screened Poisson equation'. We, however, find a '*spatiotemporal cat*' more descriptive for our field-theoretic purposes. While the generalization of (74) to d-dimensional hypercubic $\mathbb{Z}^d$ lattice is immediate, it suffices to work out the $d = 2$ spatiotemporal cat in some detail to develop intuition about the general case.

The spatiotemporal cat equation (74) can be written compactly as

$$\mathcal{J}\,\Phi = -\mathsf{M}\,, \qquad \mathcal{J} = \sigma_1 + \sigma_2 - 2s1 + \sigma_2^{-1} + \sigma_1^{-1}\,, \tag{75}$$

where σ_1, σ_2 are shift operators (11) which translate the field by one lattice spacing in the spatial, temporal direction, respectively. The inverses σ_i^{-1} translate the field in the opposite directions. The block $\mathsf{M} = \{m_{nt}\}$ is composed of symbols from alphabet

$$m_{nt} \in \mathcal{A}\,, \qquad \mathcal{A} = \{\underline{3}, \underline{2}, \underline{1}, 0, \cdots, 2s-2, 2s-1\}\,, \tag{76}$$

where symbol $\underline{m}_{nt}$ denotes m_{nt} with the negative sign, i.e., '$\underline{3}$' stands for symbol '-3'. In our explicit computational examples, we shall always set s to

$$s = 5/2 \quad \Rightarrow \quad \mathcal{A} = \{\underline{3}, \underline{2}, \underline{1}, 0, 1, 2, 3, 4\}\,, \tag{77}$$

the smallest value of the 'stretching' parameter s for which the orbit Jacobian matrix $\mathcal{J}$ is an integer-valued matrix, and the system is hyperbolic.

As for the temporal Bernoulli (10) and the temporal cat (49), one can view the spatiotemporal cat condition (75) as a zero of the function

$$F[\Phi] = \mathcal{J}\Phi + \mathsf{M} = 0\,, \tag{78}$$

with the entire periodic lattice state $\Phi_{\mathsf{M}} = \{\phi_z\}$ treated as a single fixed point within the $(\ell_1\ell_2\cdots\ell_d)$-dimensional state space unit hyper-cube $\Phi \in [0,1)^{\ell_1\ell_2\cdots\ell_d}$, where ℓ_j is the lattice period in direction j, and the $(\ell_1\ell_2\cdots\ell_d)^2$-dimensional orbit Jacobian matrix $\mathcal{J}_{zz'}$ is given by

$$\mathcal{J} = \sum_{j=1}^{d} \left(\sigma_j - s1 + \sigma_j^{-1}\right)\,. \tag{79}$$

Here σ_i is a shift operator (11) which translates the field in the ith direction by one lattice spacing. Its inverse σ_i^{-1} translates the field in the negative ith direction.

In multi-index, or 'tensorial' notation, the spatiotemporal cat equation (75) can be written as

$$\begin{aligned}
(\mathcal{J}\phi)_z \;&=\; \sum_{z'}\sum_{i=1}^{d} \left(\sigma_i - s1 + \sigma_i^{-1}\right)_{zz'} \phi_{z'} = -m_z\,, \quad m_z \in \mathcal{A}\,,\\
z \;&=\; (n_1, n_2, n_3, \cdots, n_d) \in \mathbb{Z}^d\\
\mathcal{A} \;&=\; \{-2d+1, -2d+2, \cdots, 2s-2, 2s-1\}\,,
\end{aligned} \tag{80}$$

with field ϕ_z and source m_z labelled by the d indices of lattice site z. Sources $m_z \in \mathcal{A}$ keep the field ('rotor angle' ϕ_z) within the unit interval on every site. The orbit Jacobian matrix $\mathcal{J}$, labelled by d pairs of indices, acts on the lattice state Φ by usual matrix multiplication. We illustrate how that works by working out in detail an example in Appendix A.4.3. As yet another notational choice, in (114) we recast the orbit Jacobian matrix (75) as a $[LT \times LT]$ Kronecker product block matrix.

In the lattice formulation, the spatiotemporal cat happens to involve two quite distinct lattices:

(i) In the latticization of a spacetime continuum, one replaces a time-dependent field $\phi(x,t)$ at spacetime point $(x,t) \in \mathbb{R}^d$ of *any* field theory by a discrete set of its values $\phi_z = \phi(n\Delta L, t\Delta T)$ on lattice sites, where the index $z \in \mathbb{Z}^d$ is a discrete d-dimensional spacetime *coordinate* over which the field ϕ lives. We describe the properties of this integer lattice $\mathbb{Z}^d$ and its sublattices in Sections 3.4 to 3.6.

(ii) A peculiarity of the spatiotemporal cat is that the *field* ϕ_z (74) is confined to the unit interval $[0,1)$, imparting a $\mathbb{Z}^1$ lattice structure –in any spacetime dimension d– onto the calculationally intermediate fundamental parallelepiped $\mathcal{J}$ basis vectors (see, for example, (117)). The lattice structure of periodic orbits Φ is discussed in Sections 3.7 to 5.

3.4. Symmetries of the integer lattice

The spatiotemporal cat equation (75) is *equi*variant under the discrete spacetime translations; the space σ_x and time σ_y reflections $n \to -n$, $t \to -t$; as well as under σ_a exchange $n \longleftrightarrow t$ of space and time. Spatiotemporal cat thus has the point-group symmetries of the square lattice: rotations by $\pi/2$, and reflection across x-axis, y-axis, and diagonals a and b,

$$C_{4v} = \mathrm{D}_4 = \{E, C_{4z}^+, C_{4z}^-, C_{2z}, \sigma_y, \sigma_x, \sigma_a, \sigma_b, \}\,. \tag{81}$$

In the international crystallographic notation, the square lattice space group of symmetries is referred to as $p4mm$ [40].

3.5. Bravais lattices

For the 1-dimensional temporal lattices considered so far, a sublattice is tiled by repeats of a block of temporal period T.

For a d-dimensional integer lattice $\mathbb{Z}^d$, a d-periodic sublattice that tiles the spacetime is called a *Bravais lattice*.

For a d-dimensional integer lattice $\mathbb{Z}^d$, the primitive unit cell of a d-dimensional Bravais lattice tiles the spacetime.

A 2-dimensional Bravais lattice $\mathcal{L}$ is an infinite array of points

$$\mathcal{L} = \{n_1\mathbf{a}_1 + n_2\mathbf{a}_2 \,|\, n_i \in \mathbb{Z}\}\,, \tag{82}$$

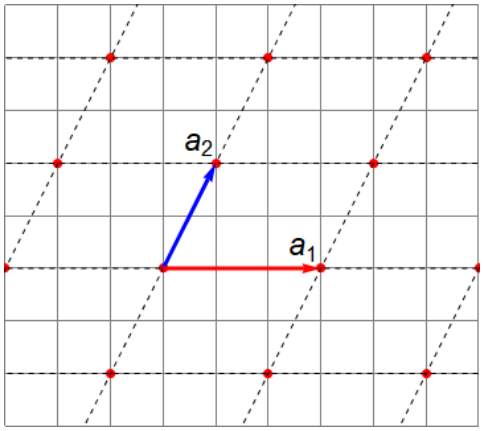

Figure 4. (Color online) The intersections of the (light grey) solid lines form the square lattice on which the discrete field ϕ_z is defined. The (red) basis vector $\mathbf{a}_1 = (3, 0)$ and the (blue) basis vector $\mathbf{a}_2 = (1, 2)$ form a $[L\times T]_S = [3\times 2]_1$ Bravais cell. The intersections (red points) of the black dashed lines form the Bravais lattice $\mathcal{L}$.

generated by the group of discrete translations $R = n_1\mathbf{a}_1 + n_2\mathbf{a}_2$, where $\{n_1, n_2\}$ are any integers, and $(\mathbf{a}_1, \mathbf{a}_2)$ is a pair of $\mathbb{Z}^2$ integer lattice vectors that span the Bravais lattice as a set of basis.

The primitive unit cell of a Bravais lattice can be chosen in different ways. In this paper we will always choose the primitive unit cell uniquely corresponding to the basis vectors:

$$C(\mathbf{a}_1, \mathbf{a}_2) = \{m_1\mathbf{a}_1 + m_2\mathbf{a}_2 \,|\, 0 \le m_i < 1\}\,, \tag{83}$$

and call $C(\mathbf{a}_1, \mathbf{a}_2)$ the *Bravais cell* of Bravais spanned by basis vectors $(\mathbf{a}_1, \mathbf{a}_2)$.

A given Bravais *lattice* $\mathcal{L}$ can be defined by any of the infinity of Bravais cells, each defined by a different pair of basis vectors $(\mathbf{a}_1, \mathbf{a}_2)$, but equivalent under unimodular, $\mathrm{SL}_2(\mathbb{Z})$ transformation [69]. Each such family contains a unique Bravais cell of the *Hermite normal form* [22], which, for a 2-dimensional square lattice, can be chosen to have the first basis vector pointing in the spatial direction [75]

$$\mathbf{a}_1 = \begin{pmatrix} L \\ 0 \end{pmatrix}\,, \qquad \mathbf{a}_2 = \begin{pmatrix} S \\ T \end{pmatrix}\,, \tag{84}$$

where L, T are respectively the spatial, temporal lattice periods, and the 'tilt' [88] $0 \le S < L$ imposes the relative-periodic 'shift' bc's [30] (in the integer lattices literature these are also referred to as *'helical'* [73] vs. *'toroidal'* [60]; *'twisted'* and *'twisting factor'* [73]; *'screw'* bc's). We label Bravais cell (84) and the corresponding Bravais lattice $\mathcal{L}$ by $[L\times T]_S$. An example is the $[3\times 2]_1$ Bravais lattice is shown in figure 4.

For each width L, height T, the number of (tilted) Hermite normal form Bravais cells is

$$\#_{[L\times T]} = \sum_{S=0}^{L-1} 1 = L\,, \tag{85}$$

and a Bravais lattices-counting zeta function (see Lind [75] Example 3.1) can by constructed by substituting $\#_{[L\times T]}$ into

$$1/\zeta(z) = \exp\left(-\sum_{L=1}^{\infty}\sum_{T=1}^{\infty}\#_{[L\times T]}\frac{z^{LT}}{LT}\right) = \exp\left(-\sum_{L=1}^{\infty}\sum_{T=1}^{\infty}\frac{(z^L)^T}{T}\right)$$
$$= \exp\left(\sum_{L=1}^{\infty}\ln(1-z^L)\right) = \prod_{L=1}^{\infty}(1-z^L)\,. \tag{86}$$

3.6. Prime Bravais lattices

It might be possible to tile a given Bravais lattice $\mathcal{L}$ by a finer lattice $\mathcal{L}_p$. Lattice $\mathcal{L}_p$, defined by a Bravais cell

$$\mathbf{a}_1^p = \begin{pmatrix} L_p \\ 0 \end{pmatrix}, \qquad \mathbf{a}_2^p = \begin{pmatrix} S_p \\ T_p \end{pmatrix}, \tag{87}$$

is a *prime* Bravais lattice, if there is no finer Bravais cell, other than the unit volume $[1\times 1]_0$ Bravais cell, that can tile it.

In order to determine all prime lattices $\mathcal{L}_p$ (87) that tile a given Bravais lattice $\mathcal{L}$ (84),

$$\mathbf{a}_1 = k\,\mathbf{a}_1^p + \ell\,\mathbf{a}_2^p$$
$$\mathbf{a}_2 = m\,\mathbf{a}_1^p + n\,\mathbf{a}_2^p\,,$$

observe that a prime tile $(\mathbf{a}_1^p, \mathbf{a}_2^p)$ tiles the larger tile only if larger tile's width L is a multiple of L_p, the height T is a multiple of T_p, and the two tile 'tilts' satisfy

$$\mathbf{a}_2 = m\,\mathbf{a}_1^p + \frac{T}{T_p}\mathbf{a}_2^p \quad \to \quad S = mL_p + \frac{T}{T_p}S_p\,.$$

Hence a prime lattice $\mathcal{L}_p$ tiles the given lattice $\mathcal{L}$ only if the area spanned by the two 'tilted' basis vectors

$$\mathbf{a}_2 \times \mathbf{a}_2^p = ST_p - TS_p \tag{88}$$

is a multiple of the prime tile area L_pT_p.

3.7. Lattice states

A *lattice state* is a set of all field values $\mathbf{\Phi} = \{\phi_z\}$ over the d-dimensional lattice $z \in \mathbb{Z}^d$ that satisfies the spatiotemporal cat equation (75), with all field values constrained to $0 \le \phi_z < 1$.

While the spatiotemporal cat equation (75) is *equivariant* under the integer lattice *space group* $p4mm$ symmetry operations (81), the individual lattice states either have no symmetry at all (they are, after all, 'turbulent'), or are invariant under subgroups of space group $p4mm$. In what follows we quotient only the translational symmetries, and postpone dazzling the captive reader with the full D_4 point group reduction to a later, more ponderous publication.

Furthermore, inspection of the temporal cat figure 3 suggests that there is a *field symmetry* under inversion though the center of the $0 \leq \phi_z < 1$ unit interval. Indeed, if $\mathsf{M} = \{m_{nt}\}$, composed of symbols from alphabet (76), corresponds to a 2-dimensional lattice state $\Phi_{\mathsf{M}} = \{\phi_{nt}\}$, its conjugation symmetry partner

$$\bar{\mathsf{M}} = \{\bar{m}_{nt}\}\,, \qquad \bar{m}_{nt} = 2(s-2) - m_{nt}\,, \tag{89}$$

corresponds to lattice state $\bar{\Phi}_{\bar{\mathsf{M}}} = \{1 - \phi_{nt}\}$. So, every lattice state either belongs to a conjugate pair $\{\Phi_{\mathsf{M}}, \bar{\Phi}_{\bar{\mathsf{M}}}\}$, or is self-dual under conjugation.

While the action of orbit Jacobian matrix $\mathcal{J}$ (80) maps fields ϕ_{nt} to values outside the unit interval, such values that are then returned back to the unit interval by integer m_{nt}. This '$\mathbb{Z}^1$ lattice action' at every spatiotemporal lattice site is a peculiarity of the coupled Bernoulli and cat map lattice models, not a condition that a spatiotemporal discretization of a generic field theory would satisfy, and should never be confused with a discretization of spacetime continuum to integer lattice $\mathbb{Z}^d$.

For brevity, we shall refer to lattice state Φ as a *periodic orbit* if it satisfies

$$\Phi(z + R) = \Phi(z) \tag{90}$$

for any discrete translation $R = n_1\mathbf{a}_1 + n_2\mathbf{a}_2 \in \mathcal{L}$, where $\{n_1, n_2\}$ are any integers, and $(\mathbf{a}_1, \mathbf{a}_2)$ is a pair of $\mathbb{Z}^2$ integer lattice vectors that define a *Bravais cell*. We shall always refer to a Bravais sublattice (sublattice of $\mathbb{Z}^2$) by its unique Hermite normal form Bravais cell (84) (basis?), and denote it $\mathcal{L} = [L \times T]_S$, a 2-dimensional doubly-periodic (relative) *periodic orbit*

$$\phi_{nt} = \phi_{n+L,t} = \phi_{n+S,t+T}\,, \qquad (n,t) \in \mathbb{Z}^2 \tag{91}$$

with periods (L, T) and tilt S.

A correct definition of a *prime* periodic orbit [29] is subtler than for the 1-dimensional temporal lattice case. If a given periodic orbit over lattice $\mathcal{L}$ is not periodic under translations $R \in \mathcal{L}_p$ on any sublattice $\mathcal{L}_p$ (except for $\mathcal{L}$ itself), we shall refer to it here as a *prime periodic orbit*, a periodic orbit of the smallest periodicity in all spacetime directions. We return to explicit construction of prime periodic orbits in section 4. Prime periodic orbits are the basic building blocks of topological zeta functions (see section 1.9 and 2.8).

Explicitly verifying the periodic lattice states counting formulas for several 2-dimensional spatiotemporal cat examples is now in order.

The simplest examples of periodic orbits are (i) spacetime equilibria over $[1 \times 1]_0$, (ii) space-equilibria over $[1 \times T]_0$, (iii) time-equilibria over $[L \times 1]_0$, and (iv) time-relative equilibria over $[L \times 1]_S$, $S \neq 0$, stationary patterns in a time-reference frame [96] moving with a constant velocity S/T.

3.7.1. Spacetime equilibria over $[1 \times 1]_0$.

3.7.2. Time-equilibria over $[L\times 1]_0$. Consider the time-equilibrium $\phi_{nt} = \phi_{n1}$ for all spatial sites n, and all times t. To see that this is the 1-dimensional lattice temporal cat tiles of period L already counted in section 2.5, note that the 5-term recurrence relation (74) reduces to the 3-term recurrence

$$\phi_{n+1,1} - 2(s_2 - 1)\,\phi_{n1} + \phi_{n-1,1} = -m_{n1}\,, \tag{92}$$

where we have temporarily added index '$_2$' to the stretching parameter s_2 to indicate that it refers to the 2-dimensional spatiotemporal cat. Comparing with the temporal cat (47), $\phi_{t+1} - s_1\,\phi_t + \phi_{t-1} = -m_t$, we see that we have already counted all lattice states on Bravais cells of form $[L\times 1]_0$, provided we replace $s_1 \to 2(s_2 - 1)$ in (69). For the values chosen in our numerical examples, $s_1 = 3$ and $s_2 = 5/2$, the two counts happen to be the same and given by (C.5).

However, already the smallest *relative*-periodic $[L\times 1]_S$ Bravais lattices are new, and perhaps surprising.

3.7.3. Relative $[2\times 1]_1$ *periodic orbit.* Consider a $[2\times 1]_1$ periodic orbit with tilt periodic bc's, periodic state $\Phi_{m_1m_2} = \begin{bmatrix} \phi_1 & \phi_2 \end{bmatrix}$, tiled by the Bravais lattice (82) with basis vectors $\mathbf{a}_1 = \{2, 0\}$ and $\mathbf{a}_2 = \{1, 1\}$, see figure 5 (a).

$$\Phi_{\underline{m}m} = \frac{1}{9}\begin{bmatrix} -m & m \end{bmatrix}\,, \qquad m \in \mathcal{A}\,, \tag{93}$$

for example

$$\mathsf{M} = \begin{bmatrix} -4 & 4 \end{bmatrix} \Rightarrow \quad \Phi_{\underline{44}} = \frac{1}{9}\begin{bmatrix} -4 & 4 \end{bmatrix}\,.$$

Note that these are 'periodic lattice state' solutions: there is one *prime* periodic orbit for each set of period-2 periodic lattice states related by cyclic permutations, $\overline{\underline{m}m} = (\Phi_{\underline{m}m}, \Phi_{m\underline{m}})$, and there are only 4 of those, as $\Phi_{00} = \Phi_0$ is a repeat of the 1-block.

By (A.36) the number of $[2\times 1]_1$ relative periodic orbits with the given Bravais lattice bc's is 9. Using the Green's function method (102) one can verify that there are indeed 9 such periodic orbits, one periodic orbit solution for each letter of alphabet (76),

3.7.4. $[2\times 1]_0$ *periodic orbit.* As an illustration of the fundamental parallelepiped (16) $s = 3$ cat map (45) acting on states ϕ_t within the unit square $(\phi_0, \phi_1) \in |0, 1)\times|0, 1)$. In 2 time steps orbit Jacobian matrix $\mathcal{J}$ unit square into the fundamental parallelepiped, with integer points within the fundamental parallelepiped corresponding to $N_2 = 5$ periodic lattice states (C.5) of period 2. These integer-valued vertices over-count the number distinct lattice states, as already noted in the construction of the topological zeta function (C.4).

But the great thing about the spatiotemporal cat is that it is a field theory defined on a lattice, a theory that can be solved by the well-developed crystallographic methods: here we follow the notation of Dresselhaus *et al* [40].

To determine the *admissible* blocks,

(7) compute Φ_p for each prime block M_p, and eliminate every Φ_p which contains a lattice site or sites on which the value of the field violates the admissibility condition $\phi_z \in [0,1)$.

For $s = 5/2$ spatiotemporal cat the pruning turns out to be very severe. Only 52 of the prime $[2\times 2]_0$ blocks are admissible. As for the repeats of smaller blocks, there are 2 admissible $[1\times 2]_0$ blocks repeating in time and 2 $[2\times 1]_0$ blocks repeating in space. There are 4 admissible 1/2-shift periodic boundary $[1\times 2]_0$ blocks. And there is 1 admissible block which is a repeat of letter 0. The total number of $[2\times 2]_0$ of periodic orbits is obtained by all cyclic permutations of admissible prime blocks,

$$\begin{aligned} N_{[2\times 2]_0} &= 225 \\ &= 52\,[2\times 2]_0 + 2\,[2\times 1]_0 + 2\,[1\times 2]_0 + 4\,[2\times 1]_1 + 1\,[1\times 1]_0\,, \end{aligned} \tag{94}$$

summarized in table 1. This explicit list of admissible prime periodic orbits verifies the counting formula (A.33).

3.7.5. $[3\times 2]_0$ *periodic orbit.* For $s = 5/2$ spatiotemporal cat only 850 prime $[3\times 2]_0$ blocks are admissible. There are 5 admissible repeating prime $[3\times 1]_0$ blocks, 2 admissible repeating prime $[1\times 2]_0$ blocks, and 1 admissible block which is a repeat of 0. The total number of admissible solutions obtained by all cyclic permutations of admissible prime blocks is:

$$N_{[3\times 2]_0} = 5120 = 850\,[3\times 2]_0 + 5\,[3\times 1]_0 + 2\,[1\times 2]_0 + 1\,[1\times 1]_0\,, \tag{95}$$

summarized in table 1. The count is in agreement with the counting formula (A.33) for the $[3\times 2]_0$ periodic orbits.

3.7.6. Relative $[3\times 2]_1$ *periodic orbit.* Consider the Bravais lattice of figure 4, tiled by periodic orbit defined by the Bravais cell with basis vectors $\mathbf{a}_1 = (3,0)$ and $\mathbf{a}_2 = (1,2)$, see figure 5 (b). There are 6 independent field values in the repeating cell, which can be written as an $[3\times 2]$ array:

$$[3\times 2]_1 = \begin{bmatrix} & \phi_{11} & \phi_{21} & \phi_{01} \\ \phi_{00} & \phi_{10} & \phi_{20} & \end{bmatrix}.$$

Example: $[2\times 2]_0$ *Bravais lattices prime blocks.*

Consider $[2\times 2]_0$ Bravais lattices prime block

$$\mathsf{M}_p = \begin{bmatrix} m_{01} & m_{11} \\ m_{00} & m_{10} \end{bmatrix}, \tag{96}$$

According to (106), the number of prime $[2\times 2]_0$ lattice states is

$$M_{[2\times 2]_0} = \frac{1}{2\cdot 2}\left(N_{[2\times 2]_0} - 2M_{[2\times 1]_0} - 2M_{[1\times 2]_0} - 2M_{[2\times 1]_1} - M_{[1\times 1]_0}\right), \tag{97}$$

We can work this out explicitly as follows:

(3) The $[2\times 1]_1$ relative-periodic block (98) is counted as the $[2\times 2]_0$ periodic orbit.

(5) Throw away all blocks which are repeats of shorter blocks. There are three kinds of repeating small blocks:

$$[2\times 1]_0 = \begin{bmatrix} a & b \\ a & b \end{bmatrix}, \quad [1\times 2]_0 = \begin{bmatrix} b & b \\ a & a \end{bmatrix}, \quad [2\times 1]_1 = \begin{bmatrix} & a & b \\ a & b & \end{bmatrix}.$$

the relative-periodic $[2\times 1]_1$ block with 1 site-shift periodic boundary, which is periodic after the second repeat in the time direction,

$$\mathsf{M}_p = \begin{bmatrix} & [m_{00} & m_{10}] \\ [m_{00} & m_{10}] & \end{bmatrix}. \tag{98}$$

Example: $[3\times 2]_0$ *Bravais lattices prime blocks.*

Consider the Bravais lattice

$$\mathsf{M} = \begin{bmatrix} m_{12} & m_{22} & m_{32} \\ m_{11} & m_{21} & m_{31} \end{bmatrix}. \tag{99}$$

According to (106), the number of prime $[3\times 2]_0$ lattice states is

$$M_{[3\times 2]_0} = \frac{1}{3\cdot 2}\left(N_{[3\times 2]_0} - 3M_{[3\times 1]_0} - 2M_{[1\times 2]_0} - M_{[1\times 1]_0}\right), \tag{100}$$

Unlike the $[2\times 2]_0$ case (98), there no sub-blocks with relative-periodic boundary contributing to the $[3\times 2]_0$ blocks count, since $[3\times 1]_0$ and $[1\times 2]_0$ sub-blocks cannot fit into the $[3\times 2]_0$ doubly-periodic Bravais lattice without a shift.

3.8. Counting spatiotemporal cat lattice states

We now show how to count the number of periodic lattice states of a 2-dimensional spatiotemporal cat, and apply the method to counting periodic orbits of the 2-dimensional spatiotemporal cat.

Periodic lattice Hill determinants, such as (16), are usually evaluated by a Fourier transform diagonalization (see Appendix A). However, due to the uniformity of Bernoulli map stretching, in case at hand lattice points counting is a combinatorial problem. Counting of $\mathbb{Z}^d$ integer lattice points within various convex domains is an important, highly developed field. For integer lattice counting powerful combinatorial methods are available, for example Barvinok multivariate generating functions algorithm for counting lattice points in convex lattice domains [11], and its online code implementations, such as the lattice point enumeration `LattE` code [34].

As in the temporal cat case (52), the total number of periodic lattice states is given by the volume of the fundamental parallelepiped

$$N_n = |\mathrm{Det}\,\mathcal{J}|\,. \tag{101}$$

3.9. Periodic orbit theory

3.10. Shadowing

As we now show, the block $\mathsf{M} = \{m_{nt} \in \mathcal{A}\,,\ (n,t) \in \mathbb{Z}^2\}$ can be used as a 2-dimensional symbolic representation of the lattice system state. By the linearity of equation (104), every solution Φ can be uniquely recovered from its symbolic representation M. Inverting (104) we obtain

$$\phi_z = \sum_{z' \in \mathbb{Z}^2} g_{zz'} m_{z'}, \qquad g_{zz'} = \left(\frac{1}{-\Box + 2(s-2)} \right)_{zz'}, \tag{102}$$

where $g_{zz'}$ is the Green's function for the 2-dimensional discretized screened Poisson equation. However, a given lattice block M is *admissible* if and only if all $\phi_z \in \Phi$ given by (102) fall into the interval $[0, 1)$.

For a given admissible source block M, the periodic field can be computed by:

$$\Phi_{i_1 j_1} = \sum_{i_2=0}^{2} \sum_{j_2=0}^{1} \mathsf{g}_{i_1 j_1, i_2 j_2} \mathsf{M}_{i_2 j_2}\,.$$

For example, if the source M is:

$$\mathsf{M} = \begin{bmatrix} 0 & 2 & 0 \\ -1 & 0 & 0 \end{bmatrix},$$

the corresponding field is:

$$\Phi_{\mathsf{M}} = \begin{bmatrix} \phi_{01} & \phi_{11} & \phi_{21} \\ \phi_{00} & \phi_{10} & \phi_{20} \end{bmatrix} = \frac{1}{35} \begin{bmatrix} 5 & 17 & 6 \\ -1 & 5 & 3 \end{bmatrix}.$$

Substitute this solution into figure 5 (b) we can see that (74) is satisfied everywhere.

3.11. Topological zeta function

3.12. Spatiotemporal cat as a continuous time dynamical system

$$(\Box - 2(s-2))\,\Phi = -\mathsf{M} \tag{103}$$

While the $d = 2$ spatiotemporal cat does have a Hamiltonian formulation [55], its Lagrangian formulation as screened Poisson equation (103), in analogy with the temporal cat (71), is a natural departure point for what follows:

$$(\Box - 2(s-2))\,\phi_{nt} = -m_{nt}\,, \qquad \phi_{nt} \in [0,1)\,, \quad m_{nt} \in \mathcal{A}\,, \quad (n,t) \in \mathbb{Z}^2 \tag{104}$$

where $\Box$ is now the discrete 2-dimensional space-time Laplacian on $\mathbb{Z}^2$,

$$\Box\,\phi_{nt} = \phi_{n,t-1} + \phi_{n-1,t} - 4\,\phi_{nt} + \phi_{n,t+1} + \phi_{n+1,t}\,, \tag{105}$$

and the alphabet is given in (76).

Spatiotemporal cat, summarized. The key insight [17, 55] –an insight that applies to coupled-map lattices [93, 94, 97], and field theories modeled by them, not only the

system considered here– is that a field $\Phi = \{\phi_z\}$ over a d-dimensional spacetime lattice $z \in \mathbb{Z}^d$ has to be described by a corresponding symbol block $\mathsf{M} = \{m_z\}$, over the same d-dimensional spacetime lattice $z \in \mathbb{Z}^d$, rather than a 1-dimensional temporal symbol sequence (**??**), as one does when describing a finite coupled "N-particle" system in the Hamiltonian formalism.

A key advantage of the spatiotemporal code M is illustrated already by the $d = 2$ case. While an Adler-Weiss type partition, forward-in time Hamiltonian evolution alphabet would grow exponentially with the "particle number" L, the number of letters (80) of the spatiotemporal code $\mathcal{A}$ is finite and the same for any spatial extent L, including the $L \to \infty$ spatiotemporal cat. For the spatiotemporal code, a field Φ over a periodic spatiotemporal domain is encoded by a doubly periodic 2-dimensional block M of symbols from a small alphabet, rather then by a 1-dimensional temporal string of symbols from the exponentially large (in L) 'L-particle' alphabet $\bar{\mathcal{A}}$.

The spatiotemporal cat is arguably the simplest example of a chaotic (or 'turbulent') classical field theory for which the local degrees of freedom are hyperbolic (anti-harmonic, 'inverted pendula') rather than oscillatory ('harmonic oscillators'). As we have shown here, it is also a field theory for which all admissible spatiotemporal patterns can be enumerated, and their recurrences (shadowing of a large periodic orbit by smaller periodic orbits) identified.

4. Enumeration of prime periodic orbits

Here we show how to enumerate the total numbers of distinct periodic states in terms of prime periodic orbits.

The enumeration of spatiotemporal cat doubly-periodic lattice states proceeds in 3 steps:

(i) Construct a hierarchy of 2-dimensional Bravais lattices Λ, starting with the smallest Bravais cells (84), list Bravais lattices by increasing $[L\times T]_S$, one per each set related by discrete symmetries (81).

(ii) For each $\Lambda = [L\times T]_S$ Bravais lattice, compute N_Λ, the number of doubly-periodic spatiotemporal cat lattice states, using the 'fundamental fact' $N_\Lambda = |\det \mathcal{J}(\Lambda)|$.

(iii) We have defined the *prime* Bravais lattice in section 3.6.

(iv) The total number of (doubly) periodic blocks is the sum of all cyclic permutations of prime blocks,

$$N_\Lambda = \sum_p N_p\, [L_p \times T_p]_{S_p}$$

where the sum goes over prime tilings of the $[L\times T]_S$ block.

The number of prime periodic orbits is given recursively by (see (36)),

$$M_p \;=\; \frac{1}{LT}\left(N_p - \sum_{p'} L_{p'} T_{p'}\, M_{p'}\right)\,, \tag{106}$$

Table 1. The numbers of the $s = 5/2$ spatiotemporal cat $[L\times T]_S$ periodic orbits: $M_{[L\times T]_S}$ is the number of prime periodic orbits, $N_{[L\times T]_S}$ is the number of doubly periodic lattice states, and $R_{[L\times T]_S}$ is the number of prime periodic orbits in the D_4 symmetries orbit.

$[L\times T]_S$	M	N	R
$[1\times 1]_0$	1	1	1
$[2\times 1]_0$	2	$5 = 2\,[2\times 1]_0 + 1\,[1\times 1]_0$	2
$[2\times 1]_1$	4	$9 = 4\,[2\times 1]_1 + 1\,[1\times 1]_0$	
$[3\times 1]_0$	5	$16 = 5\,[3\times 1]_0 + 1\,[1\times 1]_0$	
$[3\times 1]_1$	16	$49 = 16\,[3\times 1]_1 + 1\,[1\times 1]_0$	
$[4\times 1]_0$	10	$45 = 10\,[4\times 1]_0 + 2\,[2\times 1]_0 + 1\,[1\times 1]_0$	
$[4\times 1]_1$	54	$225 = 54\,[4\times 1]_1 + 4\,[2\times 1]_1 + 1\,[1\times 1]_0$	
$[4\times 1]_2$	60	$245 = 59\,[4\times 1]_2 + 2\,[2\times 1]_0 + 1\,[1\times 1]_0$	
$[2\times 2]_0$	52	$225 = 52\,[2\times 2]_0 + 2\,[2\times 1]_0 + 2\,[1\times 2]_0$	
		$+4\,[2\times 1]_1 + 1\,[1\times 1]_0$	1
$[2\times 2]_1$	60	$245 = 60\,[2\times 2]_1 + 2\,[1\times 2]_0 + 1\,[1\times 1]_0$	
$[3\times 2]_0$	850	$5\,120 = 850\,[3\times 2]_0 + 5\,[3\times 1]_0$	
		$+2\,[1\times 2]_0 + 1\,[1\times 1]_0$	
$[3\times 2]_1$	1 012	$6\,125 = 1\,012\,[3\times 2]_1 + 16\,[3\times 1]_2$	
		$+ 2\,[1\times 2]_0 + 1\,[1\times 1]_0$	
$[3\times 3]_0$	68 281	$614\,656 = 68\,281\,[3\times 3]_0 + 5\,[3\times 1]_0$	
		$+16\,[3\times 1]_1 + 16\,[3\times 1]_2 + 5\,[1\times 3]_0 + 1\,[1\times 1]_0$	1
$[3\times 3]_1$	70 400	$633\,616 = 70\,400\,[3\times 3]_1 + 5\,[1\times 3]_0 + 1\,[1\times 1]_0$	

where the sum is over p', the prime 'divisors' of p that satisfy tiling conditions (88).

The following expressions do not fit into table 2:

$$M_{[3\times 3]_0} = 2(s-2)\frac{1}{9}(256s^8 + 512s^7 - 128s^6 - 640s^5 + 16s^4 + 320s^3 - 48s^2 - 72s + 9)\,. \tag{107}$$

The last, currently unreduced formula exemplifies what is nonintuitive about the Fourier space results; it is not at all obvious that this

$$M_{[3\times 3]_1} = M_{[3\times 3]_2} = 2(s-2)\frac{1}{9}(1-2s)^2 \times \left\{\left[2s+1-2\sin\left(\frac{\pi}{18}\right)\right]^2\left[2s+1+2\cos\left(\frac{\pi}{9}\right)\right]^2 \left[(2s+1-2\cos\left(\frac{2\pi}{9}\right)\right]^2 - 1\right\} \tag{108}$$

is an integer for any half-integer or integer s. **Predrag** to Han: can you evaluate this using the fundamental fact $N_n = |\mathrm{Det}\,\mathcal{J}|$?

Note that $N_{[3\times T]_1}(s) = N_{[3\times T]_2}(s)$, by reflection symmetry, as $N_{[3\times T]_2}(s) = N_{[3\times T]_{-1}}(s)$.

$$\sum_{L=1} N_{[L\times 1]_0} z^L = \frac{s-2z}{1-sz+z^2} - \frac{2}{1-z}$$

Table 2. The numbers of spatiotemporal cat lattice states for Bravais lattices $\Lambda = [L\times T]_S$ up to $[3\times 3]_2$. Here $N_\Lambda(s)$ is the number of doubly periodic lattice states, $M_\Lambda(s)$ is the number of prime periodic orbits, and R_Λ is the number of prime periodic orbits in the D_4 symmetries orbit. The stretching parameter s can take half-integer or integer values.

Λ	$N_\Lambda(s)$	$M_\Lambda(s)$	R
$[1\times 1]_0$	$2(s-2)$	$2(s-2)$	1
$[2\times 1]_0$	$2(s-2)2s$	$2(s-2)\frac{1}{2}(2s-1)$	2
$[2\times 1]_1$	$2(s-2)2(s+2)$	$2(s-2)\frac{1}{2}(2s+3)$	
$[3\times 1]_0$	$2(s-2)(2s-1)^2$	$2(s-2)\frac{4}{3}(s-1)s$	
$[3\times 1]_1$	$2(s-2)4(s+1)^2$	$2(s-2)\frac{1}{3}(2s+1)(2s+3)$	
$[4\times 1]_0$	$2(s-2)8(s-1)^2s$	$2(s-2)\frac{1}{2}(2s-3)(2s-1)s$	
$[4\times 1]_1$	$2(s-2)8s^2(s+2)$	$2(s-2)\frac{1}{2}(s+2)(2s-1)(2s+1)$	
$[4\times 1]_2$	$2(s-2)8(s+1)^2s$	$2(s-2)\frac{1}{2}(2s+3)(2s+1)s$	
$[4\times 1]_3$	$2(s-2)8s^2(s+2)$	$2(s-2)\frac{1}{2}(s+2)(2s-1)(2s+1)$	
$[5\times 1]_0$	$2(s-2)\left(4s^2-6s+1\right)^2$	$2(s-2)\frac{4}{5}(s-1)(2s-3)(2s-1)s$	
$[5\times 1]_1$	$2(s-2)16\left(s^2+s-1\right)^2$	$2(s-2)\frac{1}{5}(2s-1)(2s+3)(4s^2+4s-5)$	
$[2\times 2]_0$	$2(s-2)8s^2(s+2)$	$2(s-2)\frac{1}{2}(2s-1)(2s^2+5s+1)$	1
$[2\times 2]_1$	$2(s-2)8s(s+1)^2$	$2(s-2)\frac{1}{2}(2s+1)(2s+3)s$	
$[3\times 2]_0$	$2(s-2)2s(2s-1)^2(2s+3)^2$	$2(s-2)\frac{2}{3}(2s-1)(4s^3+10s^2+3s-5)s$	
$[3\times 2]_1$	$2(s-2)32s^3(s+1)^2$	$2(s-2)\frac{1}{6}(2s-1)(2s+1)(8s^3+16s^2+10s+3)$	
$[3\times 3]_0$	$2(s-2)16(s+1)^4(2s-1)^4$		
$[3\times 3]_1$	$2(s-2)(2s-1)^2(8s^3+12s^2-1)^2$		

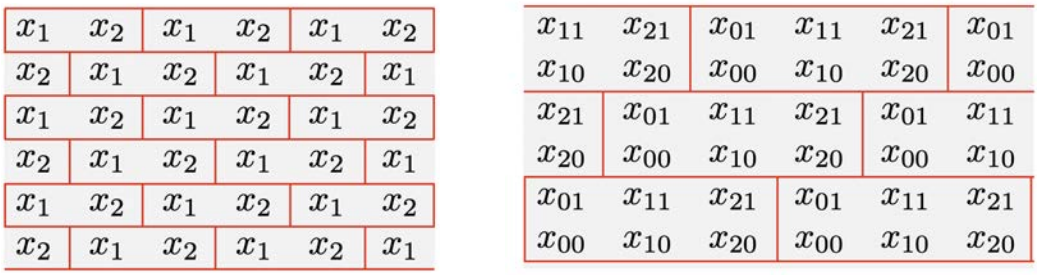

(a) (b)

Figure 5. Examples of $[L\times T]_S$ periodic orbits together with their spatiotemporal Bravais lattice tilings (82). (a) $[2\times 1]_1$, basis vectors $\mathbf{a}_1 = \{2, 0\}$ and $\mathbf{a}_2 = \{1, 1\}$; (b) $[3\times 2]_1$, basis vectors $\mathbf{a}_1 = (3, 0)$ and $\mathbf{a}_2 = (1, 2)$. Rectangles enclose the Bravais cell and its Bravais lattice translations.

$$
\begin{aligned}
&= (s-2) + (s-2)z + (s-2)(s+2)z^2 + (s-2)(s+1)^2z^3 \\
&\quad + (s-2)(s+2)\,s^2z^4 + (s-2)(s^2+s-1)^2z^5 \\
&\quad + \cdots ,
\end{aligned}
\tag{109}
$$

2020-06-09 Han Figures 6 and 7 are the plots of the periodic blocks by color. The

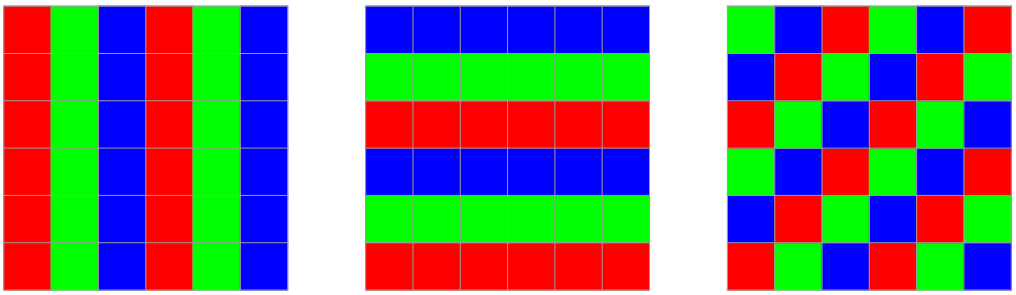

(a) (b) (c)

Figure 6. Examples of $[L\times T]_S$ periodic blocks together with their spatiotemporal Bravais lattice tilings (82). (a) $[3\times 1]_0$, basis vectors $\mathbf{a}_1 = \{3, 0\}$ and $\mathbf{a}_2 = \{0, 1\}$; (b) $[1\times 3]_0$, basis vectors $\mathbf{a}_1 = \{1, 0\}$ and $\mathbf{a}_2 = \{0, 3\}$; (c) $[3\times 1]_1$, basis vectors $\mathbf{a}_1 = \{3, 0\}$ and $\mathbf{a}_2 = \{1, 1\}$;

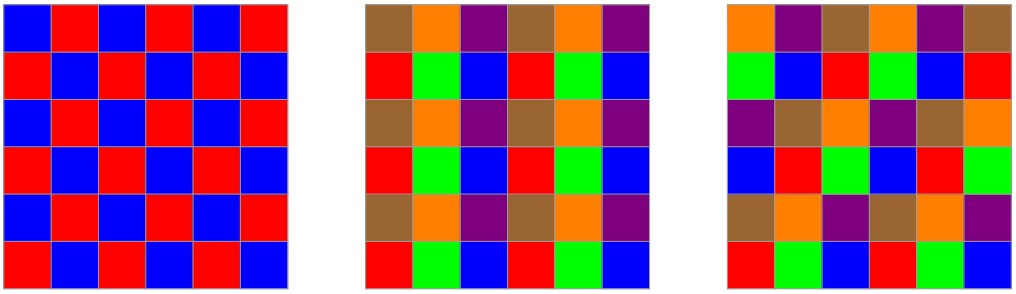

(a) (b) (c)

Figure 7. Examples of $[L\times T]_S$ periodic blocks together with their spatiotemporal Bravais lattice tilings (82). (a) $[2\times 1]_1$, basis vectors $\mathbf{a}_1 = \{2, 0\}$ and $\mathbf{a}_2 = \{1, 1\}$; (b) $[3\times 2]_0$, basis vectors $\mathbf{a}_1 = \{3, 0\}$ and $\mathbf{a}_2 = \{0, 2\}$; (c) $[3\times 2]_1$, basis vectors $\mathbf{a}_1 = \{3, 0\}$ and $\mathbf{a}_2 = \{1, 2\}$;

three figures in figure 6 are the blocks with periodicity $[1\times 3]_0$, $[3\times 1]_0$ and $[3\times 1]_1$, which can show the periodicity of the space-equilibria, time-equilibria and time-relative equilibria. Figure 7 is the color coding of the periodic blocks with periodicity $[2\times 1]_1$, $[3\times 2]_1$ and $[3\times 2]_0$.

2020-10-03 Predrag For periodic boundary conditions, the Laplacian $\Box$ in (71) and (104) has a translational zero mode, $\lambda_0 = 0$, corresponding to a constant eigenvector, so the matrix $\Box$ is singular. That is the reason why our counting formulas (69) and table 2 have a prefactor $(s-2)$; in the Laplacian limit the corresponding determinant has a zero eigenvalue, and therefore vanishes.

A hyper-cubic lattice consists of d intersecting one-dimensional lattices, with Laplacian eigenvalues being the sums of the eigenvalues of the Laplacian of the constituent one-dimensional lattices, hence for any dimension there is only one zero eigenvalue, and only a single power of the prefactor $(s-2)$ in our counting formulas.

2019-11-23 Predrag We always reduce relative-shift symmetries, so I am not happy

about the $[2\times1]_1$ relative-periodic block (98) being counted as the $[2\times2]_0$ periodic orbit. We'll have to revisit symmetry reduction...

2020-03-17 Han *PrimeTiles.nb* generates all prime tiles that can tile a larger tile. It gives some not obvious results. For example, let the large tile be $[3\times2]_1$, and consider the full-shift 9-symbol $[3\times2]_1$ blocks. The number $[3\times2]_0$ blocks is given by (**??**). The program shows that the $[3\times2]_0$ tile can only be tiled by $[1\times1]_0$, $[1\times2]_0$ and $[3\times1]_0$ tiles. So we get the result in (**??**):

$$N_{[3\times2]_0} = 9^{3\times2} = 88440\,[3\times2]_0 + 240\,[3\times1]_0 + 36\,[1\times2]_0 + 9\,[1\times1]_0\,.$$

For the full-shift the number of periodic blocks is given by the area of the larger tile, and number of $[3\times2]_S$ blocks is the same for all S. But now $[3\times1]_0$ tile cannot tile the $[3\times2]_1$ tile. Instead, the $[3\times2]_1$ can be tiled by $[1\times1]_0$, $[3\times1]_2$ and $[1\times2]_0$ tiles,

$$N_{[3\times2]_1} = 9^{3\times2} = 88440\,[3\times2]_1 + 240\,[3\times1]_2 + 36\,[1\times2]_0 + 9\,[1\times1]_0\,.$$

A priori is not obvious that $[3\times1]_2$ tile can tile a $[3\times2]_1$ tile. But if you stack $[3\times1]_2$ tile in the shifted temporal direction by 2 then the left edge of the tile is shifted by 4 in the spatial direction. With the spatial period being 3, shifted by 4 in the spatial direction is same as shifted by 1. So the bc's of $[3\times2]_1$ tile are satisfied by the $[3\times1]_2$ tiles.

5. Hill determinant: stability of an orbit vs. its time-evolution stability

The $d = 2$ lattice spatiotemporal cat equations can be recast in a matrix form, by rewriting the defining equations in terms of *block matrices* [18, 19, 39, 58], constructed by the Kronecker product $\mathbf{A}\otimes\mathbf{B}$, an operation (introduced by Zehfuss in 1858) that replaces the a_{ij} element of an $[n\times n]$ matrix $\mathbf{A}$ by $[m\times m]$ matrix block $a_{ij}\mathbf{B}$, resulting in an $[mn\times mn]$ block matrix [5, 106]

$$\mathbf{A}\otimes\mathbf{B} = \begin{bmatrix} a_{11}\mathbf{B} & \cdots & a_{1n}\mathbf{B} \\ \vdots & \ddots & \vdots \\ a_{n1}\mathbf{B} & \cdots & a_{nn}\mathbf{B} \end{bmatrix}. \tag{110}$$

Consider $\mathbf{A}$, $\mathbf{A}'$ square matrices of size $[n\times n]$, and $\mathbf{B}$, $\mathbf{B}'$ square matrices of size $[m\times m]$. The matrix product of two block matrices is a block matrix [5, 105],

$$(\mathbf{A}\otimes\mathbf{B})\,(\mathbf{A}'\otimes\mathbf{B}') = (\mathbf{A}\mathbf{A}')\otimes(\mathbf{B}\mathbf{B}')\,. \tag{111}$$

The trace and the determinant of a block matrix are given by

$$\begin{aligned} \mathrm{tr}(\mathbf{A}\otimes\mathbf{B}) &= \mathrm{tr}\,\mathbf{A}\ \mathrm{tr}\,\mathbf{B} \\ \det(\mathbf{A}\otimes\mathbf{B}) &= \det(\mathbf{A}^m)\det(\mathbf{B}^n)\ . \end{aligned} \tag{112}$$

The two $[mn\times mn]$ block matrices $\mathbf{A}\otimes\mathbf{B}$ and $\mathbf{B}\otimes\mathbf{A}$ are equivalent by a similarity transformation

$$\mathbf{B}\otimes\mathbf{A} = \mathbf{P}^\top(\mathbf{A}\otimes\mathbf{B})\,\mathbf{P}\,, \tag{113}$$

where $\mathbf{P}$ is permutation matrix. As $\det \mathbf{P} = 1$, the block matrix determinant $\det(\mathbf{A} \otimes \mathbf{B}) = \det(\mathbf{B} \otimes \mathbf{A})$ is independent of the order in which blocks are constructed.

Consider a rectangular $d = 2$ lattice $[L \times T]_0$ Bravais cell. The orbit Jacobian matrix (75) written as a $[LT \times LT]$ Kronecker product block matrix is

$$\mathcal{J} = 1_1 \otimes \left(\sigma_2 + \sigma_2^{-1}\right) - 2s\, 1_1 \otimes 1_2 + \left(\sigma_1 + \sigma_1^{-1}\right) \otimes 1_2 \,, \tag{114}$$

where the (110) matrix $\mathbf{A}$ and identity 1_1 matrix are 'spatial' $[L \times L]$ matrices, with blocks $\mathbf{B}$ and identity 1_2 'temporal' $[T \times T]$ matrix blocks. Indices '1', '2' referring to 'spatial', 'temporal' lattice directions, respectively.

Our task is to compute the Hill determinant $|\det \mathcal{J}|$. We first show how to do that directly, by computing the volume of the fundamental parallelepiped.

5.1. Hill determinant: fundamental parallelepiped evaluation

As a concrete example consider the Bravais lattice (82) with basis vectors $\mathbf{a}_1 = (3, 0)$ and $\mathbf{a}_2 = (0, 2)$. A periodic orbit over this Bravais cell has 6 field values, one for each lattice site $z = (n, t)$ on a $[3 \times 2]_0$ rectangle:

$$\begin{bmatrix} \phi_{01} & \phi_{11} & \phi_{21} \\ \phi_{00} & \phi_{10} & \phi_{20} \end{bmatrix} .$$

Stack up the columns of this lattice state and the corresponding sources into 6-dimensional vectors,

$$\Phi_{[3\times2]_0} = \begin{pmatrix} \phi_{01} \\ \hline \phi_{00} \\ \phi_{11} \\ \hline \phi_{10} \\ \phi_{21} \\ \phi_{20} \end{pmatrix} , \qquad \mathsf{M}_{[3\times2]_0} = \begin{pmatrix} m_{01} \\ \hline m_{00} \\ m_{11} \\ \hline m_{10} \\ m_{21} \\ m_{20} \end{pmatrix} . \tag{115}$$

The corresponding orbit Jacobian matrix (79) is the block-matrix (114), a block circulant matrix with circulant blocks [19],

$$\mathcal{J}_{[3\times2]_0} = \left(\begin{array}{cc|cc|cc} -2s & 2 & 1 & 0 & 1 & 0 \\ 2 & -2s & 0 & 1 & 0 & 1 \\ \hline 1 & 0 & -2s & 2 & 1 & 0 \\ 0 & 1 & 2 & -2s & 0 & 1 \\ \hline 1 & 0 & 1 & 0 & -2s & 2 \\ 0 & 1 & 0 & 1 & 2 & -2s \end{array}\right) . \tag{116}$$

of $[L \times L]$ block form, $L = 3$, with $[T \times T]$ blocks, $T = 2$.

The fundamental parallelepiped generated by the action of orbit Jacobian matrix $\mathcal{J}_{[3\times2]_0}$ is spanned by $LT = 6$ basis vectors, the columns (18) of the orbit Jacobian matrix

(116):

$$\mathcal{J}_{[3\times2]_0} = \left(\begin{array}{c|c|c|c|c|c} -2s & 2 & 1 & 0 & 1 & 0 \\ 2 & -2s & 0 & 1 & 0 & 1 \\ 1 & 0 & -2s & 2 & 1 & 0 \\ 0 & 1 & 2 & -2s & 0 & 1 \\ 1 & 0 & 1 & 0 & -2s & 2 \\ 0 & 1 & 0 & 1 & 2 & -2s \end{array}\right) . \tag{117}$$

The 'fundamental fact' (16) now yields the Hill determinant as the number of doubly-periodic lattice states,

$$N_{[3\times2]_0} = |\mathrm{Det}\, \mathcal{J}_{[3\times2]_0}| = 4(s-2)s(2s-1)^2(2s+3)^2 . \tag{118}$$

5.2. Hill determinant: time-evolution evaluation

In practice, one often computes the Hill determinant using a Hamiltonian, or 'transfer matrix' formulation. An example is the temporal cat 3-term recurrence (47),

$$\begin{aligned} \phi_t &= \phi_t \\ \phi_{t+1} &= -\phi_{t-1} + s\,\phi_t - m_t , \end{aligned}$$

in the Percival-Vivaldi [90] 'two-configuration' cat map representation (45)

$$\hat{\boldsymbol{\phi}}_{t+1} = \hat{\mathbf{J}}_1\, \hat{\boldsymbol{\phi}}_t - \hat{\mathsf{m}}_t , \tag{119}$$

with the one-time step temporal evolution $[2\times2]$ Jacobian matrix $\hat{\mathbf{J}}_1$ generating a time orbit by acting on the 2-dimensional 'phase space' of states on successive lattice sites

$$\hat{\mathbf{J}}_1 = \begin{bmatrix} 0 & 1 \\ -1 & s \end{bmatrix} , \qquad \hat{\boldsymbol{\phi}}_t = \begin{bmatrix} \phi_{t-1} \\ \phi_t \end{bmatrix} , \qquad \hat{\mathsf{m}}_t = \begin{bmatrix} 0 \\ m_t \end{bmatrix} , \tag{120}$$

Similarly, for the $d = 2$ spatiotemporal cat lattice at hand, one can recast the 5-term recurrence (74)

$$\begin{aligned} \phi_{nt} &= \phi_{nt} \\ \phi_{n,t+1} &= -\phi_{n,t-1} + (-\phi_{n-1,t} + 2s\,\phi_{nt} - \phi_{n+1,t}) - m_{nt} \end{aligned} \tag{121}$$

in the 'two-configuration' matrix form (119) by picking the vertical direction (indexed '2') as the 'time', with temporal 1-time step Jacobian $[2L\times2L]$ block matrix

$$\hat{\mathbf{J}}_1 = \left[\begin{array}{c|c} \mathbf{0} & 1_1 \\ \hline -1_1 & -\mathcal{J}_1 \end{array}\right] , \tag{122}$$

(known as a transfer matrix in statistical mechanics [83, 89]) generating a 'time' orbit by acting on a $2L$-dimensional 'phase space' lattice strip $\hat{\boldsymbol{\phi}}_t$ along the 'spatial' direction (indexed '1'),

$$\hat{\boldsymbol{\phi}}_t = \left[\begin{array}{c} \boldsymbol{\phi}_{t-1} \\ \hline \boldsymbol{\phi}_t \end{array}\right] , \quad \hat{\mathsf{m}}_t = \left[\begin{array}{c} \mathbf{0} \\ \hline \mathsf{m}_t \end{array}\right] , \qquad \boldsymbol{\phi}_t = \begin{bmatrix} \phi_{1t} \\ \vdots \\ \phi_{Lt} \end{bmatrix} , \quad \mathsf{m}_t = \begin{bmatrix} m_{1t} \\ \vdots \\ m_{Lt} \end{bmatrix} ,$$

where the hat $\hat{\ }$ indicates a $2L$-dimensional 'two-configuration' state, and $\mathcal{J}_1$ is the spatial $[L\times L]$ orbit Jacobian matrix of $d=1$ temporal cat form (50),

$$\mathcal{J}_1 = \sigma_1^{-1} - 2s\mathbb{1}_1 + \sigma_1 \tag{123}$$

The 'two-configuration' coupled cat maps system (119) is a generalization of the Bernoulli map time evolution formulation (10) to a high-dimensional spatially-coupled lattice. Just as in the temporal Bernoulli condition (13), the first order in time difference equation (119) can be viewed as a lattice state fixed point condition (13), a zero of the function $F[\hat{\Phi}] = \hat{\mathcal{J}}\hat{\Phi}+\hat{\mathsf{M}} = 0$, with the entire periodic *lattice state* $\hat{\Phi}_{\mathsf{M}}$ treated as a single fixed *point* in the $2LT$-dimensional state space unit hyper-cube, and the $[2LT\times 2LT]$ block matrix orbit Jacobian matrix given either by

$$\hat{\mathcal{J}} = \hat{\mathbb{1}} - \hat{\mathbf{J}}_1\otimes\sigma_2^{-1}\,, \tag{124}$$

or by

$$\hat{\mathcal{J}}' = \hat{\mathbb{1}} - \sigma_2^{-1}\otimes\hat{\mathbf{J}}_1\,. \tag{125}$$

Here the unity $\hat{\mathbb{1}} = \hat{\mathbb{1}}_1\otimes\mathbb{1}_2$ is a $[2LT\times 2LT]$ block matrix, and the time-evolution Jacobian matrix $\hat{\mathbf{J}}_1$ (122) is a $[2L\times 2L]$ matrix.

The order in which the block matrix blocks are composed does not matter, yielding the same the Hill determinant $\det\hat{\mathcal{J}} = \det\hat{\mathcal{J}}'$ by (113). However, written out explicitly, the two orbit Jacobian matrices (126) and (129) are of a very different form.

For example, for the $[L\times T]_0$ rectangular Bravais cell, the spatiotemporal cat orbit Jacobian matrix (124) involves the $[T\times T]$ time shift operator block matrix σ_2 (11) with the one-time-step $[2L\times 2L]$ time-evolution Jacobian matrix $\hat{\mathbf{J}}_1$ (122)

$$\hat{\mathcal{J}} = \left[\begin{array}{c|c} \mathbb{1}_1\otimes\mathbb{1}_2 & -\mathbb{1}_1\otimes\sigma_2^{-1} \\ \hline \mathbb{1}_1\otimes\sigma_2^{-1} & \mathbb{1}_1\otimes\mathbb{1}_2 + \mathcal{J}_1\otimes\sigma_2^{-1} \end{array}\right]\,, \tag{126}$$

and for spatiotemporal cat (121) this is a time-periodic $[T\times T]$ shift operator block matrix σ_2 (11), each block now a space-periodic $[2L\times 2L]$ matrix $\hat{\mathbf{J}}_1$ (122).

If a block matrix is composed of four blocks, its determinant can be evaluated using Schur's 1917 formula [101, 105]

$$\det\left[\begin{array}{c|c} \mathbf{A} & \mathbf{B} \\ \hline \mathbf{C} & \mathbf{D} \end{array}\right] = \det(\mathbf{A})\,\det(\mathbf{D}-\mathbf{C}\mathbf{A}^{-1}\mathbf{B})\,. \tag{127}$$

so, noting (111), (114) and (123), we find that

$$\begin{aligned} \det\hat{\mathcal{J}} &= \det\left[\begin{array}{c|c} \mathbb{1}_1\otimes\mathbb{1}_2 & -\mathbb{1}_1\otimes\sigma_2^{-1} \\ \hline \mathbb{1}_1\otimes\sigma_2^{-1} & \mathbb{1}_1\otimes\mathbb{1}_2 + \mathcal{J}_1\otimes\sigma_2^{-1} \end{array}\right] \\ &= \det\left[\mathbb{1}_1\otimes\mathbb{1}_2 + \mathcal{J}_1\otimes\sigma_2^{-1} + (\mathbb{1}_1\otimes\sigma_2^{-1})(\mathbb{1}_1\otimes\mathbb{1}_2)(\mathbb{1}_1\otimes\sigma_2^{-1})\right] \\ &= \det\left[\mathbb{1}_1\otimes\mathbb{1}_2 + \mathcal{J}_1\otimes\sigma_2^{-1} + \mathbb{1}_1\otimes\sigma_2^{-2}\right] \\ &= \det(\mathbb{1}_1\otimes\sigma_2^{-1})\,\det\left[\mathbb{1}_1\otimes\sigma_2^{-1} + (\sigma_1^{-1} - 2s\mathbb{1}_1 + \sigma_1)\otimes\mathbb{1}_2 + \mathbb{1}_1\otimes\sigma_2\right] \\ &= \det\mathcal{J}\,, \end{aligned} \tag{128}$$

where we have used $\det\mathbb{1}_1 = \det\mathbb{1}_2 = \det\sigma_1 = \det\sigma_2 = 1$.

This proves that $\det\hat{\mathcal{J}}$ of the 'Hamiltonian' or 'two-configuration' $[2LT\times 2LT]$ 'phase space' orbit Jacobian matrix $\hat{\mathcal{J}}$ defined by (126) equals the 'Lagrangian' Hill determinant of the $[LT\times LT]$ orbit Jacobian matrix $\mathcal{J}$.

5.3. Hill's formula

Consider next (125), the equivalent way of forming of the block matrix for the $[L\times T]_0$ rectangular Bravais cell, with temporal period taken for definitiveness $T=4$. The spatiotemporal cat orbit Jacobian matrix (125) is now constructed as the $[4\times 4]$ time shift operator block matrix σ_2 (11), with the one-time-step $[2L\times 2L]$ time-evolution Jacobian matrix $\hat{\mathbf{J}}_1$ (122) and unit matrix $\hat{1}_1$ as blocks

$$\hat{\mathcal{J}}' = 1_2\otimes\hat{1}_1 - \sigma_2^{-1}\otimes\hat{\mathbf{J}}_1 = \left[\begin{array}{c|c|c|c} \hat{1}_1 & \mathbf{0} & \mathbf{0} & -\hat{\mathbf{J}}_1 \\ \hline -\hat{\mathbf{J}}_1 & \hat{1}_1 & \mathbf{0} & \mathbf{0} \\ \hline \mathbf{0} & -\hat{\mathbf{J}}_1 & \hat{1}_1 & \mathbf{0} \\ \hline \mathbf{0} & \mathbf{0} & -\hat{\mathbf{J}}_1 & \hat{1}_1 \end{array}\right] . \tag{129}$$

The Hill determinant $\det\hat{\mathcal{J}}'$ evaluation follows essentially the same path as the Bernoulli Hill determinant evaluation of section 1.5, generalized to block matrices. From the block-matrix multiplication rule (111) and the determinant rule (112) it follows that

$$(\sigma_2^{-1}\otimes\hat{\mathbf{J}}_1)(\sigma_2^{-1}\otimes\hat{\mathbf{J}}_1) = \sigma_2^{-2}\otimes\hat{\mathbf{J}}_1^2\,, \qquad \text{so } (\sigma_2^{-1}\otimes\hat{\mathbf{J}}_1)^k = \sigma_2^{-k}\otimes\hat{\mathbf{J}}_1^k\,, \tag{130}$$

and

$$\det(\sigma_2^{-1}\otimes\hat{\mathbf{J}}_1) = (\det\sigma_2)^{-L}(\det\hat{\mathbf{J}}_1)^T = \det\hat{\mathbf{J}}_p\,, \qquad \hat{\mathbf{J}}_p = \hat{\mathbf{J}}_1^T\,, \tag{131}$$

where $\hat{\mathbf{J}}_p$ is the Jacobian matrix of a temporal periodic orbit p. Expand $\ln\det\hat{\mathcal{J}}' = \mathrm{tr}\ln\hat{\mathcal{J}}'$ as a series using (112) and (130),

$$\mathrm{tr}\ln\hat{\mathcal{J}}' = \mathrm{tr}\ln(1-\sigma_2^{-1}\otimes\hat{\mathbf{J}}_1) = -\sum_{k=1}^{\infty}\frac{1}{k}\mathrm{tr}(\sigma_2^{-k})\ \mathrm{tr}\,\hat{\mathbf{J}}_1^k\,, \tag{132}$$

and use $\mathrm{tr}\,\sigma_2^k = T$ if k is a multiple of T, 0 otherwise (follows from $\sigma_2^T = 1$):

$$\ln\det(1-\sigma_2^{-1}\otimes\hat{\mathbf{J}}_1) = -\sum_{r=1}^{\infty}\frac{1}{r}\,\mathrm{tr}\,\hat{\mathbf{J}}_p^r = \ln\det(\hat{1}_1-\hat{\mathbf{J}}_p)\,.$$

So for the spatiotemporal cat the orbit Jacobian matrix and the temporal evolution (119) stability $\hat{\mathbf{J}}_p$ are related by the remarkable (discrete time) Hill's formula [13, 77]

$$|\det\mathcal{J}| = |\det(\hat{1}_1-\hat{\mathbf{J}}_p)|\,. \tag{133}$$

which expresses the Hill determinant of the arbitrarily large orbit Jacobian matrix $\mathcal{J}$ in terms of a determinant of a small $[2L\times 2L]$ time-evolution Jacobian matrix $\hat{\mathbf{J}}_p$.

Two remarks. First, the reformulation of the spatiotemporal cat 5-term recurrence (121) as the 'two-configuration' form (119) is a passage from the Lagrangian to the Hamiltonian formulation, also known as 'transfer matrix' formulation of lattice field theories [83, 86] and Ising models [65, 89]. We chose to prove it here using only

elementary linear algebra, not only because the Lagrangian formalism [13] is not needed for the problem at hand, but because it actually obscures the generality of Hill's formula, which works equally well for dissipative systems (see Bernoulli Hill's formula (67)), systems with no Lagrangian formulation.

Second, for Hamiltonian evolution (42), the $[2 \times 2]$ Jacobian matrix J^T (the monodromy matrix of a periodic orbit) describes the growth of an initial state perturbation in T steps. For the corresponding Lagrangian system with action W, the first variation of the action $\delta W = 0$ yields the temporal cat condition (48), while the second variation, the $[T \times T]$ orbit Jacobian matrix (50), describes the stability of the *entire* given periodic orbit. In this, classical mechanics context, Bolotin and Treschev [13] refer to $\mathcal{J}$ as the 'Hessian operator', but, as it is clear from our Bernoulli discussion of section 1.3, and applications to Kuramoto-Sivashinsky and Navier-Stokes systems [51], this notion of global stability of orbits is general, and applies to all dynamical systems, not only the Hamiltonian ones.

Accordingly, by the discrete time Hill's formula (133), just as for the Bernoulli example (24) these two expressions are equivalent,

$$|\mathrm{Det}\, \mathcal{J}_{\mathsf{M}}| = |\det(\mathbf{1} - J_{\mathsf{M}})|\,. \tag{134}$$

As the cat map hyperbolicity is the same everywhere and does not depend on a particular solution Φ_p, counting periodic orbits is all that is needed to solve a cat-map dynamical system completely; once periodic orbits are counted, all cycle averaging formulas [26] follow.

6. Summary and discussion

In this paper we have analyzed the spatiotemporal cat (80) linear symbolic dynamics. We now summarize our main findings.

6.1. Discussion.

While the setting is classical, such classical field-theory advances offer new semi-classical approaches to quantum field theory and many-body problems.

Acknowledgments

Work of P. C. was in part supported by the family of late G. Robinson, Jr.. We are grateful to Sara A. Solla's many perspicacious comments on this manuscript. No actual cats, graduate or undergraduate were harmed during this research. This paper sets up the necessary underpinnings for the quantum field theory of spatiotemporal cat, the details of which we leave to our friends Jon Keating and Marcos Saraceno.

Appendix A. Discrete Fourier transforms

In this appendix we show how compute the orbit Jacobian matrix or Hill determinants $|\mathrm{Det}\,\mathcal{J}|$ using crystallographer's favorite tool, the discrete Fourier transform.

Appendix A.1. Temporal Bernoulli

Due to the time-translation invariance of Bernoulli time evolution law (9), the orbit Jacobian matrix $\mathcal{J} = \mathsf{1} - s\,\sigma^{-1}$ is an $[n\times n]$ is a circulant matrix. A circulant matrix is constant along each diagonal,

$$C = \begin{pmatrix} c_0 & c_{n-1} & \dots & c_2 & c_1 \\ c_1 & c_0 & c_{n-1} & & c_2 \\ \vdots & c_1 & c_0 & \ddots & \vdots \\ c_{n-2} & & \ddots & \ddots & c_{n-1} \\ c_{n-1} & c_{n-2} & \dots & c_1 & c_0 \end{pmatrix}, \qquad C_{jk} = c_{j-k}\,, \tag{A.1}$$

diagonalizable by a discrete Fourier transform,

$$U^\dagger C U = \mathrm{diag}(\lambda)\,, \qquad U_{jk} = \frac{1}{\sqrt{n}}\,\epsilon^{(j-1)(k-1)}\,, \tag{A.2}$$

with discrete Fourier mode eigenvectors

$$\tilde{e}_k = \frac{1}{\sqrt{n}}(1, \epsilon^k, \epsilon^{2k}, \dots, \epsilon^{k(n-1)})^{\mathrm{T}}\,, \qquad k = 0, 1, \dots, n-1\,, \tag{A.3}$$

and eigenvalues $C\tilde{e}_k = \lambda_k \tilde{e}_k$,

$$\lambda_k = c_0 + c_{n-1}\epsilon^k + c_{n-2}\epsilon^{2k} + \dots + c_1\epsilon^{k(n-1)}\,, \tag{A.4}$$

where

$$\epsilon = \mathrm{e}^{2\pi \mathrm{i}/n} \tag{A.5}$$

is an nth root of unity. The eigenvalues of the Bernoulli orbit Jacobian matrix $(\mathsf{1} - s\,\sigma^{-1})$ are given by the nonzero coefficients $c_0 = 1$, $c_1 = -s$,

$$\lambda_k = 1 - s\,\epsilon^{-k}\,, \tag{A.6}$$

with discrete Fourier transform diagonalizing the Bernoulli equation (10),

$$(\mathsf{1} - s\,\sigma^{-1})\,\tilde{\Phi}_k = (1 - s\,\epsilon^{-k})\,\tilde{\Phi}_k = -\,\tilde{\mathsf{M}}_k\,, \tag{A.7}$$

where the $\tilde{\Phi}_k$ and $\tilde{\mathsf{M}}_k$ are the kth Fourier modes of the lattice state Φ and symbol block M:

$$\tilde{\Phi}_k = \left(\tilde{e}_k{}^\top\,\Phi\right)\tilde{e}_k\,, \quad \tilde{\mathsf{M}}_k = \left(\tilde{e}_k{}^\top\,\mathsf{M}\right)\tilde{e}_k\,. \tag{A.8}$$

The total number of the solutions of the fixed point condition (13) is given by (16), the 'fundamental fact' Hill determinant $|\mathrm{Det}\,\mathcal{J}|$, i.e., the product of the orbit Jacobian matrix eigenvalues,

$$N_n = |\mathrm{Det}\,\mathcal{J}| = \prod_{k=0}^{n-1} \left|1 - s\,\epsilon^{-k}\right| = \prod_{k=0}^{n-1} \left|s - \epsilon^k\right| = s^n - 1\,, \tag{A.9}$$

where the last equality follows from ϵ^k being the kth root of equation $s^n - 1 = 0$, so

$$s^n - 1 = \prod_{k=0}^{n-1} (s - \epsilon^k) \,.$$

This verifies the 'fundamental fact' count of Bernoulli solutions (21).

Appendix A.2. Temporal cat

The temporal cat orbit Jacobian matrix $\mathcal{J} = \sigma - s\,\mathbf{1} + \sigma^{-1}$ is an $[n \times n]$ circulant matrix (51), with eigenvalues (A.4)

$$\lambda_k = \epsilon^{-k} - s + \epsilon^k = -s + 2\cos(2\pi k/n) \,, \tag{A.10}$$

and the Hill determinant

$$N_n = |\mathrm{Det}\,\mathcal{J}| = \prod_{k=0}^{n-1} |s - 2\cos(2\pi k/n)| \,. \tag{A.11}$$

It is not immediately obvious that such products of trigonometric functions should be integer-valued [41], and establishing that usually requires some work [107].

In case at hand we observe that as the Chebyshev polynomials of the first kind [15] satisfy $T_n(\cos(x)) = \cos(nx)$, for $x = 2\pi k/n$, $k = 0, 1, ..., n-1$, $\cos(2\pi k/n)$ is the kth root of equation

$$T_n(x) - 1 = 0 \,.$$

This equation, in analogy with the Bernoulli eigenvalue product (A.9), can be written as a product over the eigenvalues (A.10)

$$T_n(x) - 1 = 2^{n-1} \prod_{k=0}^{n-1} [x - \cos(2\pi k/n)] \,. \tag{A.12}$$

Here the coefficient 2^{n-1} comes from matching the coefficient of x^n term in the definition of $T_n(x) = \cdots + 2^{n-1}x^n$. For $x = s/2$, this is the Hill determinant formula (56)

$$N_n = \prod_{k=0}^{n-1} [s - 2\cos(2\pi k/n)] = 2T_n(s/2) - 2 \,. \tag{A.13}$$

Appendix A.3. Spatiotemporal cat

In order to count the periodic lattice states as we did for the temporal cat (A.11), we need to compute the eigenvalues and eigenvectors of the orbit Jacobian matrix (79). The eigenvalues determine the Hill determinant of the orbit Jacobian matrix, and thus count the number of the periodic lattice states. The eigenvectors enable us to diagonalize the orbit Jacobian matrix.

In the spatiotemporal cat equation (80) the operators, fields and sources are defined on the spatiotemporally infinite 2-dimensional cubic lattice. This equation is also satisfied on a single tile, provided the translation operators satisfy the periodic bc's

on the tile. Thus, in order to count the periodic orbits, it suffices to determine the eigenvalues of the orbit Jacobian matrix on finite tiles.

Now consider 2-dimensional spatiotemporal cat. The periodicity is described by 2-dimensional Bravais lattice (82).

Periodic fields with the periodicity described by Bravais lattice $\mathcal{L}$ satisfy:

$$f(z+R) = f(z)\,, \quad R \in \mathcal{L}\,. \tag{A.14}$$

The orbit Jacobian matrix (79) is constructed from 2 commuting translation operators $\{\sigma_1, \sigma_2\}$. The eigenvectors of these translation operators are plane waves:

$$f_k(z) = e^{ik\cdot z}\,, \tag{A.15}$$

where $\mathbf{k}$ is a 2-dimensional wave vector. A general plane wave does not satisfy the periodicity (A.14), unless

$$e^{ik\cdot R} = 1\,. \tag{A.16}$$

Since R is a vector from the Bravais lattice $\mathcal{L}$, the wave vector $\mathbf{k}$ must lie in the reciprocal lattice of $\mathcal{L}$:

$$\mathbf{k} \in \mathcal{L}^*\,, \quad \mathcal{L}^* = \left\{ \sum_{i=1}^{2} m_i \mathbf{b}_i \,|\, m_i \in \mathbb{Z} \right\}\,, \tag{A.17}$$

where the primitive reciprocal lattice vectors $\mathbf{b}_i$ satisfy:

$$\mathbf{b}_i \cdot \mathbf{a}_j = 2\pi\delta_{ij}\,. \tag{A.18}$$

To get the eigenvectors and the corresponding eigenvalues of the orbit Jacobian matrix, note that

$$(\sigma_j + \sigma_j^{-1})e^{ik\cdot z} = e^{i(k\cdot z - k_j)} + e^{i(k\cdot z + k_j)} = (2\cos k_j)e^{ik\cdot z}\,, \tag{A.19}$$

where the $\mathbf{k} = (k_1, k_2)$. Hence the eigenvalue of the orbit Jacobian matrix (79) corresponding to the eigenvector with the wave vector $\mathbf{k}$ is

$$\lambda_k = -2s + 2\cos k_1 + 2\cos k_2\,. \tag{A.20}$$

Choosing primitive vectors with Hermite normal form (84), the reciprocal lattice is:

$$\mathcal{L}^* = \{n_1\mathbf{b}_1 + n_2\mathbf{b}_2 \,|\, n_i \in \mathbb{Z}\}\,, \tag{A.21}$$

where the primitive reciprocal lattice vectors $\mathbf{b}_1$ and $\mathbf{b}_2$ are:

$$\begin{bmatrix} \mathbf{b}_1 & \mathbf{b}_2 \end{bmatrix} = \frac{2\pi}{LT} \begin{bmatrix} T & 0 \\ -S & L \end{bmatrix}\,, \tag{A.22}$$

so (A.18) is satisfied. The eigenvectors of the translation operator have the form of a plane wave

$$f_k(z) = e^{ik\cdot z}\,, \quad k \in \mathcal{L}^*\,, \tag{A.23}$$

and, in addition, satisfy the Bravais lattice (82) periodicity. The eigenvalues are:

$$\lambda_k = 2\cos k_1 + 2\cos k_2 - 2s\,, \tag{A.24}$$

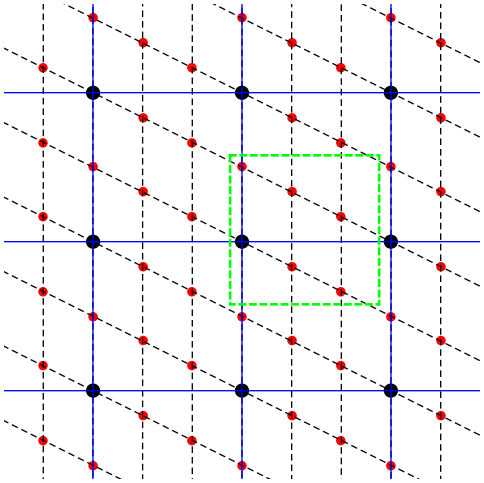

Figure A1. (Color online) The reciprocal lattices of both the Bravais lattice $\mathcal{L}$ and the integer square lattice. The red points are the reciprocal lattice $\mathcal{L}^*$ of the Bravais lattice $\mathcal{L}$ in figure 4. The black points are the reciprocal lattice of the square lattice. Each of these squares enclosed by the blue lines has edge length 2π. Two wave vectors are equivalent if they are different by a reciprocal lattice vector of the square lattice.

where $\mathbf{k} = (k_1, k_2)$. If $\mathbf{k} = n_1\mathbf{b}_1 + n_2\mathbf{b}_2$, then k_1 and k_2 are:

$$\mathbf{k} = \begin{bmatrix} k_1 \\ k_2 \end{bmatrix} = \begin{bmatrix} \mathbf{b}_1 & \mathbf{b}_2 \end{bmatrix} \begin{bmatrix} n_1 \\ n_2 \end{bmatrix} = \frac{2\pi}{LT} \begin{bmatrix} n_1 T \\ -n_1 S + n_2 L \end{bmatrix} . \tag{A.25}$$

As the field has support only on the integer lattice sites, it suffices to use the wave vectors $\mathbf{k} = n_1\mathbf{b}_1 + n_2\mathbf{b}_2$ with n_1 from 0 to $L-1$ and n_2 from 0 to $T-1$ to get all of the eigenvectors.

This range contains all the wave vectors in one primitive cell of reciprocal lattice of the square lattice, as shown in figure A1, where the wave vectors with n_1 from 0 to $L-1$, and n_2 from 0 to $T-1$ are enclosed by the green dashed square. Any wave vector on the reciprocal lattice $\mathcal{L}^*$ outside of this range will give an eigenvector which is equivalent to an eigenvector with the wave vector within this range. So the number of eigenvectors is LT, which is equal to the number of integer lattice sites in the Bravais cell of the Bravais lattice $\mathcal{L}$.

The number of periodic lattice states is then given by the Hill determinant of the orbit Jacobian matrix, which is the product of the eigenvalues:

$$\begin{aligned} N_{[L\times T]_S} &= \left| \prod_k \lambda_k \right| \\ &= \prod_{n_1=0}^{L-1} \prod_{n_2=0}^{T-1} \left[2s - 2\cos(\frac{2\pi n_1}{L}) - 2\cos(-\frac{2\pi n_1 S}{LT} + \frac{2\pi n_2}{T}) \right] . \end{aligned} \tag{A.26}$$

Appendix A.4. Backup from s previous version of spatiotemporal cat

The set of all wave vectors $\mathbf{K}_m$ that yield plane waves with the periodicity of a given Bravais lattice defines its reciprocal lattice. The $\mathbf{K}_m$ are called reciprocal lattice vectors.

Let $\langle \cdot, \cdot \rangle$ be the scalar product on $\mathbb{R}^d$. Let $\mathcal{L} \subset \mathbb{R}^d$ be a lattice, and let $\mathcal{L}^* \subset \mathbb{R}^d$ be its *reciprocal* lattice

$$\mathcal{L}^* = \left\{ x \in \mathbb{R}^d : \quad \langle x, y \rangle \in \mathbb{Z} \quad \text{for all} \quad y \in \mathcal{L} \right\}. \tag{A.27}$$

The reciprocal lattice of the Bravais lattice (82) is spanned by reciprocal basis (A.18)

$$\mathcal{L}^* = \{ n_1 \mathbf{b}_1 + n_2 \mathbf{b}_2 \,|\, n_i \in \mathbb{Z} \}. \tag{A.28}$$

The eigenvectors of the translation operator have the form of a plane wave

$$f_k(z) = e^{ik \cdot z}, \quad k \in \mathcal{L}^*, \tag{A.29}$$

and, in addition, satisfy the Bravais lattice (82) periodicity.

Then the basis vectors of the reciprocal lattice are:

$$\begin{bmatrix} \mathbf{b}_1 & \mathbf{b}_2 \end{bmatrix} = \frac{2\pi}{LT} \begin{bmatrix} T & 0 \\ -S & L \end{bmatrix}. \tag{A.30}$$

A plane wave with wave vector $\mathbf{k}$ in the reciprocal lattice $\mathcal{L}^*$ is an eigenvector of the orbit Jacobian matrix (80) that satisfies the periodic condition of Bravais lattice $\mathcal{L}$. The eigenvector with wave vector $\mathbf{k} = n_1 \mathbf{b}_1 + n_2 \mathbf{b}_2$ is

$$f_k(z) = e^{ik \cdot z} = \exp\left(i \frac{2\pi}{LT} (n_1 T z_1 - n_1 S z_2 + n_2 L z_2) \right), \tag{A.31}$$

where the $z = (z_1, z_2)$, with the orbit Jacobian matrix eigenvalue

$$\lambda_k = \sum_{j=1}^{2} (s - 2\cos k_j) = 2s - 2\cos 2\pi (\frac{n_1}{L}) - 2\cos 2\pi (\frac{n_1 S}{LT} - \frac{n_2}{T}). \tag{A.32}$$

As the field has support on the square lattice sites, it suffices to use the wave vectors $\mathbf{k} = n_1 \mathbf{b}_1 + n_2 \mathbf{b}_2$ with n_1 from 0 to $L-1$ and n_2 from 0 to $T-1$ to get all the reciprocal lattice eigenvectors.

This range contains all of the wave vectors in one lattice cell of reciprocal lattice of the square lattice, as shown in figure A1, where wave vectors with n_1 from 0 to $L-1$, and n_2 from 0 to $T-1$ are enclosed by the green dashed square. Any wave vector on the reciprocal lattice $\mathcal{L}^*$ outside of this range will give an eigenvector which is equivalent to an eigenvector with the wave vector within this range. So the number of eigenvectors is LT, which is the number of square lattice sites within the minimal repeating tile.

The 4-index orbit Jacobian matrix (80) is a matrix with indices in a finite range. The orbit Jacobian matrix has LT eigenmodes. We know that the number of periodic orbits is equal to the Hill determinant of the orbit Jacobian matrix, which is the product of all the eigenvalues,

$$N_{[L\times T]_S} = 2^{LT} \prod_{k_1=0}^{L-1} \prod_{k_2=0}^{T-1} \left[s - \cos\left(\frac{2\pi k_1}{L} \right) - \cos\left(\frac{2\pi k_2}{T} - \frac{2\pi k_1}{L} \frac{S}{T} \right) \right] \tag{A.33}$$

Given the eigenmodes with a given periodic condition, one can reduce the 2-dimensional square lattice to a finite repeating tile. The screened Poisson equation in this tile is still (80). But now the fields and sources are defined over an $[L\times T]_S$ lattice.

$$N_{[1\times 1]_0} = 2s - 4 = 1\,. \tag{A.34}$$

$$N_{[L\times 1]_0} = \prod_{k_1=0}^{L-1} \left[2s_2 - 2 - 2\cos\left(\frac{2\pi k_1}{L}\right)\right]\,. \tag{A.35}$$

Comparing with the temporal cat count (A.13) we see that the count is the same, provided we replace $s_1 \to 2(s_2-1)$, in agreement with the 3-term recurrence (92).

Appendix A.4.1. $[2\times 1]_1$ *periodic orbits.* For $s = 5/2$ spatiotemporal cat.

$$N_{[2\times 1]_1} = \prod_{l=0}^{1} \left[2s - 4\cos 2\pi\left(\frac{l}{2}\right)\right] = 9\,. \tag{A.36}$$

Appendix A.4.2. $[2\times 2]_0$ *periodic orbits.* For $s = 5/2$ spatiotemporal cat.

$$N_{[2\times 2]} = 2^4(s-2)(s-\cos\pi-1)(s-1-\cos\pi)(s-\cos\pi-\cos\pi) = 225\,.$$

Appendix A.4.3. $[3\times 2]_0$ *periodic orbits.* For $s = 5/2$ only 850 prime $[3\times 2]_0$ blocks are admissible. The integer points count (**??**) is in agreement with the counting formula (A.33) for the $[3\times 2]_0$ periodic orbits:

$$N_{[3\times 2]_0} = \prod_{l=0}^{2}\prod_{t=0}^{1} \left[2s - 2\cos\left(\frac{2\pi l}{3}\right) - 2\cos\left(\frac{2\pi t}{2}\right)\right] = 5120\,.$$

Appendix B. Temporal Bernuolli

Applied to a temporal lattice state Φ of period n, the shift operator (11) acts as a cyclic permutation that translates the lattice state Φ by one site, $(\sigma\Phi)^\top = (\phi_2, \phi_3, \cdots, \phi_n, \phi_1)$, with '1' in the lower left corner assuring periodicity.

After n shifts, the lattice state Φ returns to the initial state, $\sigma^n = 1$. This relation leads to the explicit expression for the orbit Jacobian matrix (28),

$$\mathsf{g} = \frac{\sigma}{s\,1-\sigma} = \frac{1}{1-\frac{\sigma}{s}}\frac{\sigma}{s} = \sum_{k=1}^{\infty}\frac{\sigma^k}{s^k} = \frac{s^n}{s^n-1}\sum_{k=1}^{n}\frac{\sigma^k}{s^k}\,. \tag{B.1}$$

From (28) it then follows that the last field in Φ is the field at lattice site n

$$\phi_n = \frac{s^n}{s^n-1}.m_1m_2m_3\cdots m_n = \frac{1}{s-1}\,\frac{s^{n-1}m_1+\cdots+s\,m_{n-1}+m_n}{s^{n-1}+\cdots+s+1}\,, \tag{B.2}$$

and the rest are obtained by cyclic permutations of M.

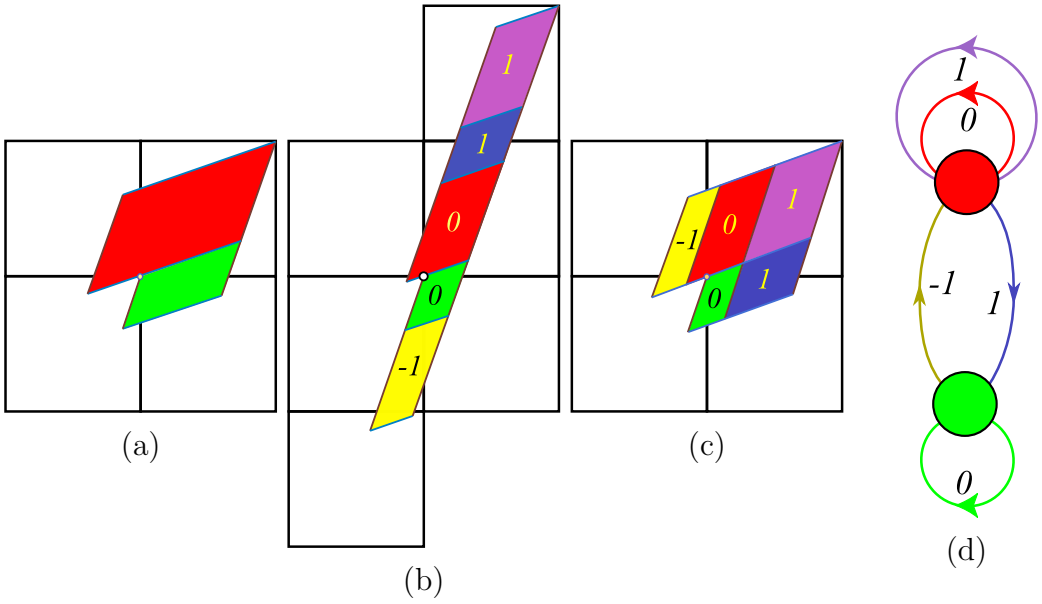

Figure C1. (Color online) (a) An Adler-Weiss generating partition of the unit torus for the $s = 3$ Percival-Vivaldi cat map (45), with rectangle $\mathcal{M}_A$ (red) and $\mathcal{M}_B$ (green) borders given by the cat map stable (blue) and unstable (dark red) manifolds, i.e., along the two eigenvectors corresponding to the eigenvalues (43). (b) Mapped one step forward in time, the rectangles are stretched along the unstable direction and shrunk along the stable direction. Sub-rectangles $\mathcal{M}_j$ that have to be translated back into the partition are indicated by color and labeled by their lattice translation $m_j \in \mathcal{A} = \{\underline{1}, 0, 1\}$, which also doubles as the 3-letter alphabet $\mathcal{A}$. (c) The sub-rectangles $\mathcal{M}_j$ translated back into the initial partition yield a generating partition, with the finite grammar given by the transition graph (d). The nodes refer to the rectangles A and B, and the five links correspond to the five sub-rectangles induced by one step forward-time dynamics. For details, see ChaosBook [31].

For example, for $s = 2$, the lattice fields are rational-valued,

$$\begin{aligned}\phi_{m_1 m_2 \cdots m_n} &= \sum_{k=1}^{n} \frac{m_k}{2^k} \sum_{m=0}^{\infty} \frac{1}{2^{nm}} = \frac{2^n}{2^n - 1} . m_1 m_2 \cdots m_n \\ &= \frac{1}{2^n - 1} \sum_{k=1}^{n} m_k 2^{n-k} \,, \end{aligned} \tag{B.3}$$

where $p = \overline{m_1 m_2 \cdots m_n}$ is a prime cycle of period n, with stability multiplier $\Lambda_p = 2^n$.

For a Bernoulli map, the rational ϕ_0 are either periodic or land eventually on a periodic orbit (the base-s version of the familiar fact that the decimal expansion of a rational number is eventually periodic), while the orbit of a normal irrational ϕ_0 is ergodic.

Appendix C. Cat map: Hamiltonian formulation

Appendix C.1. Adler-Weiss partition of the cat map state space

Cat maps, also known as Thom-Anosov diffeomorphisms, or Thom-Anosov-Arnol'd-Sinai cat maps [6, 35, 104], have been extensively studied as the simplest examples of chaotic Hamiltonian systems.

Percival-Vivaldi cat map (45) is a discrete time non-autonomous Hamiltonian system, time-forced by 'pulses' m_t. The m_t translations reshuffle the state space, as in figure C1, thus partitioning it into regions $\mathcal{M}_m$, labeled with letters m of the $|\mathcal{A}|$-letter alphabet $\mathcal{A}$, and associating a symbol sequence $\{m_t\}$ to the dynamical trajectory $\{\phi_t\}$. As the relation (45) between the trajectory ϕ_t and its symbolic dynamics encoding m_t is linear, Percival and Vivaldi refer to m_t as a 'linear code'.

As explained in the companion paper [52], the deep problem with the Percival-Vivaldi code prescription is that it does not yield a generating partition; the borders (i.e., ϕ_0, ϕ_1 axes) of their unit-square partition $(\phi_{t-1}, \phi_t) \in (0,1]\times(0,1]$ do not map onto themselves, resulting in the infinity of, to us unknown, grammar rules for inadmissible symbol sequences.

This problem was resolved in 1967 by Adler and Weiss [1, 2, 6] who utilized the stable/unstable manifolds of the fixed point at the origin to cover a unit area torus by a two-rectangles generating partition; for the Percival-Vivaldi cat map (45), such partition [31] is drawn in figure C1. Following Bowen [14], one refers to parallelograms in figure C1 as 'rectangles'; for details see Devaney [35], Robinson [100], or ChaosBook [31]. Siemaszko and Wojtkowski [103] refer to such partitions as the 'Berg partitions', and Creagh [23] studies their generalization to weakly nonlinear mappings. Symbolic dynamics on this partition is a subshift of finite type, with the 3-letter alphabet

$$\mathcal{A} = \{\underline{1}, 0, 1\} \tag{C.1}$$

that indicates the translation needed to return the given sub-rectangle $\mathcal{M}_j$ back into the two-rectangle partition $\mathcal{M} = \mathcal{M}_A \cup \mathcal{M}_B$.

While Percival and Vivaldi were well aware of Adler-Weiss partitions, they felt that their "coding is less efficient in requiring more symbols, but it has the advantage of linearity." Our construction demonstrates that one can have both: an Adler-Weiss generating cat map partition, and a linear code. The only difference from the Percival-Vivaldi formulation [90] is that one trades the single unit-square cover of the torus of (45) for the dynamically intrinsic, two-rectangles cover of figure C1, but the effect is magic - now every infinite walk on the transition graph of figure C1 (d) corresponds to a unique admissible orbit $\{\phi_t\}$, and the transition graph generates all admissible itineraries $\{m_t\}$.

To summarize: an explicit Adler-Weiss generating partition, such as figure C1, completely solves the Hamiltonian cat map problem, in the sense that it generates all admissible orbits. Rational and irrational initial states generate periodic and

ergodic orbits, respectively [66, 91], with every state space orbit uniquely labeled by an admissible bi-infinite itinerary of symbols from alphabet $\mathcal{A}$.

Appendix C.2. Counting Hamiltonian cat map periodic orbits

The five sub-rectangles $\mathcal{M}_j$ of the two-rectangle Adler-Weiss partition of figure C1 (c) motivate introduction of a 5-letter alphabet

$$\bar{\mathcal{A}} = \{1,2,3,4,5\} = \{A^0A, B^1A, A^1A, B^0B, A^1B\}\,, \tag{C.2}$$

see figure C2 (b), which encodes the links of the transition graph of figure C1 (d). The loop expansion of the determinant [27] of the transition graph T of figure C2 (b) is given by all non-intersecting walks on the graph

$$\det(1-zT) = 1 - z(t_1+t_3+t_4) - z^2(t_{25} - (t_1+t_3)t_4)\,, \tag{C.3}$$

where t_p are traces over fundamental cycles, the three fixed points $t_1 = T_{A^0A}, t_3 = T_{A^1A}, t_4 = T_{B^0B}$, and the 2-cycle $t_{25} = T_{B^1A}T_{A^1B}$.

As the simplest application, consider counting all admissible cat map periodic orbits. This is accomplished by setting the non-vanishing links of the transition graph to $T_{ji} = 1$, resulting in the $s = 3$ cat map topological zeta function [31, 59],

$$1/\zeta_{\rm top}(z) = \frac{1-3z+z^2}{(1-z)^2}\,, \tag{C.4}$$

where the numerator $(1-z)^2$ corrects the overcounting of the fixed point at the origin due to assigning it to both $\mathcal{M}_A$ (twice) and $\mathcal{M}_B$ rectangles [79].

The number of *periodic points* of period n is given by (33), the logarithmic derivative of the topological zeta function. Substituting the cat map topological zeta function (C.4) we obtain

$$\begin{aligned}\sum_{n=1} N_n z^n = {} & z + 5z^2 + 16z^3 + 45z^4 + 121z^5 + 320z^6 + 841z^7 \\ & + 2205z^8 + 5776z^9 + 15125z^{10} + 39601z^{11} + \cdots\end{aligned} \tag{C.5}$$

WolframAlpha says, compare with (69):

$$\sum_{n=1} N_n z^n = \frac{s-2z}{1-sz+z^2} - \frac{2}{1-z} \tag{C.6}$$

The number of *prime* cycles is given by (36),

$$\begin{aligned}\sum_{n=1} M_n z^n = {} & z + 2z^2 + 5z^3 + 10z^4 + 24z^5 + 50z^6 + 120z^7 \\ & + 270z^8 + 640z^9 + 1500z^{10} + 3600z^{11} + \cdots\,,\end{aligned} \tag{C.7}$$

in agreement with the Bird and Vivaldi [12] census.

This derivation was based on the Adler-Weiss generating partition, a clever explicit visualization of the cat map dynamics, whose generalization to several coupled maps (let alone spatially infinite coupled cat maps lattice) is far from obvious: one would have to construct covers of high-dimensional fundamental parallelepipeds by sets of

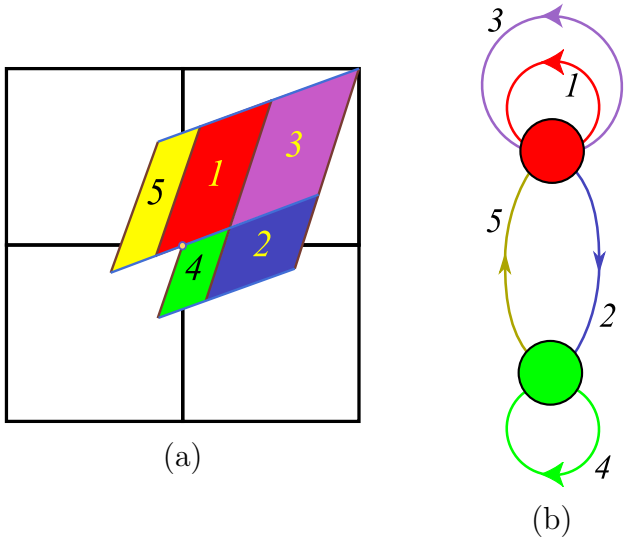

Figure C2. (Color online) (a) The sub-rectangles $\mathcal{M}_j$ of figure C1 (c). (b) Admissible orbits correspond to walks on the transition graph of figure C1 (d), with rectangles $\mathcal{M}_A$ (red) and $\mathcal{M}_B$ (green) as nodes, and the links labeled by 5-letter alphabet (C.2), see the loop expansion (C.3).

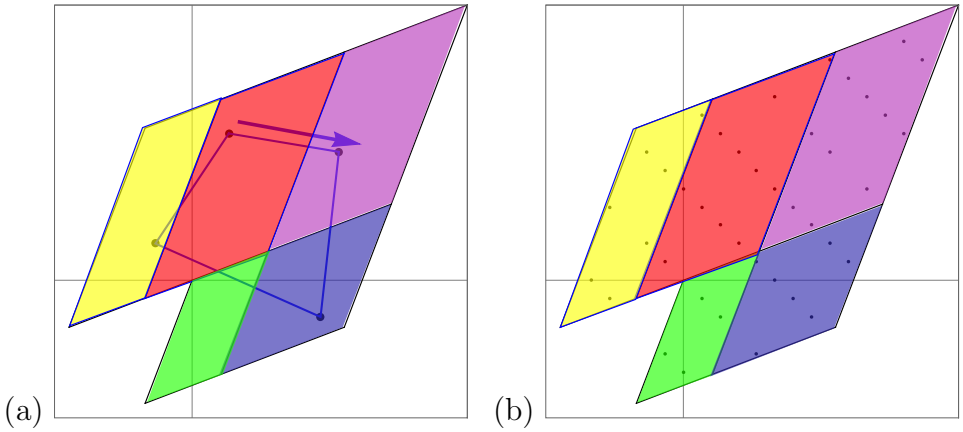

Figure C3. (a) An example of a 4-cycle: $\Phi_{011\underline{1}}$. (b) All prime period-4 lattice states land in the partition of figure C2 (a).

sub-volumes. However, as Keating [66] explains, no such explicit generating partition is needed to count cat map periodic orbits. Cat map (45) lattice states are the fixed points of

$$\begin{bmatrix} q_t \\ p_t \end{bmatrix} = \begin{bmatrix} q_{t+n} \\ p_{t+n} \end{bmatrix} = J^n \begin{bmatrix} q_t \\ p_t \end{bmatrix} \pmod 1 ,$$

so on the unwrapped phase space lattice, tiled by repeats of the unit square of the cat map torus,

$$(J^n - \mathbf{1}) \begin{bmatrix} q_t \\ p_t \end{bmatrix} = \begin{bmatrix} m_t^q \\ m_t^p \end{bmatrix} , \qquad (m_t^q, m_t^p) \in \mathbb{Z}^2 , \tag{C.8}$$

matrix $(J^n - \mathbf{1})$ stretches the unit square into the 'fundamental parallelepiped'.

Appendix C.3. An example: period-4 prime cycles

As a hands-on example, let us count the $M_4 = 10$ admissible prime 4-cycles, as stated in (**??**). The admissible blocks M_p can be read off as walks on either the 5-letter alphabet (C.2) graph, see figure C2 (b), or the 3-letter alphabet (C.1) graph, see figure C1 (d). They are, in 5-letter (top), and 3-letter (bottom) alphabets

$$\begin{array}{ccccc} \overline{1113} & \overline{1125} & \overline{1245} & \overline{1253} & \overline{1325} \\ 0001 & 001\underline{1} & 010\underline{1} & 01\underline{1}1 & 011\underline{1} \\ \overline{1133} & \overline{3325} & \overline{3331} & \overline{3245} & \overline{4452} \\ 0011 & 111\underline{1} & 1110 & 110\underline{1} & 00\underline{11} \end{array} \ . \tag{C.9}$$

The corresponding periodic orbits Φ_p are computed using Green's function (66) (the inverse of the $[4 \times 4]$ orbit Jacobian matrix (51), easiest to evaluate by discrete Fourier transforms, see Appendix A):

$$\mathsf{M}_{0001} \Rightarrow \quad \Phi_{0001} = g \begin{bmatrix} 0 \\ 0 \\ 0 \\ 1 \end{bmatrix} = \frac{1}{15} \begin{bmatrix} 3 \\ 2 \\ 3 \\ 7 \end{bmatrix} .$$

Likewise,

$$\begin{aligned} \Phi^\top_{001\underline{1}} &= \frac{1}{15} \begin{bmatrix} -1 & 1 & 4 & -4 \end{bmatrix} , & \Phi^\top_{010\underline{1}} &= \frac{1}{15} \begin{bmatrix} 0 & 5 & 0 & -5 \end{bmatrix} \\ \Phi^\top_{01\underline{11}} &= \frac{1}{15} \begin{bmatrix} 4 & 6 & -1 & 6 \end{bmatrix} , & \Phi^\top_{011\underline{1}} &= \frac{1}{15} \begin{bmatrix} 2 & 8 & 7 & -2 \end{bmatrix} \\ \Phi^\top_{0011} &= \frac{1}{15} \begin{bmatrix} 5 & 5 & 10 & 10 \end{bmatrix} , & \Phi^\top_{111\underline{1}} &= \frac{1}{15} \begin{bmatrix} 9 & 11 & 9 & 1 \end{bmatrix} \\ \Phi^\top_{1110} &= \frac{1}{15} \begin{bmatrix} 12 & 13 & 12 & 8 \end{bmatrix} , & \Phi^\top_{110\underline{1}} &= \frac{1}{15} \begin{bmatrix} 7 & 8 & 2 & -2 \end{bmatrix} \\ \Phi^\top_{00\underline{11}} &= \frac{1}{15} \begin{bmatrix} 1 & -1 & -4 & 4 \end{bmatrix} . \end{aligned} \tag{C.10}$$

One can verify that for each of these 10 prime 4-cycles the lattice states (ϕ_t, ϕ_{t+1}) visit the rectangles $\mathcal{M}_A$ or $\mathcal{M}_B$ of figure C1 (b) in the temporal order dictated by the transition graph, and thus they are all admissible cycles.

Appendix D. Spatiotemporal stability

Here we address two questions: (i) how is the high-dimensional orbit Jacobian matrix $\mathcal{J}$ related to the temporal $[d \times d]$ Jacobian matrix J? and (ii) how does one evaluate the orbit Jacobian matrix $\mathcal{J}$?

Appendix D.1. Temporal lattice

$$\mathcal{J}_{\mathsf{M}} = 1 - J \otimes \sigma^{-1} \,, \tag{D.1}$$

the temporal Bernoulli condition (10) is the zero of function

$$F[\Phi; \mathsf{M}[= \mathcal{J}\Phi + \mathsf{M} = 0 \,, \qquad \mathcal{J} = 1 - s\sigma^{-1} \,, \tag{D.2}$$

For a d-dimensional discrete time map f, with the lattice state Φ of discrete period n, every temporal lattice site satisfies

$$\phi_{t+1} = f(\phi_t) \,, \tag{D.3}$$

where ϕ_t is a d-dimensional field at lattice site t. Consider an approximate lattice state, known only to a finite precision

$$\hat{\Phi} = (\hat{\phi}_1, \hat{\phi}_2, \cdots, \hat{\phi}_n) \,, \quad \hat{\phi}_t = \phi_t + \Delta\phi_t \,, \tag{D.4}$$

where ϕ_t is the exact field at lattice site t. Define the error field by $F[\hat{\Phi}] = f(\hat{\Phi}) - \sigma^{-1} \otimes \hat{\Phi}$, an operator which compares the forward map of every point in $\hat{\Phi}$ with the next point $\hat{\Phi} \otimes \sigma$.

$F[\hat{\Phi}]$ is a $(n \times d)$-dimensional temporal lattice field obtained by stacking a d-dimensional field $\hat{\phi}_t$ at each of the n lattice sites,

$$F[\hat{\Phi}] \;=\; F \begin{pmatrix} \hat{\phi}_1 \\ \hat{\phi}_2 \\ \cdots \\ \hat{\phi}_n \end{pmatrix} = \begin{pmatrix} \hat{\phi}_1 - \hat{f}_n \\ \hat{\phi}_2 - \hat{f}_1 \\ \cdots \\ \hat{\phi}_n - \hat{f}_{n-1} \end{pmatrix} , \qquad \hat{f}_t = f(\hat{\phi}_t) \,, \tag{D.5}$$

which measures the misalignment of every finite forward-in-time segment $f(\hat{\phi})_t$ with the next site $\hat{\phi}_{t+1}$ on the lattice state $\hat{\Phi}$.

By (D.3), the exact lattice state Φ is a zero of this vector field, $F[\Phi] = 0$. Assuming that the d-dimensional error vectors $\Delta\phi_t$ are small in magnitude, and Taylor expanding the one discrete time-step map f to linear order around the exact solution,

$$f(\phi_t + \Delta\phi_t) = \phi_{t+1} + J_t \Delta\phi_t + (\cdots) \,,$$

where

$$[J_t]_{ij} = \frac{\partial f_i(\phi_t)}{\partial \phi_j} \,, \quad t = (1, 2, \cdots, n) \,, \quad i, j \;=\; (1, 2, \cdots, d) \tag{D.6}$$

one finds that the neighborhood of entire cycle p is linearly deformed by the $[nd \times nd]$ orbit Jacobian matrix

$$\Delta\phi' = \mathcal{J}(\phi)\, \Delta\phi \,, \qquad \mathcal{J}_{ij}(\phi) = \frac{\delta F[\phi]_i}{\delta \phi_j} \,, \tag{D.7}$$

with

$$\mathcal{J} \;=\; 1 - \sigma J \,,$$

the one discrete time-step temporal $[d\times d]$ Jacobian matrix J evaluated on the entire cycle p, and σ the shift operator

$$\sigma = \begin{pmatrix} 0 & & & & & 1 \\ 1 & 0 & & & & \\ & 1 & 0 & & & \\ & & 1 & & & \\ & & & \ddots & 0 & \\ & & & & 1 & 0 \end{pmatrix}, \quad J = \begin{pmatrix} J_1 & & & & & \\ & J_2 & & & & \\ & & J_3 & & & \\ & & & \ddots & & \\ & & & & J_{n-1} & \\ & & & & & J_n \end{pmatrix}, \tag{D.8}$$

with 1 in the upper right corner assuring periodicity, $\sigma^n = 1$.

Consider a d–dimensional map $\phi_{t+1} = f(\phi_t)$, where $\phi_t = \{\phi_{t,1}, \phi_{t,2}, \ldots, \phi_{t,d}\}$ is the state of the system at time t. In case at hand, the one time step Jacobian matrix

$$J(\phi_t)_{ij} = \left.\frac{\partial f(\phi)_i}{\partial \phi_j}\right|_{\phi_i=\phi_{i,t}} \tag{D.9}$$

stretches uniformly, so the Jacobian matrix does not depend on the field value ϕ_t or time t, $J(\phi_t) = J$.

For a lattice state Φ_p with period n, the orbit Jacobian matrix is a $[nd \times nd]$ block matrix

$$\mathcal{J} = \begin{pmatrix} \mathbf{1} & & & & -J \\ -J & \mathbf{1} & & & \\ & \cdots & \mathbf{1} & & \\ & & \cdots & \mathbf{1} & \\ & & & -J & \mathbf{1} \end{pmatrix} = 1 - J \otimes \sigma^{-1}\,, \tag{D.10}$$

where $\mathbf{1}$ is a d–dimensional identity matrix, J is the one time step $[d \times d]$ Jacobian matrix (D.9), and σ is the $[n \times n]$ shift operator matrix with period n.

To evaluate the Hill determinant of the orbit Jacobian matrix, expand $\ln \mathrm{Det}\, \mathcal{J}_p = \mathrm{Tr} \ln \mathcal{J}_p$:

$$\begin{aligned} \ln \mathrm{Det}\, \mathcal{J}_p &= \mathrm{Tr} \ln(1 - J \otimes \sigma^{-1}) \\ &= -\sum_{k=1}^{\infty} \frac{\mathrm{Tr}(J \otimes \sigma^{-1})^k}{k}\,. \end{aligned} \tag{D.11}$$

Note that $(J\otimes\sigma^{-1})^k = J^k \otimes \sigma^{-k}$ and $\mathrm{Tr}(J^k \otimes \sigma^{-k}) = \mathrm{Tr}(J^{nr} \otimes 1_{[n\times n]})\delta_{k,nr} = n\,\mathrm{tr}(J^{nr})\delta_{k,nr}$ which is not 0 only when k is a multiple of n.

$$\begin{aligned} \ln \mathrm{Det}\, \mathcal{J}_p &= -\sum_{r=1}^{\infty} \frac{n\,\mathrm{tr}(J^{rn})}{rn} = \mathrm{tr}[-\sum_{r=1}^{\infty} \frac{(J^n)^r}{r}] \\ &= \mathrm{tr} \ln(1 - J^n) = \ln \det(1 - J^n)\,. \end{aligned} \tag{D.12}$$

So the Hill determinant of the orbit Jacobian matrix is $\mathrm{Det}\, \mathcal{J} = \det(1 - J^{n_p})$.

Appendix D.2. Temporal stability

To summarize, a discretized, temporal lattice periodic orbit linear stability can be computed in two ways - either by computing the $[nd\times nd]$ orbit Jacobian matrix $jMorb$, or by computing J_p

$$\text{Det}\,\mathcal{J}_{\mathsf{M}} = \det(1 - J_{\mathsf{M}})\,, \tag{D.13}$$

where J_{M} is the n time-steps $[d\times d]$ forward-time Jacobian matrix. In the limit of discretization $n\to\infty$ the left hand side is a *functional* Hill determinant of an ∞-dimensional *operator*. Nevertheless, thanks to the discrete Fourier diagonalization of $\mathcal{J}(x)$, Appendix A, the Hill determinant $\text{Det}\,\mathcal{J}_{\mathsf{M}}$ is easier to compute than the ill-posed J_{M}.

The projection operator on the kth Fourier mode is

$$P_k = \prod_{j\neq k} \frac{\sigma - \omega_j 1}{\omega_k - \omega_j}\,. \tag{D.14}$$

The set of the projection operators is complete,

$$\sum_k P_k = 1\,, \tag{D.15}$$

and orthonormal

$$P_k P_j = \delta_{kj} P_k \qquad (\text{no sum on } k)\,. \tag{D.16}$$

[TO BE CONTINUED]

Appendix E. Spatiotemporal lattice

In spatiotemporal settings, J_p can be defined only for finite numbers of spatial sites, and it gets funkier and funkier as the spatial direction increases (that is why we are able to work only with very small spatial domain Kuramoto-Sivashinsky discretizations). But, as shown for the spatiotemporal cat in [33], $\text{Det}\,\mathcal{J}_p$ works just fine on any spatiotemporal torus. In particular, for any periodic orbit Kuramoto-Sivashinsky discretization.

Appendix F. Symbolic dynamics: a glossary

Analysis of a low-dimensional chaotic dynamical system typically starts [31] with establishing that a flow is locally stretching, globally folding. The flow is then reduced to a discrete time return map by appropriate Poincaré sections. Its state space is partitioned, the partitions labeled by an alphabet, and the qualitatively distinct solutions classified by their temporal symbol sequences. Thus our analysis of the cat map and the spatiotemporal cat requires recalling and generalising a few standard symbolic dynamics notions.

Partitions, alphabets. A division of state space $\mathcal{M}$ into a disjoint union of distinct regions $\mathcal{M}_A, \mathcal{M}_B, \ldots, \mathcal{M}_Z$ constitutes a *partition*. Label each region by a symbol m from an N-letter *alphabet* $\mathcal{A} = \{A, B, C, \cdots, Z\}$, where $N = n_{\mathcal{A}}$ is

the number of such regions. Alternatively, one can distinguish different regions by coloring them, with colors serving as the "letters" of the alphabet. For notational convenience, in alphabets we sometimes denote negative integer m by underlining it, as in $\mathcal{A} = \{-2,-1,0,1\} = \{\underline{2},\underline{1},0,1\}$.

Itineraries. For a dynamical system evolving in time, every state space point $\phi_0 \in \mathcal{M}$ has the *future itinerary*, an infinite sequence of symbols $S^+(\phi_0) = m_1 m_2 m_3 \cdots$ which indicates the temporal order in which the regions shall be visited. Given a trajectory $\phi_1, \phi_2, \phi_3, \cdots$ of the initial point ϕ_0 generated by a time-evolution law $\phi_{n+1} = f(\phi_n)$, the itinerary is given by the symbol sequence

$$m_n = m \qquad \text{if} \qquad \phi_n \in \mathcal{M}_m \,. \tag{F.1}$$

The *past itinerary* $S^-(\phi_0) = \cdots m_{-2} m_{-1} m_0$ describes the order in which the regions were visited up to arriving to the point ϕ_0. Each point ϕ_0 thus has associated with it the bi-infinite itinerary

$$S(\phi_0) = S^-.S^+ = \cdots m_{-2} m_{-1} m_0 . m_1 m_2 m_3 \cdots \,, \tag{F.2}$$

or simply 'itinerary', if we chose not to use the decimal point to indicate the present,

$$\{m_t\} = \cdots m_{-2} m_{-1} m_0 m_1 m_2 m_3 \cdots \tag{F.3}$$

Shifts. A forward iteration of temporal dynamics $x \to x' = f(x)$ shifts the entire itinerary to the left through the 'decimal point'. This operation, denoted by the shift operator σ,

$$\sigma(\cdots m_{-2} m_{-1} m_0 . m_1 m_2 m_3 \cdots) = \cdots m_{-2} m_{-1} m_0 m_1 . m_2 m_3 \cdots \,, \tag{F.4}$$

demotes the current partition label m_1 from the future S^+ to the past S^-. The inverse shift σ^{-1} shifts the entire itinerary one step to the right.

The set of all itineraries that can be formed from the letters of the alphabet $\mathcal{A}$ is called the *full shift*

$$\hat{\Sigma} = \{(m_k) : m_k \in \mathcal{A} \quad \text{for all} \quad k \in \mathbb{Z}\} \,. \tag{F.5}$$

The itinerary is infinite for any trapped (non-escaping or non–wandering set orbit) orbit (such as an orbit that stays on a chaotic repeller), and infinitely repeating for a periodic orbit p of period n_p. A map f is said to be a *horseshoe* if its restriction to the non–wandering set is hyperbolic and topologically conjugate to the full $\mathcal{A}$-shift.

Lattices. Consider a d-dimensional hypercubic lattice infinite in extent, with each site labeled by d integers $z \in \mathbb{Z}^d$. Assign to each site z a letter m_z from a finite alphabet $\mathcal{A}$. A particular fixed set of letters m_z corresponds to a particular lattice state $\mathsf{M} = \{m_z\}$. In other words, a d-dimensional lattice requires a d-dimensional code $\mathsf{M} = \{m_{n_1 n_2 \cdots n_d}\}$ for a complete specification of the corresponding state Φ. In the lattice case, the *full shift* is the set of all d-dimensional symbol blocks that can be formed from the letters of the alphabet $\mathcal{A}$

$$\hat{\Sigma} = \{\{m_z\} : m_z \in \mathcal{A} \quad \text{for all} \quad z \in \mathbb{Z}^d\} \,. \tag{F.6}$$

Commuting discrete translations. For an autonomous dynamical system, the evolution law f is of the same form for all times. If f is also of the same form at every lattice site, the group of lattice translations (sometimes called multidimensional shifts), acting along jth lattice direction by shift σ_j, is a spatial symmetry that commutes with the temporal evolution. A temporal mapping f that satisfies $f \circ \sigma_j = \sigma_j \circ f$ along the $d-1$ spatial lattice directions is said to be *shift invariant*, with the associated symmetry of dynamics given by the d-dimensional group of discrete spatiotemporal translations.

Assign to each site z a letter m_z from the alphabet $\mathcal{A}$. A particular fixed set of letters m_z corresponds to a particular lattice symbol array $\mathsf{M} = \{m_z\} = \{m_{n_1 n_2 \cdots n_d}\}$, which yields a complete specification of the corresponding state Φ. In the lattice case, the *full shift* is the set of all d-dimensional symbol arrays that can be formed from the letters of the alphabet $\mathcal{A}$

as in (F.6)

A d-dimensional spatiotemporal field $\Phi = \{\phi_z\}$ is determined by the corresponding *d-dimensional* spatiotemporal symbol array $\mathsf{M} = \{m_z\}$. Consider next a finite block of symbols $\mathsf{M}_\mathcal{R} \subset \mathsf{M}$, over a finite rectangular $[L_1 \times L_2 \times \cdots \times L_d]$ lattice region $\mathcal{R} \subset \mathbb{Z}^d$. In particular, let M_p over a finite rectangular $[L_1 \times L_2 \times \cdots \times L_d]$ lattice region be the $[L_1 \times L_2 \times \cdots \times L_d]$ d-periodic block of M whose repeats tile $\mathbb{Z}^d$.

Blocks. In the case of temporal dynamics, a finite itinerary $\mathsf{M}_\mathcal{R} = m_{k+1} m_{k+2} \cdots m_{k+L}$ of symbols from $\mathcal{A}$ is called a *block* of length $L = n_\mathcal{R}$. More generally, let $\mathcal{R} \subset \mathbb{Z}^d$ be a $[L_1 \times L_2 \times \cdots L_d]$ rectangular lattice region, $L_k \geq 1$, whose lower left corner is the $n = (n_1 n_2 \cdots n_d)$ lattice site

$$\mathcal{R} = \mathcal{R}_n^{[L_1 \times L_2 \times \cdots L_d]} = \{(n_1 + j_1, \cdots n_d + j_d) \mid 0 \leq j_k \leq L_k - 1\}\,. \tag{F.7}$$

The associated finite block of symbols $m_z \in \mathcal{A}$ restricted to $\mathcal{R}$, $\mathsf{M}_\mathcal{R} = \{m_z | z \in \mathcal{R}\} \subset \mathsf{M}$ is called the block $\mathsf{M}_\mathcal{R}$ of volume $n_\mathcal{R} = L_1 L_2 \cdots L_d$. For example, for a 2-dimensional lattice a $\mathcal{R} = [3 \times 2]$ block is of form

$$\mathsf{M}_\mathcal{R} = \begin{bmatrix} m_{12} & m_{22} & m_{32} \\ m_{11} & m_{21} & m_{31} \end{bmatrix} \tag{F.8}$$

and volume (in this case, an area) equals $3 \times 2 = 6$. In our convention, the first index is 'space', increasing from left to right, and the second index is 'time', increasing from bottom up.

Cylinder sets. While a particular admissible infinite symbol array $\mathsf{M} = \{m_z\}$ defines a point Φ (a unique lattice state) in the state space, the *cylinder set* $\mathcal{M}_{\mathsf{M}_\mathcal{R}}$, corresponds to the totality of state space points Φ that share the same given finite block $\mathsf{M}_\mathcal{R}$ symbolic representation over the region $\mathcal{R}$. For example, in $d = 1$ case

$$\mathcal{M}_{\mathsf{M}_\mathcal{R}} = \{\cdots a_{-2} a_{-1}\,.\, m_1 m_2 \cdots m_L a_{L+1} a_{L+2} \cdots\}\,, \tag{F.9}$$

with the symbols a_j outside of the block $\mathsf{M}_\mathcal{R} = [m_1 m_2 \cdots m_L]$ unspecified.

Periodic orbits, invariant d-tori. A state space point $\phi_z \in \Phi$ is spatiotemporally *periodic*, $\phi_z = \phi_{z+L}$, if its spacetime orbit returns to it after a finite lattice shift

$L = (L_1, L_2, \cdots, L_d)$ over region $\mathcal{R}$ defined in (F.7). The infinity of repeats of the corresponding block $\mathsf{M}_\mathcal{R}$ then tiles the lattice. For a spatiotemporally periodic state Φ, a *prime* block M_p (or p) is a smallest such block $L_p = (L_1, L_2, \cdots, L_d)$ that cannot itself be tiled by repeats of a shorter block.

The periodic tiling of the lattice by the infinitely many repeats of a prime block is denoted by a bar: $\overline{\mathsf{M}}_p$. We shall omit the bar whenever it is clear from the context that the state is periodic.

In $d = 1$ dimensions, prime block is called a *prime* cycle p, or a single traversal of the orbit; its label is a block of n_p symbols that cannot be written as a repeat of a shorter block. Each *periodic point* $\phi_{m_1 m_2 \cdots m_{n_p}}$ is then labeled by the starting symbol m_1, followed by the next $(n_p - 1)$ steps of its future itinerary. The set of periodic points $\mathcal{M}_p$ that belong to a given periodic orbit form a *cycle*

$$p = \overline{m_1 m_2 \cdots m_{n_p}} = \{\phi_{m_1 m_2 \cdots m_{n_p}}, \phi_{m_2 \cdots m_{n_p} m_1}, \cdots, \phi_{m_{n_p} m_1 \cdots m_{n_p - 1}}\} . \quad \text{(F.10)}$$

More generally, a state space point is *spatiotemporally periodic* if it belongs to an invariant d-torus, i.e., its symbolic representation is a block over region $\mathcal{R}$ defined by (F.7),

$$\mathsf{M}_p = \mathsf{M}_\mathcal{R} , \qquad \mathcal{R} = \mathcal{R}_0^{[L_1 \times L_2 \times \cdots \times L_d]} , \quad \text{(F.11)}$$

that tiles the lattice state M periodically, with period L_j in the jth lattice direction.

Generating partitions. A temporal partition is called *generating* if every bi-infinite itinerary corresponds to a distinct point in state space. In practice almost any generating partition of interest is infinite. Even when the dynamics assigns a unique infinite itinerary $\cdots m_{-2} m_{-1} m_0 . m_1 m_2 m_3 \cdots$ to each distinct orbit, there generically exist full shift itineraries (F.5) which are not realized as orbits; such sequences are called *inadmissible*, and we say that the symbolic dynamics is *pruned*.

Dynamical partitions. If the symbols outside of given temporal block b remain unspecified, the set of all admissible blocks of length n_b yield a dynamically generated partition of the state space, $\mathcal{M} = \cup_b \mathcal{M}_b$.

Subshifts. A dynamical system $(\mathcal{M}, f)$ given by a mapping $f : \mathcal{M} \to \mathcal{M}$ together with a partition $\mathcal{A}$ induces *topological dynamics* (Σ, σ), where the *subshift*

$$\Sigma = \{(m_k)_{k \in \mathbb{Z}}\} , \quad \text{(F.12)}$$

is the set of all *admissible* itineraries, and $\sigma : \Sigma \to \Sigma$ is the shift operator (F.4). The designation 'subshift' comes from the fact that Σ is a subset of the full shift.

Let $\hat{\Sigma}$ be the full lattice shift (F.5), i.e., the set of all possible lattice state M labelings by the alphabet $\mathcal{A}$, and $\hat{\Sigma}(\mathsf{M}_\mathcal{R})$ is the set of such blocks over a region $\mathcal{R}$. The principal task in developing the symbolic dynamics of a dynamical system is to determine Σ, the set of all *admissible* itineraries/lattice states, i.e., all states that can be realized by the given system.

Pruning, grammars, recoding. If certain states are inadmissible, the alphabet must be supplemented by a *grammar*, a set of pruning rules. Suppose that the grammar

can be stated as a finite number of pruning rules, each forbidding a block of finite size,

$$\mathcal{G} = \{b_1, b_2, \cdots b_k\} \ , \tag{F.13}$$

where a *pruned block* b is an array of symbols defined over a finite $\mathcal{R}$ lattice region of size $[L_1 \times L_2 \times \cdots \times L_d]$. In this case we can construct a finite Markov partition by replacing finite size blocks of the original partition by letters of a new alphabet. In the case of a 1-dimensional, the temporal lattice, if the longest forbidden block is of length $L+1$, we say that the symbolic dynamics is Markov, a shift of finite type with L-step memory.

Subshifts of finite type. A topological dynamical system (Σ, σ) for which all admissible states M are generated by recursive application of the finite set of pruning rules (F.13) is called a subshift of *finite type*.

If a map can be topologically conjugated to a linear map, the symbolic dynamics of the linear map offers a dramatically simplified description of all admissible solutions of the original flow, with the temporal symbolic dynamics and the state space dynamics related by linear recoding formulas. For example, if a map of an interval, such as a parabola, can be conjugated to a piecewise linear map, the kneading theory [82] classifies *all* of its admissible orbits.

References

[1] R. L. Adler and B. Weiss, "Entropy, a complete metric invariant for automorphisms of the torus", Proc. Natl. Acad. Sci. USA **57**, 1573–1576 (1967).

[2] R. L. Adler and B. Weiss, *Similarity of automorphisms of the torus*, Vol. 98, Memoirs Amer. Math. Soc. (Amer. Math. Soc., Providence RI, 1970).

[3] E. Allroth, "Ground state of one-dimensional systems and fixed points of 2n-dimensional map", J. Phys. A **16**, L497 (1983).

[4] A. M. Ozorio de Almeida and J. H. Hannay, "Periodic orbits and a correlation function for the semiclassical density of states", J. Phys. A **17**, 3429 (1984).

[5] G. B. Arfken, H. J. Weber, and F. E. Harris, *Mathematical Methods for Physicists: A Comprehensive Guide*, 7th ed. (Academic, New York, 2013).

[6] V. I. Arnol'd and A. Avez, *Ergodic Problems of Classical Mechanics* (Addison-Wesley, Redwood City, 1989).

[7] M. Artin and B. Mazur, "On periodic points", Ann. Math. **81**, 82–99 (1965).

[8] R. Artuso, E. Aurell, and P. Cvitanović, "Recycling of strange sets: I. Cycle expansions", Nonlinearity **3**, 325–359 (1990).

[9] M. Baake, J. Hermisson, and. A. B. Pleasants, "The torus parametrization of quasiperiodic LI-classes", J. Phys. A **30**, 3029–3056 (1997).

[10] A. Barvinok, Lattice Points, Polyhedra, and Complexity, tech. rep. (Univ. of Michigen, Ann Arbor MI, 2004).

[11] A. I. Barvinok, "A polynomial time algorithm for counting integral points in polyhedra when the dimension is fixed", Math. Oper. Res. **19**, 769–779 (1994).

[12] N. Bird and F. Vivaldi, "Periodic orbits of the sawtooth maps", Physica D **30**, 164–176 (1988).

[13] S. V. Bolotin and D. V. Treschev, "Hill's formula", Russ. Math. Surv. **65**, 191 (2010).

[14] R. Bowen, "Markov partitions for Axiom A diffeomorphisms", Amer. J. Math. **92**, 725–747 (1970).

[15] J. P. Boyd, *Chebyshev and Fourier Spectral Methods*, 2nd ed. (Dover, New York, 2000).

[16] R. B. S. Brooks, R. F. Brown, J. Pak, and D. H. Taylor, "Nielsen numbers of maps of tori", Proc. Amer. Math. Soc. **52**, 398–398 (1975).

[17] L. A. Bunimovich and Y. G. Sinai, "Spacetime chaos in coupled map lattices", Nonlinearity **1**, 491 (1988).

[18] B. L. Buzbee, G. H. Golub, and C. W. Nielson, "On direct methods for solving Poisson's equations", SIAM J. Numer. Anal. **7**, 627–656 (1970).

[19] M. Chen, "On the solution of circulant linear systems", SIAM J. Numer. Anal. **24**, 668–683 (1987).

[20] B. V. Chirikov, "A universal instability of many-dimensional oscillator system", Phys. Rep. **52**, 263–379 (1979).

[21] W. G. Choe and J. Guckenheimer, "Computing periodic orbits with high accuracy", Computer Meth. Appl. Mech. and Engin. **170**, 331–341 (1999).

[22] H. Cohen, *A Course in Computational Algebraic Number Theory* (Springer, Berlin, 1993).

[23] S. C. Creagh, "Quantum zeta function for perturbed cat maps", Chaos **5**, 477–493 (1995).

[24] P. Cvitanović, "Invariant measurement of strange sets in terms of cycles", Phys. Rev. Lett. **61**, 2729–2732 (1988).

[25] P. Cvitanović, "Recurrent flows: The clockwork behind turbulence", J. Fluid Mech. Focus Fluids **726**, 1–4 (2013).

[26] P. Cvitanović, "Trace formulas", in *Chaos: classical and quantum*, edited by P. Cvitanović, R. Artuso, R. Mainieri, G. Tanner, and G. Vattay (Niels Bohr Inst., Copenhagen, 2017).

[27] P. Cvitanović, "Counting", in *Chaos: Classical and Quantum* (Niels Bohr Inst., Copenhagen, 2020).

[28] P. Cvitanović, "Why cycle?", in *Chaos: Classical and Quantum*, edited by P. Cvitanović, R. Artuso, R. Mainieri, G. Tanner, and G. Vattay (Niels Bohr Inst., Copenhagen, 2020).

[29] P. Cvitanović, "World in a mirror", in *Chaos: Classical and Quantum* (Niels Bohr Inst., Copenhagen, 2020).

[30] P. Cvitanović, R. Artuso, R. Mainieri, G. Tanner, and G. Vattay, *Chaos: Classical and Quantum* (Niels Bohr Inst., Copenhagen, 2020).

[31] P. Cvitanović, R. Artuso, R. Mainieri, G. Tanner, and G. Vattay, *Chaos: Classical and Quantum* (Niels Bohr Inst., Copenhagen, 2020).

[32] P. Cvitanović and Y. Lan, Turbulent fields and their recurrences, in Correlations and Fluctuations in QCD : Proceedings of 10. International Workshop on Multiparticle Production, edited by N. Antoniou (2003), pp. 313–325.

[33] P. Cvitanović and H. Liang, Spatiotemporal cat: a chaotic field theory, in preparation, 2020.

[34] J. A. De Loera, R. Hemmecke, J. Tauzer, and R. Yoshida, "Effective lattice point counting in rational convex polytopes", J. Symbolic Comp. **38**, 1273–1302 (2004).

[35] R. L. Devaney, *An Introduction to Chaotic Dynamical systems*, 2nd ed. (Westview Press, 2008).

[36] X. Ding, H. Chaté, P. Cvitanović, E. Siminos, and K. A. Takeuchi, "Estimating the dimension of the inertial manifold from unstable periodic orbits", Phys. Rev. Lett. **117**, 024101 (2016).

[37] X. Ding and P. Cvitanović, "Periodic eigendecomposition and its application in Kuramoto-Sivashinsky system", SIAM J. Appl. Dyn. Syst. **15**, 1434–1454 (2016).

[38] E. J. Doedel, A. R. Champneys, T. F. Fairgrieve, Y. A. Kuznetsov, B. Sandstede, and X. Wang, *AUTO: Continuation and Bifurcation Software for Ordinary Differential Equations* (2007).

[39] F. W. Dorr, "The direct solution of the discrete Poisson equation on a rectangle", SIAM Rev. **12**, 248–263 (1970).

[40] M. S. Dresselhaus, G. Dresselhaus, and A. Jorio, *Group Theory: Application to the Physics of Condensed Matter* (Springer, New York, 2007).

[41] J. Dubout, Zeta functions of graphs, their symmetries and extended Catalan numbers.

[42] H. R. Dullin and J. D. Meiss, "Stability of minimal periodic orbits", Phys. Lett. A **247**, 227–234 (1998).

[43] E. N. Economou, *Green's Functions in Quantum Physics* (Springer, Berlin, 2006).

[44] S. Elaydi, *An Introduction to Difference Equations* (Springer, Berlin, 2005).

[45] A. L. Fetter and J. D. Walecka, *Theoretical Mechanics of Particles and Continua* (Dover, New York, 2003).

[46] E. Fradkin, *Field Theories of Condensed Matter Physics* (Cambridge Univ. Press, Cambridge UK, 2013).

[47] G. Giacomelli, S. Lepri, and A. Politi, "Statistical properties of bidimensional patterns generated from delayed and extended maps", Phys. Rev. E **51**, 3939–3944 (1995).

[48] F. Ginelli, P. Poggi, A. Turchi, H. Chaté, R. Livi, and A. Politi, "Characterizing dynamics with covariant Lyapunov vectors", Phys. Rev. Lett. **99**, 130601 (2007).

[49] J. W. von Goethe, *Faust I, Studierzimmer 2.* M. Greenberg, transl. (Yale Univ. Press, 1806).

[50] J. Guckenheimer and B. Meloon, "Computing periodic orbits and their bifurcations with automatic differentiation", SIAM J. Sci. Comput. **22**, 951–985 (2000).

[51] M. N. Gudorf and P. Cvitanović, Spatiotemporal tiling of the Kuramoto-Sivashinsky flow, in preparation, 2020.

[52] B. Gutkin, L. Han, R. Jafari, A. K. Saremi, and P. Cvitanović, Linear encoding of the spatiotemporal cat map, Nonlinearity, to appear, 2020.

[53] B. Gutkin and V. Osipov, "Clustering of periodic orbits and ensembles of truncated unitary matrices", J. Stat. Phys. **153**, 1049–1064 (2013).

[54] B. Gutkin and V. Osipov, "Clustering of periodic orbits in chaotic systems", Nonlinearity **26**, 177 (2013).

[55] B. Gutkin and V. Osipov, "Classical foundations of many-particle quantum chaos", Nonlinearity **29**, 325–356 (2016).

[56] G. W. Hill, "On the part of the motion of the lunar perigee which is a function of the mean motions of the sun and moon", Acta Math. **8**, 1–36 (1886).

[57] W. G. Hoover and K. Aoki, "Order and chaos in the one-dimensional ϕ^4 model : N-dependence and the Second Law of Thermodynamics", Commun. Nonlinear Sci. Numer. Simul. **49**, 192–201 (2017).

[58] G. Y. Hu, J. Y. Ryu, and R. F. O'Connell, "Analytical solution of the generalized discrete Poisson equation", J. Phys. A **31**, 9279 (1998).

[59] S. Isola, "ζ-functions and distribution of periodic orbits of toral automorphisms", Europhys. Lett. **11**, 517–522 (1990).

[60] N. S. Izmailian, K. B. Oganesyan, and C.-K. Hu, "Exact finite-size corrections for the square-lattice Ising model with Brascamp-Kunz boundary conditions", Phys. Rev. E **65**, 056132 (2002).

[61] L. P. Kadanoff, *Statistical Physics: Statics, Dynamics and Renormalization* (World Scientific, Singapore, 2000).

[62] K. Kaneko, "Transition from torus to chaos accompanied by frequency lockings with symmetry breaking: In connection with the coupled-logistic map", Prog. Theor. Phys. **69**, 1427–1442 (1983).

[63] K. Kaneko, "Period-doubling of kink-antikink patterns, quasiperiodicity in antiferro-like structures and spatial intermittency in coupled logistic lattice: Towards a prelude of a "field theory of chaos"", Prog. Theor. Phys. **72**, 480–486 (1984).

[64] H. Kantz and P. Grassberger, "Chaos in low-dimensional Hamiltonian maps", Phys. Let. A **123**, 437–443 (1987).

[65] B. Kastening, "Simplified transfer matrix approach in the two-dimensional Ising model with various boundary conditions", Phys. Rev. E **66**, 057103 (2002).

[66] J. P. Keating, "The cat maps: quantum mechanics and classical motion", Nonlinearity **4**, 309–341 (1991).

[67] H.-T. Kook and J. D. Meiss, "Application of Newton's method to Lagrangian mappings", Physica D **36**, 317–326 (1989).

[68] Y. Lan and P. Cvitanović, "Variational method for finding periodic orbits in a general flow", Phys. Rev. E **69**, 016217 (2004).

[69] S. Lang, *Linear Algebra* (Addison-Wesley, Reading, MA, 1987).

[70] S. Lepri, A. Politi, and A. Torcini, "Chronotopic Lyapunov analysis. I. A detailed characterization of 1D systems", J. Stat. Phys. **82**, 1429–1452 (1996).

[71] S. Lepri, A. Politi, and A. Torcini, "Chronotopic Lyapunov analysis. II. Towards a unified approach", J. Stat. Phys. **88**, 31–45 (1997).

[72] J. Li and S. Tomsovic, "Exact relations between homoclinic and periodic orbit actions in chaotic systems", Phys. Rev. E **97**, 022216 (2017).

[73] T. M. Liaw, M. C. Huang, Y. L. Chou, S. C. Lin, and F. Y. Li, "Partition functions and finite-size scalings of Ising model on helical tori", Phys. Rev. E **73**, 041118 (2006).

[74] A. J. Lichtenberg and M. A. Lieberman, *Regular and Chaotic Dynamics*, 2nd ed. (Springer, New York, 2013).

[75] D. A. Lind, "A zeta function for Z^d-actions", in *Ergodic Theory of Z^d Actions*, edited by M. Pollicott and K. Schmidt (Cambridge Univ. Press, 1996), pp. 433–450.

[76] E. N. Lorenz, "Deterministic nonperiodic flow", J. Atmos. Sci. **20**, 130–141 (1963).

[77] R. S. MacKay and J. D. Meiss, "Linear stability of periodic orbits in Lagrangian systems", Phys. Lett. A **98**, 92–94 (1983).

[78] R. S. MacKay, J. D. Meiss, and I. C. Percival, "Transport in Hamiltonian systems", Physica D **13**, 55–81 (1984).

[79] A. Manning, "Axiom A diffeomorphisms have rational zeta function", Bull. London Math. Soc. **3**, 215–220 (1971).

[80] J. D. Meiss, "Symplectic maps, variational principles, and transport", Rev. Mod. Phys. **64**, 795–848 (1992).

[81] B. D. Mestel and I. Percival, "Newton method for highly unstable orbits", Physica D **24**, 172 (1987).

[82] J. Milnor and W. Thurston, "Iterated maps of the interval", in *Dynamical Systems (Maryland 1986-87)*, edited by A. Dold and B. Eckmann (Springer, New York, 1988), pp. 465–563.

[83] I. Montvay and G. Münster, *Quantum Fields on a Lattice* (Cambridge Univ. Press, Cambridge, 1994).

[84] B. Mramor and B. Rink, "Ghost circles in lattice Aubry-Mather theory", J. Diff. Equ. **252**, 3163–3208 (2012).

[85] S. Müller, S. Heusler, P. Braun, F. Haake, and A. Altland, "Semiclassical foundation of universality in quantum chaos", Phys. Rev. Lett. **93**, 014103 (2004).

[86] G. Münster and M. Walzl, Lattice gauge theory - A short primer, 2000.

[87] J. Nielsen, "Über die Minimalzahl der Fixpunkte bei den Abbildungstypen der Ringflächen", Math. Ann. **82**, 83–93 (1920).

[88] Y. Okabe, K. Kaneda, M. Kikuchi, and C.-K. Hu, "Universal finite-size scaling functions for critical systems with tilted boundary conditions", Phys. Rev. E **59**, 1585–1588 (1999).

[89] L. Onsager, "Crystal statistics. I. A Two-dimensional model with an order-disorder transition", Phys. Rev. **65**, 117–149 (1944).

[90] I. Percival and F. Vivaldi, "A linear code for the sawtooth and cat maps", Physica D **27**, 373–386 (1987).

[91] I. Percival and F. Vivaldi, "Arithmetical properties of strongly chaotic motions", Physica D **25**, 105–130 (1987).

[92] Y. B. Pesin and Y. G. Sinai, "Space-time chaos in the system of weakly interacting hyperbolic systems", J. Geom. Phys. **5**, 483–492 (1988).

[93] S. D. Pethel, N. J. Corron, and E. Bollt, "Symbolic dynamics of coupled map lattices", Phys. Rev. Lett. **96**, 034105 (2006).

[94] S. D. Pethel, N. J. Corron, and E. Bollt, "Deconstructing spatiotemporal chaos using local symbolic dynamics", Phys. Rev. Lett. **99**, 214101 (2007).

[95] H. Poincaré, "Sur les déterminants d'ordre infini", Bull. Soc. Math. France **14**, 77—90 (1886).

[96] A. Politi and A. Torcini, "Periodic orbits in coupled Hénon maps: Lyapunov and multifractal analysis", Chaos **2**, 293–300 (1992).

[97] A. Politi and A. Torcini, "Towards a statistical mechanics of spatiotemporal chaos", Phys. Rev. Lett. **69**, 3421–3424 (1992).

[98] A. Politi, A. Torcini, and S. Lepri, "Lyapunov exponents from node-counting arguments", J. Phys. IV **8**, 263 (1998).

[99] C. Pozrikidis, *An Introduction to Grids, Graphs, and Networks* (Oxford Univ. Press, Oxford , UK, 2014).

[100] R. C. Robinson, *An Introduction to Dynamical Systems: Continuous and Discrete* (Amer. Math. Soc., New York, 2012).

[101] I. Schur, "Über Potenzreihen, die im Innern des Einheitskreises beschränkt sind", J. reine angewandte Math. **147**, 205–232 (1917).

[102] M. Sieber and K. Richter, "Correlations between periodic orbits and their role in spectral statistics", Phys. Scr. **2001**, 128 (2001).

[103] A. Siemaszko and M. P. Wojtkowski, "Counting Berg partitions", Nonlinearity **24**, 2383–2403 (2011).

[104] R. Sturman, J. M. Ottino, and S. Wiggins, *The Mathematical Foundations of Mixing* (Cambridge Univ. Press, 2006).

[105] Wikipedia contributors, Block matrix — Wikipedia, The Free Encyclopedia, 2020.

[106] Wikipedia contributors, Kronecker product — Wikipedia, The Free Encyclopedia, 2020.

[107] F. Y. Wu, "Theory of resistor networks: the two-point resistance", J. Phys. A **37**, 6653–6673 (2004).

[108] A. Zee, *Quantum Field Theory in a Nutshell*, 2nd ed. (Princeton Univ. Press, Princeton NJ, 2010).